MOLECULAR MECHANISMS INVOLVING PPARY IN THE PLACENTAL PATHOPHYSIOLOGY OF PREECLAMPSIA

By

Brooke A. Grimaldi

A DISSERTATION

Submitted to
Michigan State University
in partial fulfillment of the requirements
for the degree of

Genetics—Doctor of Philosophy

2022

ABSTRACT

MOLECULAR MECHANISMS INVOLVING PPARY IN THE PLACENTAL PATHOPHYSIOLOGY OF PREECLAMPSIA

By

Brooke A. Grimaldi

Preeclampsia (PE) is a hypertensive disorder of pregnancy that effects 5-7% of all pregnancies and is the main cause of maternal-fetal morbidity and mortality worldwide. Despite significant advancements in obstetric and neonatal care, the prevalence of PE has remained steady over the past thirty years. There is no cure for PE other than placental and fetal delivery. The exact etiology of the PE syndrome remains unclear however, maternal vascular malperfusion and placental ischemia are prominent features of the PE placenta that cause abnormal trophoblast differentiation and function. PE is considered a two-stage disease due to the ischemic-diseased placenta releasing altered secretion of placental proteins that negatively impact the maternal endothelium causing hypertension and end organ damage. The placental dysfunction is as well characterized by a reduction of the transcription factor, peroxisome proliferator activated receptor γ (PPARγ) which normally promotes trophoblast differentiation and healthy placental function. This dissertation has aimed to understand the link between PPARγ-driven trophoblast dysfunction and the imbalance of secreted proteins in PE. The restoration of these disrupted pathways by PPARγ actions in the placenta could offer potential therapeutic pathways to reverse the disease, extend pregnancy duration, and dampen maternal sequalae. This dissertation has utilized a collection of first trimester and term healthy and preeclamptic placentas in addition to immortalized cell lines to understand the effect of PPARγ activation by the drug, Rosiglitazone, during preeclamptic or in vitro

ischemic conditions. These studies revealed several molecules that are regulated by PPARγ in the human placenta, including the anti-angiogenic soluble fms-like tyrosine kinase 1 (sFLT1) and the cytoprotective heme oxygenase (HO1). Both proteins were restored to normal levels in PE by treatment with the PPARγ activating drug, Rosiglitazone. Furthermore, PPARγ activation improved the anti-angiogenic environment in the PE placenta as shown by increasing the pro-angiogenic and growth factor proteins: placental growth factor, fibroblast growth factor 2, follistatin and heparin-binding epidermal growth factor. Placental activation of PPARγ further restored the angiogenic balance in PE through significant reductions in the anti-angiogenic proteins, angiopoietin-2 and soluble endoglin. Using an endothelial cell model representing the maternal response to the placental protein secretion, these works revealed improved angiogenesis in endothelial cells during culture with conditioned medium from Rosiglitazone-treated PE placentas. These studies collectively show the beneficial effects of placental activation of PPARγ to improve placental and vascular function in PE. Future works should aim to understand global changes from PPARγ regulation in the human placenta and focus on compounds that hold promise to be safely used during pregnancy with the goal to improve pregnancy outcomes.

This work is dedicated to all those who are affected by preeclampsia.

ACKNOWLEDGMENTS

There are many people who I need to thank for making it possible to carry out this work. First, I would like to thank the BioMolecular Science program at Michigan State University for my acceptance into this PhD program. I am very grateful for the Genetics and Genome Sciences program and Dr. Cathy Ernst (former director) for the support and guidance throughout my PhD coursework and research-related milestones. I am very thankful to have participated in the Reproductive and Developmental Biology Program T32 (RDSP T32) which provided financial support for my stipend and thesis work. I have thoroughly enjoyed participating in the courses, scientific meetings, and weekly seminars through the RDSP which have all greatly enriched my scientific learning. The department of Obstetrics, Gynecology, and Reproductive Biology also largely contributed to my success through supporting the needs of my projects and I thank them for their generosity.

I would like to thank Dr. Sascha Drewlo, for accepting me as his PhD student and for providing all the opportunities to execute this work. Dr. Drewlo had a significant role in the conceptualization of my projects, as well supported everything that was required for this work to be completed. I have loved researching the placenta and I am so grateful to have participated in the research goals of this lab. Much of my success is also attributed to guidance and mentorship from Dr. Hamid-Reza Kohan-Ghadr. I am so thankful to have worked with Dr. Kohan as he has helped with executing many of my experiments. I am thankful for his help and discussions on data analysis and interpretations. I have learned many lessons from Dr. Drewlo and Dr. Kohan which have led to my exponential improvement in scientific skills since the beginning of my PhD. I am grateful to have worked with this team.

I would like to thank all my committee members (Dr. Ronald Chandler, Dr. Margaret Petroff, and Dr. Asgerally Fazleabas) for taking an interest in my research and scientific development. I appreciate all the time they have invested in also serving as a mentor to me and for providing many resources that I needed to perform my experiments and carry out data analysis.

I would like to thank the many collaborators whom I had the opportunities to work with, especially Dr. John Kingdom and Dr. Elizabeth Enninga. I am especially grateful for team at Spectrum Health and all their work in collecting/processing fresh placentas for our culture. As well, I am thankful for all the women who donated their placentas for research purposes. These studies would have not been possible without their donations.

Lastly, I would like to thank my family for their support in my interests since the beginning of my scientific career. My dad especially has always told me to “bet on myself” and without those words of encouragement, I would have never pursued this path towards earning a PhD. I want to thank my mom, for always listening to me share about my day and for offering advice. I want to thank my husband, Mike, for all his support and for being my inspiration to finish this work and continue a career as a research scientist.

TABLE OF CONTENTS

LIST OF TABLES

LIST OF FIGURES

KEY TO ABBREVIATIONS

GDM	Gestational diabetes mellitus
PE	Preeclampsia
IUGR	Intrauterine growth restriction
DC	Dendritic cell
VT	Villous trophoblast
EVT	Extra villous trophoblast
PPARγ	Peroxisome proliferator activated receptor gamma
GCM1	Glial cell missing 1
iEVT	Interstitial EVT
eEVT	Endovascular EVT
sPE	Severe PE
VEGF / VEGF-A	Vascular endothelial growth factor
PlGF	Placental growth factor
NO	Nitric oxide
sFLT1	Soluble fms-like tyrosine kinase 1
FLT1 / VEGFR1	Vascular endothelial growth factor receptor 1
VEGFR2	Vascular endothelial growth factor receptor 2
sEng	Soluble Endoglin
TGFβ	Transforming growth factor β
ECs	Endothelial cells
HO1	Heme oxygenase 1

ROS	Reactive oxygen species
NFκB	Nuclear factor κ B
TNFα	Tumor necrosis factor-α
IL-1	Interleukin 1
PPRE	PPARγ response element
RXRα	retinoid X receptor α
STB	Syncytiotrophoblast
IL-6	Interleukin 6
AF-1	Activating function-1
AF-2	Activating function-2
GLUT4	Glucose transporter 4
FABPs	Fatty acid binding proteins
EGF	Epidermal growth factor
PDGF	Platelet derived growth factor
NCoR	Nuclear receptor corepressor
AP-1	Activating protein 1
TZDs	Thiazolidinediones
TS cell	Trophoblast stem cells
hCG	Human chorionic gonadotropin
RUPP	Reduced uterine perfusion pressure
VSMCs	Vascular smooth muscle cells
eNOS	Endothelial nitric oxidate synthase
sGC	soluble guanylyl cyclase

ET-1	Endothelin-1
Ang-2	Angiopoietin-2
Ang-1	Angiopoietin-1
FGF-2	Fibroblast growth factor-2
HB-EGF	Heparin-binding epidermal growth factor
FST	Follistatin
CO	Carbon monoxide
BV	Biliverdin
BR	Bilirubin
Fe^{2+}	Free iron
HIF	Hypoxia inducible factor
NRF2	Nuclear factor E2-related factor 2
TLR4	Toll-like receptor 4
IL-10	Interleukin-10
SDF-1	Stromal cell-derived factor 1
MCP1	Monocyte chemotactic protein 1
IL-8	Interleukin-8
Tregs	Regulatory T cells
PTC	Preterm control
NT	No treatment
DMSO	Dimethyl sulfoxide
Rosi	Rosiglitazone
DMEM/F-12	Dulbecco's modified Eagle's medium/Ham's F-12 nutrient mixture

FBS	Fetal bovine serum
mRNA	Messenger RNA
ELISA	Enzyme linked immunosorbent assay
T007	T0070907
IP	Immunoprecipitation
CUT&RUN	Cleavage under targets and release using nuclease
ConA	Concalvalin A
pAG-MNase	Protein A and Protein G Micrococcal nuclease
LASAGNA	Length-Aware Site Alignment Guided by Nucleotide Association
H/R or HR	Hypoxia re-oxygenation
FABP4	Fatty acid binding protein 4
PPARγ SC	Santa Cruz PPARγ antibody
PPARγ TH	ThermoFisher PPARγ antibody
PPARγ CST	Cell Signaling Technology PPARγ antibody
HUVECs	Human umbilical vein endothelial cells

1. INTRODUCTION

1.1. An introduction to maternal adaptations in pregnancy

Since the middle of the 20th century, there has been significant advancements in women's health and obstetric care. Yet, the prevalence of pregnancy complications has remained steady over the past thirty to forty years and knowledge of the mechanisms required for the new formation of life remains to be discovered. Part of this is attributed to the difficulty of studying fetal and placental development in ongoing human pregnancies. These challenges fail to allow early identification and development of interventions for women experiencing pregnancy complications. With the recent development of novel model systems and technologies, current research beings to grasp the molecular underpinnings of establishing and maintaining a healthy pregnancy and the perturbations that lead to disease.

Pregnancy is an overall test of maternal health and fitness. There are significant adaptions that must occur in the mother to support a growing and developing fetus. Maternal health prior to conception has an equally significant role in determining the mother's ability to carry a child, as poor health in pre-conception increases the risk for developing adverse pregnancy complications that pose immediate and life-long problems for both the mother and fetus [1]. For example, pre-conception obesity is a high-risk factor for many pregnancy complications including gestational diabetes mellitus (GDM), preeclampsia (PE), fetal macrosomia and others, which can also lead to transgenerational effects on the fetus in the long term [1]. Moreover, obesity is one example that can lead to chronic inflammation in the mother which may be amplified during pregnancy and lead to lasting effects on the mother's health. High systemic

inflammation that compromises the maternal adaptions to pregnancy can further enhance systemic damage to the endothelial cells lining the vasculature, leading to an increase in blood pressure and impairment of nutrient transfer to surrounding organs and tissues. While these effects are largely problematic, more than 50% of all pregnancies in the United States involve overweight or obese women, therefore it is essential to further investigate molecular processes contributing to these poor pregnancy outcomes and identify means of intervention [1].

Part of the maternal adaptions involve metabolically adjusting to the needs of the fetus. In the first half of pregnancy, the maternal metabolism favors an anabolic state to build up a storage of fats [1]. At the start of the second half of pregnancy, the mother undergoes a metabolic switch to a catabolic state to promote lipolysis which provides an increase of nutrients needed to support the growing and developing fetus. Disruptions in maternal metabolism can lead to GDM or PE, and a lack of nutrient transfer to the fetus can result in intrauterine growth restriction (IUGR).

Besides metabolic adaptations, the mother also will adapt their immune system to establish tolerance for the allogenic fetus [2]. The placenta and fetus have been described similar to that of organ transplants, where the recipient host (mother) must dampen or alter their immune-cell environment in the uterus to allow the implantation of the embryo and transformation of the uterus. This process is regulated through the reduction of pro-inflammatory immune cells such T effector cells, inhibition of dendritic cell (DC) activation, and a higher presence of anti-inflammatory T regulatory cells and M2 macrophages [2]. The first trimester is referred to as a pro-inflammatory state, which switches to a greater anti-inflammatory state during fetal development and growth in the second trimester, and

a final switch to a pro-inflammatory state at the end of gestation which helps to initiate the signaling cascades for parturition [3-5]. Disruption of the immunologic harmony in the maternal-placental environment can be a major cause of infertility, spontaneous abortion, miscarriage, and other pregnancy complications. As well, the maternal-placental immune environment should be positioned to manage pathological inflammation such as from infections [4, 5]. When the immunologic balance is tipped towards excessive pro-inflammatory conditions, it leaves the placenta and fetus susceptible to rejection and results in tissue damage which has a multitude of negative effects throughout gestation and lifelong in the offspring.

These pathways systemically must be altered to protect both the mother and fetus from harm. Without a doubt, a successful pregnancy relies on sufficient communication and harmony between the mother and placenta; the mother being able to adapt to support all fetal needs without compromising the mother's health or putting the fetus and placenta in an unfavorable environment. Many of these pathways beyond metabolic and immunological that must be altered, are in-part directed by the human placenta. Deficiencies in placenta development significantly contributes to pregnancy complications, therefore a clear understanding of placental development and function in healthy pregnancies and disease are required to unveil the pathophysiological mechanisms that drive diseases in pregnancy.

1.2. Human placental development and function

An intricate network of tissues and blood vessels give rise to the placenta as the baby's first organ. The placenta serves to support fetal growth and development throughout pregnancy and its absence in proper formation and function can significantly impair the development of new life [1, 6, 7]. The placenta conducts a range of functions

such as temperature regulation, protection of the maternal micro-environment from infection, establishment of maternal immunologic tolerance of the fetus, and it provides the exchange of gases, nutrients, and waste from fetal and maternal blood [7, 8].

Placentation begins with differentiation and proliferation of the extra embryonic layer of the blastocyst, known as the trophectoderm. This trophectoderm layer differentiates into trophoblast cells that form into a branching network of placental villi composing the functional units of the placenta [9]. The cytotrophoblasts are the progenitor cells of the placenta which proliferate and differentiate into two trophoblast lineages to form the villous trophoblast (VT) and the extra villous trophoblast (EVT) (Figure 1.1) [7, 9-11].

VTs are present along the outer layer of the placental villi (Figure 1.1). Throughout pregnancy, VTs fuse together forming a multi-nucleated syncytiotrophoblast layer covering the entire outer surface of the placenta, known as the syncytium (Figure 1.1). This layer is also referred to as the maternal-fetal interface due to its contact with maternal blood to conduct an exchange of gas, nutrients and waste that can be transferred between the maternal blood and fetal blood vessels that are centered in the heart of the placental villi [8]. Simultaneously, the placental villi act as a protective barrier for the fetus and prevent maternal blood from reaching the developing fetal tissues and as well preventing mixing of maternal and fetal blood.

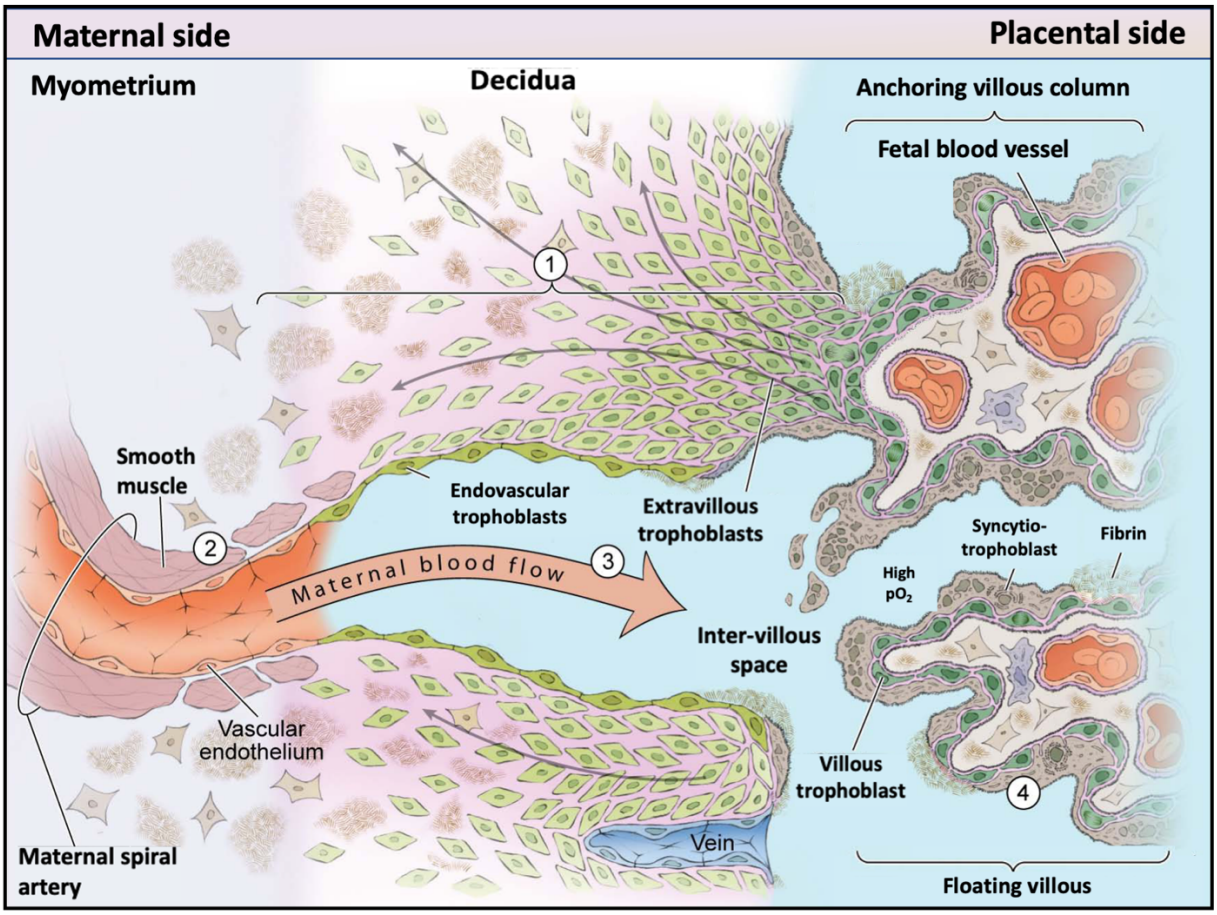

Figure 1.1: Maternal-fetal interface in healthy pregnancies. A healthy pregnancy relies on sufficient invasion of extravillous trophoblasts from the tips of the anchoring villi into the maternal decidua (1). The endovascular trophoblasts work to expand the maternal spiral arteries (2) for an increased and steady blood flow into the intervillous space (3). The villous trophoblast line the placental villi and undergo asymmetric differentiation to form the syncytium (4) which contacts the maternal blood and undergoes an exchange of gas, nutrients, and waste between mother and fetus. Image adapted with permission from Kingdom and Drewlo, Blood 118(18), 4780-4788, 2011.

Several proteins are involved in the molecular regulation of trophoblast differentiation. Notably, the transcription factor and steroid nuclear receptor, peroxisome proliferator activated receptor gamma (PPARγ) has a significant role in regulating both EVT and VT differentiation [12-14]. PPARγ is well known to activate another transcription factor, glial cell missing 1 (GCM1) which enhances expression of syncytin-1 which promotes VT fusion to form the syncytiotrophoblast [15-17]. The roles of PPARγ in regulating EVT

differentiation are less clear. Some studies show that activating PPARγ in first trimester explants inhibits EVT outgrowth [18] however histological staining of the human placenta show that PPARγ is expressed throughout the EVT differentiation pathway [12]. Inflammatory targets are known to increase EVT differentiation while PPARγ is known to inhibit inflammatory pathways [19] thus more research is needed to fully understand the role for PPARγ throughout EVT differentiation.

By the end of the first trimester, the placental villi are completely submerged in maternal blood and thus exposed to 8% physiologic oxygen tension (Figure 1.1) [10]. Many of the tips of the placental villi will directly contact the maternal endometrium, allowing for the placenta to anchor itself into the uterus [7]. These anchoring villi are composed of cytotrophoblasts which undergo multiple differentiation stages forming into proliferative column cytotrophoblasts, distal column cytotrophoblasts and become invasive extravillous trophoblasts (EVTs) as the cells detach from the column and invade into the endometrium (Figure 1.1) [7].

The EVTs can further differentiate into various subtypes to carry out specialized functions. Interstitial EVTs (iEVTs) invade through the first third of the myometrium and form into multinucleated placental bed giant cells. The iEVTs interact with macrophages, natural killer cells, and decidual stromal cells to assist in maternal-fetal immune tolerance and to further regulate EVT function [7]. In the early first trimester, the EVTs will “plug” the material spiral arteries which completely prevents the exposure of maternal blood to the developing placenta. Consequently, the placenta develops in a low oxygen (hypoxic) environment at approximately 1-2% physiologic oxygen tension [10]. Without the maternal blood supply, the placenta relies on the uterine glands to supply nutrients to the placenta

via histotrophic nutrition. These nutrients are established from iEVT invasion into the uterine glands which then adopt an endoglandular EVT phenotype by disintegrating the uterine glands to open the gland lumen and increase the glandular secretions [7, 19].

The EVT plugs slowly dissolve between 8-12 weeks of pregnancy which allows maternal blood to slowly fill into the implantation site and gradually increases the oxygen tension [10]. Prior to formation of the fully oxygenated placental environment, the iEVTs are recruited to spiral arteries by the uterine natural kills cells and differentiate into endovascular EVTs (eEVTs) [19]. The eEVTs adopt an endothelial-like phenotype as they invade the maternal spiral arteries and cause apoptosis of the endothelial lining. This permits the eEVTs to replace the monolayer of endothelial cells while simultaneously expanding and transforming the maternal spiral arteries into low pressure, high-capacity vessels. This expansion of the material spiral arteries is a key step in establishing sufficient blood flow to the fetus that is maintained throughout pregnancy (Figure 1.1) [20, 21].

Among the many important functions of the human placenta, its role as a secretory organ has a substantial impact in systemically regulating maternal physiologic response and adaptations to pregnancy [1]. The placenta functions as an endocrine organ to secrete hormones and peptides that regulate maternal metabolism. Beyond the production and secretion of hormones and peptides, the placenta naturally secretes angiogenic proteins that are essential for healthy placental and endothelial function [22]. Many of the molecules that regulate trophoblast differentiation and function also work to regulate how proteins are secreted from the placenta into maternal circulation which can systemically impact maternal response to pregnancy. Maintaining a proper balance of

these secreted protein for placental development and function is at the center of providing a healthy pregnancy for both the mother and baby.

1.3. Preeclampsia

Deficiencies in placental development and function are a major contribution to several adverse pregnancy complications, such as preeclampsia (PE) [23]. PE is a hypertensive disorder of pregnancy originated from the placenta, that affects up to 7% of all pregnancies and is the main cause of maternal-fetal morbidity and mortality worldwide [24]. PE is characterized by the new onset of maternal hypertension occurring after 20 weeks of gestation, involving systemic endothelial dysfunction in the presence or absence of proteinuria [25]. Severe forms of PE often involve higher maternal hypertension and evidence of organ damage to the kidneys and liver. If untreated, PE can progress into eclampsia and impair the hepatic and coagulation systems, causing seizures, brain damage, or maternal death.

Knowledge of PE was reported in ancient civilizations of China, Egypt, and India mostly based on the signs of eclampsia [26]. It was not until the 19th century when doctors made the association between proteinuria, maternal hypertension, and eclampsia, and realized that these pregnancy complications subsided after delivery. To date, there is still no cure for PE and while many clinical trials for treatment of PE are ongoing, there are no approved therapies and the primary method for preventing severe disease remains to be placental and fetal delivery [24]. In severe cases, PE requires early delivery that can result in preterm birth which poses immediate and long-term health complications for the fetus and mother [14,16].

It is not fully known what causes the manifestation of PE, and this is partly attributed to the heterogeneity of the condition. Some women may develop PE as early

as 20 weeks of gestation and classified as early-onset pre-term PE (if diagnosed before 37 weeks), while other women may not express clinical symptoms of PE until the end of gestation around 38-39 weeks and are classified as late-onset PE. To add a greater depth of variability, some women will go on to progress into PE with severe features (sPE) in either early pregnancy (early-onset sPE) or in late pregnancy (late-onset sPE).

The idea of different subtypes occurring within PE has been postulated recently [27] and can be partially explained by maternal health and fitness pre-conception. Women who have pre-existing conditions prior to pregnancy, such as hypertension, diabetes, and obesity have a significantly higher risk for developing PE compared to the general population [6]. Evidence of high blood pressure in early pregnancy is also an indicator for increased risk of PE. These conditions are associated with maternal predisposition to cardiovascular disease and chronic inflammation that may already pose vascular and metabolic dysfunction which is then heightened during pregnancy and results in PE [6].

Besides metabolic and cardiovascular comorbidities, PE has a higher prevalence in primiparity women, during subsequent pregnancies with new paternity, and in women of an advanced maternal age [6]. Genetically, there has yet to be one specific gene mutation responsible for the cause of PE. There is more likely to be non-mendelian transmission of several variants that could all collectively contribute to PE. Any variation in genes involved in the dynamic processes of pregnancy and maternal response to pregnancy could have a contributing role in PE predisposition. However, there is familial aspect that leads to a higher risk of developing PE, based on the observation that PE occurs more frequently in women of the same family, with a 20-40% increased risk of developing PE when born to a mother who had PE during their pregnancy [6].

Although the etiology of PE remains unclear, significant molecular and histopathological evidence suggests that PE manifests from abnormal placental development and function. Especially in sPE and pre-term PE, studies have found a very high association between maternal vascular malperfusion to the placenta that is likely the cause for abnormal VT differentiation [6, 19, 28, 29]. Studies have associated these placentas with high expression of hypoxic genes when collected at term, suggesting the placentas could be developing in a pro-longed hypoxic environment [24]. A major hallmark of the dysfunctional placenta is shallow extra-villous trophoblast (EVT) invasion that prevents the spiral artery remodeling and expansion required for an increased and steady blood flow to the placenta throughout pregnancy (Figure 1.2) [30]. This intermittent perfusion of maternal blood to the implantation site causes ischemia of the developing placental villi [30-32], enhancing oxidative stress in the placenta, and further contributing to defective VT differentiation and function [33].

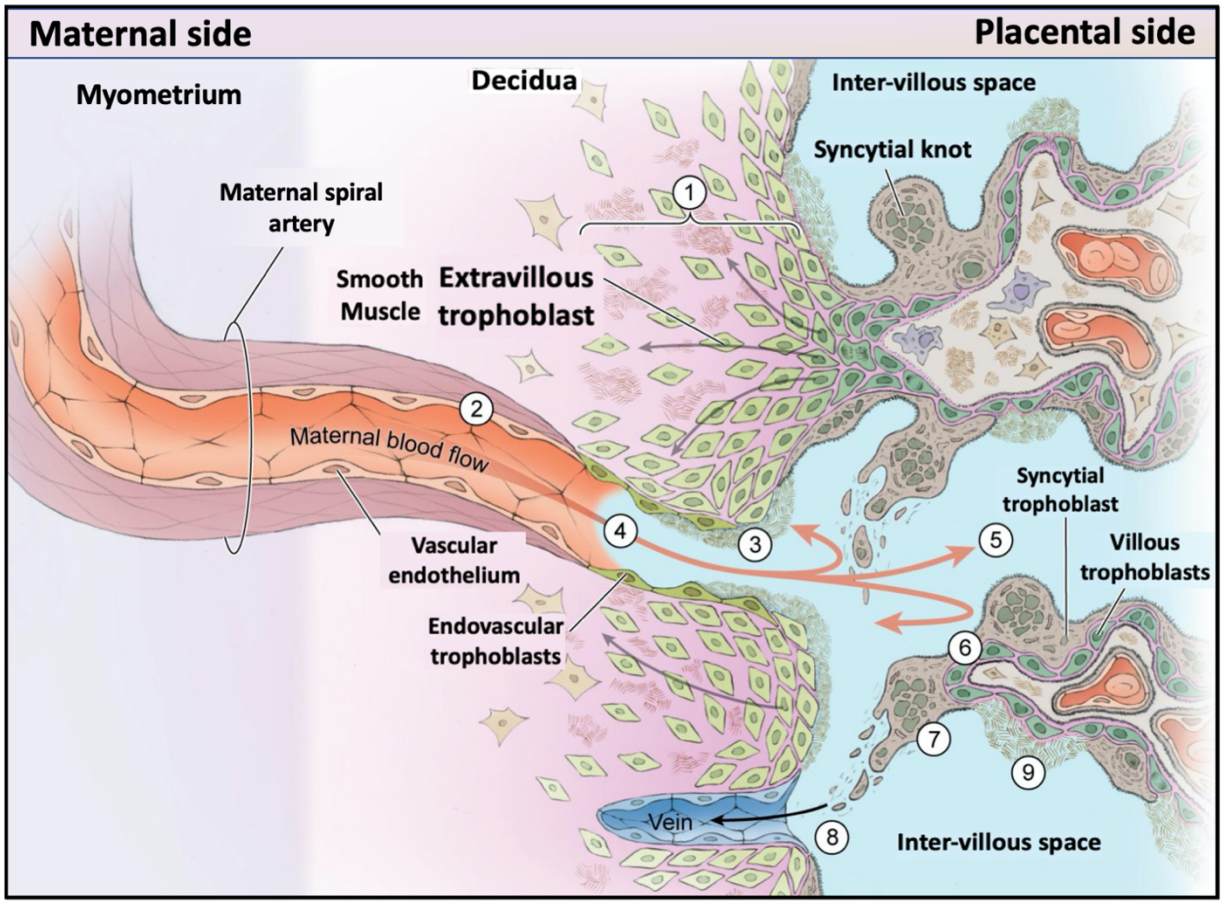

Figure 1.2: Maternal-fetal interface in preeclamptic pregnancies. Preeclampsia (PE) often involves shallow extra villous trophoblast invasion (1) which reduces maternal spiral artery remodeling (2) causing damage to the villous trophoblast (3) due to intermittent perfusion (4). The lack of blood flow to the intervillous space (5) causes impaired villous trophoblast differentiation (6) and accumulation of syncytial knots (7) that are released into maternal circulation (8) and further evidence of increased fibrin deposition at the site of syncytial shedding. Image adapted with permission from Kingdom and Drewlo, Blood 118(18), 4780-4788, 2011.

The dysfunctional VT are hypothesized to be at least partially responsible for the imbalance of pro- and anti-angiogenic proteins secreted by the placenta into maternal-fetal circulation. The ischemic conditions leading to trophoblast dysfunction which can be observed histologically by the presence of syncytial knots on the placental villi (Figure 1.3). The PE placenta exhibits increased shedding of the syncytiotrophoblast basement membrane into maternal circulation due to accelerated apoptosis, and this can promote

inflammation to the surrounding endothelium [34]. Further molecular characterization of the PE placenta shows abnormal expression and activity of transcription factors that regulate trophoblast proliferation and differentiation, such as PPARγ and GCM1 [16, 23, 35, 36].

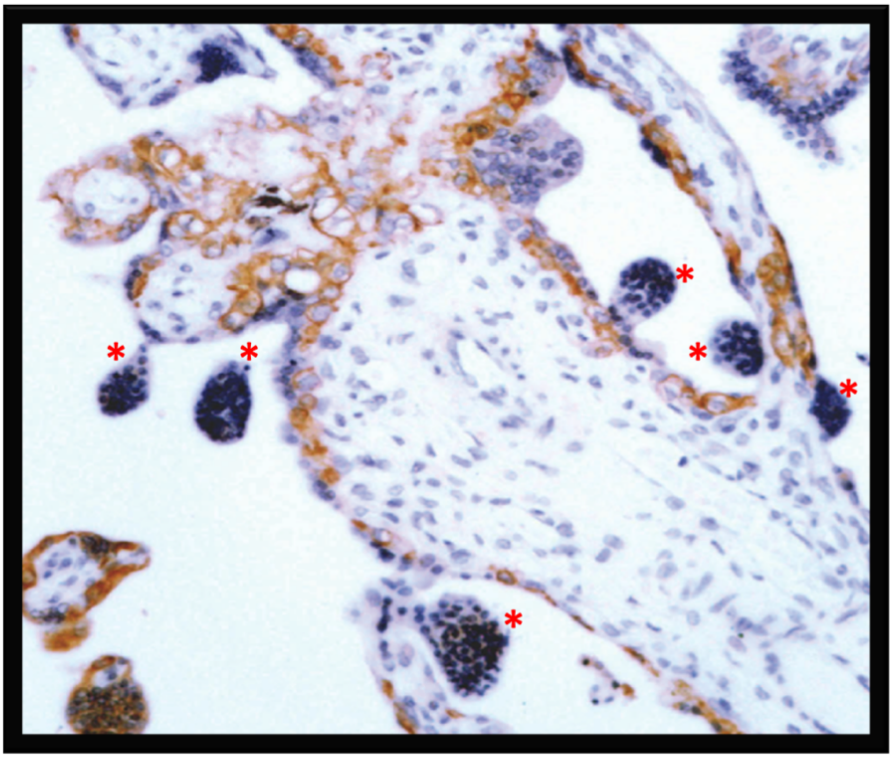

Figure 1.3: Syncytial knots present in the preeclamptic placenta. Aberrant villous trophoblast differentiation and enhanced apoptosis leads to the formation of syncytial knots, indicated by the red asterisks. The syncytial knots undergo excessive shedding and exacerbates inflammation in the maternal endothelium, contributing to endothelial dysfunction. *Image was adapted with permission from the owner, Dr. Sascha Drewlo.*

PE is described as a two-stage disease, which begins with atypical trophoblast differentiation and placental function, that stimulates the aberrant release of angiogenic proteins to cause systemic maternal endothelial dysfunction leading to end organ damage and hypertension in the mother [37]. Normal endothelial function is regulated largely by the vascular endothelial growth factor (VEGF) and placental growth factor (PIGF) and the

production of nitric oxide (NO) molecules that simulate angiogenic pathways and lead to endothelial vasodilation. The high abundance of soluble FLT1 (sFLT1) acts as a decoy to prevent VEGF and PIGF from binding to their cell surface receptors VEGF receptor 1 (VEGFR1 or FLT1) and VEGF receptor 2 (VEGFR2) which prevents the activation of angiogenic signaling cascades [20, 38-40]. Secondly, the secretion of soluble Endoglin (sEng) binds to transforming growth factor β (TGFβ), which prevents TGFβ from binding to the endothelial Endoglin cell surface receptor, and ultimately prevents the induction of NO, which is necessary for the endothelial cells (ECs) to undergo vasodilation. As well, there are reduced levels of the cytoprotective, heme oxygenase 1 (HO1) molecule, which adds to the dysfunctional endothelial and trophoblast apoptosis in PE (Figure 1.4).

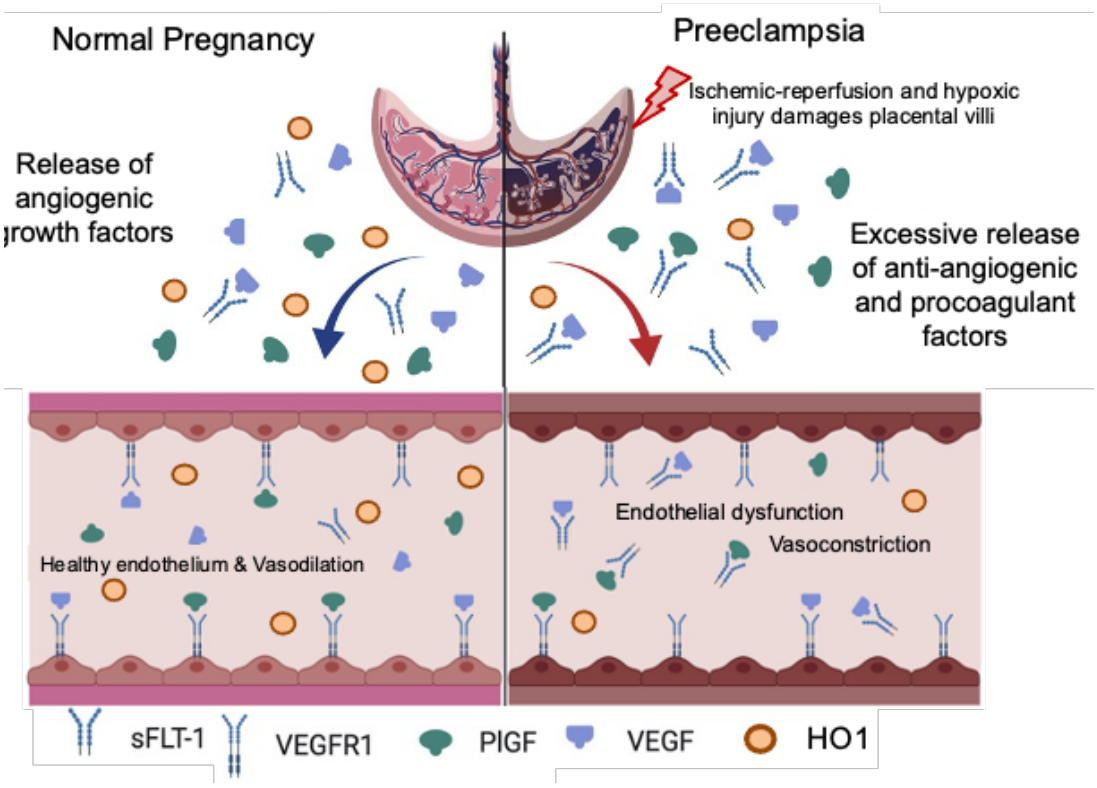

Figure 1.4: Preeclampsia is a two-stage disease. Preeclampsia (PE) is burdened by placental ischemia that causes damage to the placenta villi, resulting in an imbalance of secreted angiogenic and cytoprotective proteins such as soluble FLT1 (sFLT1) which bind to placental growth factor (PIGF) and vascular endothelial growth factor (VEGF) in

Figure 1.4 (cont'd)
circulation preventing their interactions of cell surface receptors such as fms-like tyrosine kinase 1 (FLT1) which poses endothelial dysfunction. Moreover, the reduction in levels of cytoprotective molecules, like heme oxygenase 1 (HO1) exacerbate trophoblast apoptosis and endothelial dysfunction in PE. *Image adapted with permission from Rana et al., Am J Obstet Gynecol. 226(2S), S1019-S1034, 2020.*

These perturbed pathways prevent the vasodilation needed to maintain a steady blood flow into the placenta and as well to other organ systems. Overtime the vasoconstriction can cause hypertension in the mother. Moreover, the inhibited neovascular and angiogenesis pathways are likely responsible for the reduced placental vasculature observed in PE placentas. Endothelial dysfunction can initiate the later development of vascular diseases and is a prominent feature in women with PE [41]. Some women may have a predisposition to developing PE due to primary endothelial dysfunction prior to conception. A secondary endothelial injury in pregnancy due to placental malperfusion could trigger a series of events resulting in endothelial dysfunction and the manifestation of PE [41].

In addition to the dysregulation of angiogenic proteins, there could be multiple sources of exacerbated inflammation that lead to endothelial damage in PE [24]. Reactive oxygen species (ROS) are generated either in the endothelium directly or from the ischemic placenta to act on the ECs to activate NFκB producing high levels of pro-inflammatory cytokines such as tumor necrosis factor-α (TNFα) and interleukin 1 (IL-1) that further promote pro-inflammatory cascades [26, 42]. An activated maternal immune system may also serve as a source of pro-inflammatory cytokines which interfere with EC function [26, 42]. HO1 is another molecule that is released by the placenta and acts to regulate expression of angiogenic proteins, dampen maternal immune response to pregnancy and sequester ROS to prevent placental and endothelial dysfunction. When

HO1 is perturbed in PE, it can further contribute to these disease phenotypes by increasing oxidative stress and causing disruption to the maternal immunological balance and acceptance to the fetus.

An abnormal endothelium poses significant risks to the mother and fetus' health due to the increased endothelial permeability, leukocyte adhesion and generation of cytokines which serve as the foundation for vascular disease that can poorly impact maternal health and well beyond pregnancy [42]. Nearly half of all women with PE have high blood pressure through 12 weeks post-partum [43, 44] and are at risk of developing chronic hypertension within a few years after giving birth [6]. PE poses a greater risk for cardiovascular disease than smoking [6] and women in the United States who have sPE have a 9.4 fold increased risk for cardiovascular-related deaths when the newborn is born within 34 weeks of gestation [45]. Thus, it would be beneficial to identify the pathways that regulate the immunologic and angiogenic harmony in placental and endothelial function. Restoring these regulatory pathways could provide therapeutic opportunity to improve placental and endothelial function and dampen maternal sequalae.

1.4. Peroxisome Proliferator Activated Receptor-γ: A key molecule in the development and function of the human placenta

Among the significant number of molecules that regulate placental development and function, the steroid nuclear receptor and transcription factor, peroxisome proliferator activated-receptor (PPAR)-γ, is of major focus in this study. PPARγ has critical roles in regulating several aspects of placental development and function that are perturbed in PE, which makes PPARγ an attractive target to prevent severe disease. PPARγ is part of the PPAR family of proteins that regulate cell differentiation, metabolism, inflammation, and immune tolerance pathways (Figure1.5) [46-48].

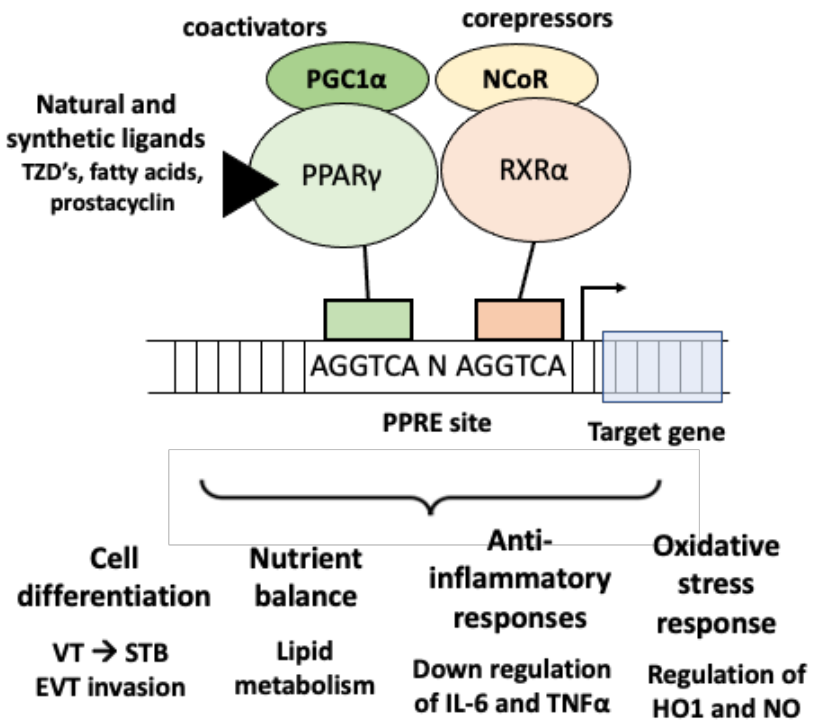

Figure 1.5: Peroxisome proliferator activated receptor γ activation and effects on downstream pathways in the human placenta. Peroxisome proliferator activated receptor γ (PPARγ) undergoes ligand binding to initiate translocation to the nucleus where it forms a heterodimer with its co factor, retinoid X receptor α (RXRα), and binds to the DNA at specific PPARγ response elements (PPREs). Upon activation, PPARγ initiates genes effects cell differentiation, nutrient balance, anti-inflammatory, and oxidative stress responses. In the placenta, PPARγ regulates villous trophoblast (VT) differentiation to form syncytiotrophoblasts (STB) and regulates extra villous trophoblast invasion. PPARγ modulates lipid metabolisms and down regulates interleukin 6 (IL-6) and tumor necrosis factor α (TNFα) as well as increases expression of heme oxygenase 1 (HO1) and nitric oxide (NO) from the placenta.

The PPAR family of proteins contains PPARα, PPARβ, and PPARγ which have unique functions and are generally expressed in different tissue types. PPARα is active is highly metabolic tissue to influences genes in fatty acid metabolism and acts to decrease lipid levels [49]. PPARβ is ubiquitously expressed and is most known for its role in regulating oxidative phosphorylation in skeletal and cardiac muscles but it also aids in the regulation of blood glucose levels [49]. PPARγ has many functions related to adipogenesis, energy balance, maintenance of vascular integrity, lipid biosynthesis and

inflammation, and it is expressed in white and brown adipose tissue, the large intestine, spleen and also the placenta [49].

PPARγ is known as a steroid nuclear receptor due to its actions being regulated through ligand binding [47]. PPARγ has six protein domains. The N-terminus contains domains A and B where the activating function-1 (AF-1) domain is located. AF-1 allows for cis-transcriptional activity without the need for ligand binding [46]. The DNA binding domain is located in Domain C and consists of two zinc-fingers that bind at specific response elements at the conserved DNA sequence, AGGTCANAGGTCA, which are often found in gene promoter regions [48]. This domain also allows for protein-protein interactions. Domain D serves as a hinge to allow flexibility for protein movement and is followed by Domains E and F [47]. These C-terminal domains contain the ligand binding pocket, which upon ligand binding, allows for protein dimerization and contains the activating function-2 (AF-2) domain that permits PPARγ-induced gene expression [46, 47]. The confirmation changes that occur from ligand binding in the AF-2 domain also allow interactions with coactivator proteins, such as PPARγ co-activating protein 1-α (PGC1α), that assist in permissive transcriptional activity [46]. Once in the nucleus, PPARγ forms a heterodimer with its cofactor, Retinoid X Receptor-α (RXRα) [47] then proceeds to bind DNA at PPRE sites.

Natural ligands for PPARγ are derived from metabolic processes, such as poly unsaturated fatty acids, prostaglandins, and others, which activate PPARγ allowing for increased glucose uptake and insulin sensitivity such as through increasing expression of glucose transporter 4 (GLUT4) and fatty acid binding proteins (FABPs) [14, 48]. For these reasons, PPARγ is often described as a ‘metabolic sensor’ for the cell. In

adipocytes, PPARγ can induce adipogenesis and production of hormones such as leptin and adiponectin, which act to induce insulin sensitivity [48]. PPARγ can increase lipid accumulation in adipocytes which helps to reduce excessive lipid production and lower serum lipid levels; part of these actions is the reason why PPARγ is a common target for dyslipidemia [47]. PPARγ is also an attractive target for treating a variety of metabolically related diseases such as obesity, type 2 diabetes, and nonalcoholic fatty liver disease [47, 48].

PPARγ acts very dynamically to both activate (cis-activation) and repress (trans-repression) a variety of genes, and these actions are largely mediated through post translational modifications. Phosphorylation is a major factor in the negative regulation of PPARγ activity. PPARγ phosphorylation can be influenced by the MAPK and ERK pathways which are activated by various factors such as epidermal growth factor (EGF), prostaglandin F2α, platelet derived growth factor (PDGF), TGFβ, and even cellular stress [50-53]. These pathways can lead to phosphorylation at the serine 112 (S112) residue located within the AF-1 domain [52, 53]. S112 phosphorylation decreases PPARγ transcriptional activity by causing dissociation with coactivators and initiation of corepressor binding [47]. Phosphorylation at the serine 273 residue (S273) is also shown to inhibit PPARγ activity [54-56]. Studies in obese mice show enhanced phosphorylation at S273 leading to inhibited PPARγ regulation of insulin-sensitizing hormones and increased production of obesity related genes [54]. Phosphorylation of S273 is also shown to be enhanced by proinflammatory cytokines, which is thought to be one of the mechanisms behind obesity-driven inhibition of PPARγ activity [55]. Fortunately, these actions can be reversed by blocking phosphorylation at S273 in obese mice [56] as well,

synthetic PPARγ ligands are shown to block S273 phosphorylation to aid in inducing PPARγ activity [46]. Dephosphorylation of this residue results in increased expression of insulin sensitizing genes [47].

SUMOylation is also used to control PPARγ expression. SUMOylation can occur at the lysine 107 and 395 (K107 and K395) residues within the PPARγ protein and are associated with the trans-repression activity of PPARγ [46]. This repressive activity is induced by the binding to its corepressor proteins, nuclear receptor corepressor (NCoR) and histone deacetylase, which permits PPARγ binding with the nuclear factor κ B (NFκB) and activating protein 1 (AP-1) transcription factors to inhibit their activity [46]. NFκB and AP-1 regulate genes in inflammatory pathways and PPARγ repression of their activity can induce anti-inflammatory effects [57].

Acetylation can occur at lysine residues K98, K107, K218, K268 and K293 and is another method of inhibiting PPARγ transcriptional activity [47]. Acetylation at these locations acts similarly to the SUMOylation by recruitment of NCoR to inhibit PPARγ activity [46]. Specifically, acetylation of K268 and K293 can occur in response to obesity, but the de-acetylation of these residues can result in increased insulin sensitivity [54, 58-60]. One type of PPARγ agonist, Rosiglitazone, partially acts to induce PPARγ activity by preventing acetylation at K268 and K293 [47].

In 1995, PPARγ was identified as one of the major targets of the Thiazolidinediones (TZD) class of drugs which were previously used to treat metabolic diseases such as type 2 diabetes and dyslipidemia [61]. TZD drugs increase PPARγ activity to reduce fatty acid levels, increase lipid storage and decrease lipid toxicity in skeletal muscle and the liver [48]. Rosiglitazone belongs to the TZD drug class and was

a primary therapeutic treatment for diabetes until the mid 2000s. Rosiglitazone was taken off the market in Europe and its use in the United States was restricted due to major off target effects [46]. Some individuals undergoing this therapy experienced excessive weight gain, and it was thought this occurred from PPARγ activity in the brain which increases hunger response [46, 62, 63]. This hypothesis was introduced from mouse studies where brain-selective knock-out of PPARγ prevented weight gain in mice treated with Rosiglitazone and when fed a high-fat diet [63]. Patients given Rosiglitazone for the treatment of diabetes also experienced fluid retention due to increased sodium and water retention in the kidneys [64]. It was found that Rosiglitazone may lead to bone loss through inhibition of bone formation and enhancing mechanisms of bone resorption [65]. Lastly, Rosiglitazone poses a major risk of congestive heart failure and myocardial infarction [65]. These off-target effects highlight the lack of knowledge for the molecular activities of Rosiglitazone *in vivo* and point out the areas where more research is needed to fully understand the physiological role of Rosiglitazone. Despite all these negative effects, there are a considerable number of benefits from PPARγ activation, such as improved lipid profiles and inhibiting vascular inflammation. Therefore, it would be advantageous to better understand the mechanisms underlying Rosiglitazone-mediated PPARγ activation throughout several tissues in the body, besides skeletal muscles and adipose tissues which are some of the most studied tissue types. The use of Rosiglitazone may be beneficial in research settings to understand molecular actions of PPARγ activity. Beyond this, developing PPARγ-activating drugs that are tissue specific might overcome many of these off-target effects.

Murine studies with complete PPARγ-knock out provide significant detail on the essential roles of PPARγ, especially in the placenta. Murine embryos lacking PPARγ die *in utero* from placental and cardiovascular abnormalities [12] thus, PPARγ is essential for placental development. PPARγ has critical functions in the placenta through regulation of trophoblast differentiation, oxidative stress response, nutrient balance, and anti-inflammatory response pathways [66-68]. Parast et al. show PPARγ is upregulated in murine trophoblast stem (TS) cells as they differentiate [69]. PPARγ-null mouse TS cells prematurely differentiate into an invasive trophoblast subtype while activation of PPARγ in wild-type mouse TS cells promotes differentiation toward the labyrinthine (villous) lineage [69]. In the murine and human placenta, PPARγ initiates VT differentiation and fusion through the transcription factor, glial cell missing 1 (GCM1) [16]. PPARγ also regulates secretion of placental proteins and hormones, such as human chorionic gonadotropin (hCG), in VTs and syncytiotrophoblast [68]. Expression of PPARγ and its co-activators normally increase in the human placenta as gestation advances and cause uterine relaxation to prevent onset of labor [68].

Significant evidence points towards the lack of placental activity of PPARγ serving as a large contribution to the development of PE [23]. Abnormal PPARγ activity in the placenta produces PE-like phenotypes in animal models as shown by McCarthy et al. [35] In this study, healthy pregnant rats were treated with PPARγ antagonists, and they developed hypertension, proteinuria, reduced pup weight, and endothelial dysfunction [35]. They also exhibit high secretion of anti-angiogenic and low secretion of pro-angiogenetic proteins – all key features of PE [35]. Interestingly, in a separate study, McCarthy et al. show that activation of PPARγ by Rosiglitazone in the hypoxia-induced

rat model of PE can improve placental function [70]. This PE-phenotype was achieved by performing surgical clamping of the uterine artery to simulate placental hypoxia (reduced uterine placental perfusion - RUPP model) [70]. These rats developed hypertension, decreased pro-angiogenic protein secretion, and endothelial dysfunction [70]. Rosiglitazone decreased blood pressure and significantly increased secretion of vasodilatory proteins to improve endothelial health [70].

Beyond these animal studies, it has been shown that women with PE have a decrease in the natural production of PPARγ ligands 10-15 weeks before onset of maternal symptoms in PE [68]. It still is not fully known what mechanisms are driving the altered PPARγ expression, although it could be partially due to aberrant metabolic mechanisms in pregnancy, since a high number of downstream metabolic proteins are responsible for the induction of PPARγ activity which are perturbed in PE. Some women may also have a higher risk for developing PE based on variants in the PPARγ protein. PE is highly associated with a proline to leucine substitution at residue 467 (P467L) [71] and a cystine to a threonine substitution at residue 1431 [72]. Both sets of alterations negatively impact PPARγ activity and pose a high risk of PE.

The evidence presented here highlights that 1. mechanisms governed by PPARγ such as metabolic and inflammatory pathways are perturbed in PE, 2. PPARγ is required for normal trophoblast differentiation and healthy placental development, 3. a lack of PPARγ activity in the placenta promotes PE phenotypes, and 4. increasing PPARγ activity in pathological conditions improves placental function and pregnancy outcome in the rodent models. While the translational use of Rosiglitazone in pregnancy is controversial, understanding mechanisms governed by PPARγ in the healthy and

preeclamptic placenta is fundamental for the future targeting of PPARγ to improve pregnancy outcome. Next generation of PPARγ-targeting drugs that have less off-target effects are warranted for development, such as drugs that directly target the placenta without crossing into fetal circulation could resolve the many complications that arise in women with PE.

1.5. Roles of secreted proteins in healthy pregnancy and preeclampsia

A healthy pregnancy relies on synergistic communication between mother and fetus which largely occurs through the secretion of placental proteins that can impact maternal metabolic adaptation, immune responses, and local and systemic endothelial function. The ischemic nature of the placenta in PE can alter the secretion of various hormones and peptides to negatively impact the mother and fetus, such as through the imbalance of pro- and anti-angiogenic proteins that impair endothelial function to cause end organ damage and hypertension in the mother.

The endothelium is composed of a mono-layer of endothelial cells (ECs) that are surrounded by vascular smooth muscle cells (VSMCs) and function to regulate hemodynamic blood flow through vascular tone and uptake of nutrients by surrounding organs and tissues [41]. ECs will undergo drastic changes for new blood vessel development in the placenta, known as neovascularization, and expand on existing vasculature, known as angiogenesis [73]. These processes occur during wound healing, ischemia, inflammation, tumor development, as well as during pregnancy, and are directly proportional to the metabolic needs of the surrounding tissues. Angiogenesis involves major changes in ECs and VSMCs initiated by several proteins secreted from neighboring cells that cause EC activation and proliferation. The ECs will secrete proteases that degrade the extracellular matrix to permit migration to an angiogenic stimuli, such as

vascular endothelial growth factor-A (VEGF-A), which is the leading molecule for initiation of angiogenesis [73]. Other chemotactic and mitogenic factors will act on the ECs to cause EC sprouting and tube formation [73]. Subsequently, the ECs will transform into a quiescent state in newly developed angiogenic/tube structures and will require reformation and stabilization through recruitment of pericytes, which are embedded in the basement membrane of the micro vessels [74].

In addition to angiogenesis, normal endothelial functions are largely regulated by the VEGF and placental growth factor (PIGF) molecules which interact with cell surface receptors, VEGF receptor 1 (VEGFR1 or FLT1) and VEGF receptor 2 (VEGFR2) [20, 38-40]. PIGF binds to both VEGF-receptors (VEGFR1 and VEGFR2) and its only known function is to compete with VEGF for binding to VEGFR1 to encourage VEGF-VEGFR2 interaction on ECs which elicits signaling cascades needed to maintain EC survival, proliferation, and migration [75]. PIGF is known to be downregulated in PE and many studies are providing more convincing evidence that a reduction of maternal plasma levels of PIGF can predict the risk of later developing PE especially in unsuspecting women [76-78].

VEGFR1, also known as FLT1, is expressed on the placenta, and is increased in tissues during vascular reoxygenation in response to hypoxic/ischemic insult [79]. FLT1 can undergo alternative splicing to generate different isoforms where some will contain only the extracellular ligand binding domain, known as soluble FLT1 (sFLT1). In early pregnancy, the first trimester placenta secretes significantly high levels of sFLT1, which normally would decrease throughout pregnancy [80]. However, sFLT1 levels are shown to remain consistently high in PE throughout pregnancy. In 2003, Maynard et al.

discovered that sFLT1 is a major target for endothelial dysfunction, hypertension, and proteinuria in women with PE which was supported by their studies of pregnant rats who were administered sFLT1 and developed PE-like symptoms [81]. sFLT1 is released from the placental cells into maternal-fetal circulation in excessive levels during ischemic injury to the placenta [82]. sFLT1 binds to PIGF and VEGF in circulation, preventing their interactions with cell surface receptors to cause impaired endothelial function and angiogenesis. sFLT1 has since been one of the most well-known anti-angiogenic molecules that contribute to the manifestation of PE.

Alterations in secretory proteins not only impair the process of angiogenesis, but they can also negatively impact aspects of endothelial function, such as vasodilation which is thought to be one of the most damaging mechanisms that lead to endothelial dysfunction in PE [34]. Vasodilation is regulated through many molecules, including transforming growth factor-β (TGFβ) which acts as a ligand for Endoglin, a cell surface receptor on ECs [83]. TGFβ initiates endothelial nitric oxidate synthase (eNOS) which works together with L-arginine and BF_4 to generate nitric oxide (NO) [42]. NO is one of the most important vasodilatory proteins that acts on both the endothelium and in the placenta. The production of NO is an important aspect of maintaining endothelial function by transferring across VSMC membranes to stimulate soluble guanylyl cyclase (sGC) which then decreases the intracellular calcium concentration, allowing for EC vasodilation [42]. NO also assists in preventing inflammation and oxidative stress in ECs as well as inhibiting platelet aggregation and VSMC migration [42]. Inhibition of eNOS, such as through eNOS uncoupling, poses major complications by reducing the bioavailability of NO and increasing ROS [26, 42].

While Endoglin remains an important cell surface receptor in this process, it can also undergo alternative splicing to generate alternate protein variants, one of them being soluble Endoglin (sEng) which contains the extra-cellular protein domain that is secreted from the cell and binds to TGFβ in circulation. In high levels, sEng can block these crucial vasodilation pathways, including inhibiting the production of NO, which is a common occurrence in PE and is a large contribution to the endothelial dysfunction [26, 42].

Endothelin-1 (ET-1) acts as a vasoconstrictor counterpart to NO and is constitutively expressed and secreted from ECs. ET-1 acts on both ECs and VSMCs to cause vasoconstriction through its receptor, ETA [84]. ET-1 expression and activity is increased in response to endothelial shear stress, cytokines, and free radicals in the endothelium [84]. ET-1 is known it be highly expressed in diseases involving endothelial dysfunction, such as cardiovascular disease, pulmonary hypertension, and PE [85]. Despite ET-1 having an anti-angiogenic role in many diseases, a murine model with heterozygous ET-1 gene-knockout surprisingly results in hypertension which suggests that drastic alterations of ET-1 expression may not promote an expected vasodilatory effect [86]. ET-1 can also bind to the ETB receptor which activates pathways to upregulate NO and prostacyclin that subsequently downregulates ET-1 expression.

Angiopoietin-2 (Ang-2) is an important angiogenic protein that belongs to the angiopoietin/Tie2 pathway and is necessary for endothelial cell survival, maturation and morphogenesis [87]. Ang-2 is most known for its anti-angiogenic roles through serving as an antagonist to Angiopoietin-1 (Ang-1) by competing for interaction with the EC surface receptor, Tie2 [87-89]. Ang-1 is very important for the reorganization of ECs, promoting structural integrity of the blood vessels and preventing EC leakage and migration of

leukocytes to surrounding tissues by inhibiting EC activation [87] whereas blocking these effects through Ang-2 can largely contribute to vascular disease. Ang-2 expression is tightly regulated and can be increased during inflammation and hypoxia [88]. The full spectrum of Ang-2 functions is still being elucidated, as Ang-2 can exert pro- and anti-angiogenic actions that are dependent on the context of the tissue types, interactions of other molecules and disease pathology [88]. In the presence of VEGF, Ang-2 can act in a pro-angiogenic manner by promoting neovascularization. Without VEGF, Ang-2 tends to serve more anti-angiogenic roles such as causing endothelial cell apoptosis and vessel regression [87]. Ang-2 has a central role in cardiovascular diseases and is used as a biomarker to assess deleterious vascular permeability [89-91].

In pregnancy, Ang-2 is mainly produced by the placenta and regulates EC survival, angiogenic sprouting and vascular regression [87, 88]. Some studies report that maternal plasma Ang-2 levels are increased in healthy pregnancies, as compared to non-pregnant and post-partum women [92]. However, there have been conflicting evidence reporting Ang-2 levels in PE. Some studies show that maternal blood plasma Ang-2 levels are decreased in PE [92] while others describe an increase of Ang-2 placental mRNA expression and higher maternal Ang-2 plasma levels in PE compared to healthy pregnancies [93]. Furthermore, additional research suggests that measuring the Ang-1/Ang-2 ratio could be a method for predicting sPE onset, as the Ang-1/Ang-2 ratio has been shown to decrease during 25-28 weeks of gestation in women who later developed sPE [94].

Fibroblast growth factor-2 (FGF-2) is an angiogenic factor that regulates cell migration and differentiation as well as tissue remodeling and regeneration [95, 96]. While

FGF-2 is known to affect several organ and pathways, its ability to regulate growth and function of the vasculature is one of its most well-known functions. FGF-2 can stimulate quiescent ECs to undergo proliferation and migration as part of the angiogenesis pathway [97]. Surprisingly, FGF-2 is not required for embryonic development as murine knockout studies revealed offspring are fertile and viable, however, inhibition of FGF-2 during mid-gestation has led to significant impairment in vasculature development in murine models [97, 98]. FGF-2 has a direct role in the production of NO, which is very important due to NO being the main vasodilatory agent in the placenta that contributes to regulation of trophoblast invasion, uterine vascular remodeling, and placental perfusion [99]. FGF-2 acts on ECs to regulate the expression of VEGFR2, and studies have shown reductions of FGF-2 cause subsequent reductions of VEGFR2 which can impair production of NO and angiogenesis [96, 100]. FGF-2 is normally produced by placental ECs and from the syncytium in pregnancy and women with sPE are shown to have significantly reduced blood serum levels of FGF-2 compared to women of healthy pregnancies [101].

Besides the impaired endothelial function, maternal metabolism is altered in PE which can lead to placental dysfunction. Leptin is a secreted hormone that can regulate maternal metabolism through its roles in increasing energy storage and regulation of food intake by suppressing appetite [102]. Despite the needs for increasing fat storage throughout pregnancy, leptin levels normally increase throughout pregnancy and leptin resistance during pregnancy must occur to maintain increased energy intake to support fetal growth in the second and third trimester [103]. Leptin acts on its receptors in the hypothalamus where it influences secretion of thyroid hormones, sex hormones, and growth hormones [104]. Leptin has important roles beyond metabolism, such as

regulating the menstrual-cycle, oocyte maturation [105], and embryo implantation and development [106, 107]. Leptin can also induce autocrine/paracrine functions in the placenta such as positive regulation of trophoblast differentiation, promotion of placental angiogenesis and nutrient transport, and local immunomodulation at the maternal-fetal interface [108, 109].

Leptin levels are known to be higher in women with PE however, they vary among those with early-onset PE and late-onset PE. Taylor et al. reported that only women who had late-onset PE were shown to have significantly higher levels of leptin in maternal serum as compared to the normotensive controls [110]. However, these results contradicted findings from Salimi et al. who showed that early-onset PE had significantly higher leptin levels than late-onset PE, where both groups show significantly high maternal leptin levels in comparison to the healthy controls [111]. High leptin levels are thought to be due to placental hypoxia and thus these results could as well be dependent on the degree of placental dysfunction that occurs in PE.

Epidermal growth factor (EGF) signaling pathways have important functions throughout gestation especially in the establishment of pregnancy to regulate uterine receptivity. Both EGF and heparin-binding EGF (HB-EGF) bind to EGF receptors, also known as HER1-4, and are expressed on the placenta and throughout the decidua to regulate endometrial function [112-114]. HB-EGF binds specifically to EGFR and HER4 and enacts specific functions depending on the cell type. Activation of these EGF receptors in early gestation by EGF and HB-EGF permits communication between trophoblasts and endometrial stromal cells for implantation and trophoblast invasion [112-114]. Studies show that ablation of EGF receptors can lead to early pregnancy loss due

to defects in decidualization and reduced cell proliferation and survival [115]. In the first trimester placenta, HB-EGF is increased from hypoxia to protect trophoblasts from apoptosis however this natural induction of HB-EGF does not occur in hypoxic term placentas [116]. Studies have shown that exogeneous addition of HB-EGF to term placentas cultured in hypoxia inhibits trophoblast apoptosis [113].

Impairments in EGFR signaling is prominent in pregnancy complications including intrauterine growth restriction, pre-term labor, and PE [117]. Deficiencies in HB-EGF and EGF expression and signaling can occur in the PE placenta although, it is not entirely clear at what point in pregnancy HB-EGF signaling is impaired. In early pregnancy, loss of HB-EGF expression and signaling can impair trophoblast differentiation, invasion and survival ultimately causing placental perfusion [118]. HB-EGF is reduced in PE placentas at term however, activating HB-EGF in the term PE placenta can significantly reduce trophoblast apoptosis, positioning HB-EGF as a cytoprotective agent in both early and late pregnancy [116].

Follistatin (FST) is an important growth factor that mediates TGFβ signaling. FST is highly expressed in early pregnancy in the decidua and helps to regulate uterine receptivity and decidualization [119]. FST blocks the production of Gonadotropin-releasing hormone (GnRH) to prevent pituitary release of follicle stimulating hormone and prevent follicular development [120] and as well regulates human chorionic gonadotropin (hCG) in early pregnancy [121]. FST serum levels increase throughout gestation leading to ovarian quiescence [120]. While aberrant expressions of FST are associated with abortions [122], miscarriages [123, 124] and implantation failure in IVF [125], there has

been less investigation of FST expression and contribution to other gestational complications such as PE and IUGR.

Among the many dysregulated placental proteins in PE, the reduction of heme oxygenase 1 (HO1) has a profound impact on PE pathology. HO1 is a potent cytoprotective molecule that functions as the rate limiting enzyme in the metabolism of heme into carbon monoxide (CO), biliverdin (BV) which is further converted to bilirubin (BR), and free iron (Fe^{2+}) [2, 126-130]. HO1 is one of three isoforms of HO and its inducible role is to elicit cellular and tissue response to injury during pathologic conditions [131]. HO-2 is constitutively expressed in every cell [2] and its role is primarily to regulate cellular functions including redox sensing, neovascularization and neuroprotection [131]. HO3 does not appear to have any specific function as it is thought to be a pseudogene [2].

HO1 expression is regulated by several transcription factors such as activator protein-1 (AP1), nuclear factor-kappa B (NFκB), Hypoxia inducible factor (Hif) and nuclear factor E2-related factor 2 (Nrf2) which bind at specific enhancer sequences found in the *HMOX1* promoter region [132]. Certain conditions and cell stimuli such as heavy metals, UV radiation, reactive oxygen species, prostaglandins, cytokines, nitric oxide, and hypoxia activate these transcription factors that further leads to upregulation of HO1 [132]. HO1 expression can also vary from person to person, based on genotype and the number of (GT)n dinucleotide repeats in the *HMOX1* promoter region [2]. Generally, a greater number of repeats lead to a reduction of HO1 expression and low number of repeats lead to an increase of HO1 expression [2]. Individuals with long (GT)n repeats are also at an increased risk for developing cardiovascular disease and hypertension [131] and

polymorphic (GT)n dinucleotide repeats greater than 25 in the promoter for *HMOX1* are known to be associated with non-severe PE and late-onset PE due to the reduction of HO1 [2, 133]. However, overexpression of HO1 could as well be harmful as studies have identified in some women with (GT)n repeats less than 27 were associated with recurrent miscarriages [134].

HO1 itself as well as heme metabolites have anti-inflammatory and antioxidative properties which help to dampen injury from oxidative stress and inflammation. HO1 metabolizes heme into CO, BV/BR and Fe^{2+} which all have beneficial effects on inflammation and oxidative stress. The HO1-derived metabolism of heme into CO is responsible for the largest production of CO in the body [132]. HO1-derived CO production assists in regulation of hemodynamics by promoting vasodilation in ECs though the NO pathway and in VSMCs through ion channels [131]. CO can also promote endothelial relaxation by inhibiting responsiveness to vasoconstrictive enzymes [131]. CO prevents apoptosis and exhibits anti-proliferative actions in VSMCs and ECs which are both beneficial for maintaining endothelial relaxation and function [131, 132]. In macrophages, CO prevents ROS-mediated recruitment of Toll-like receptor 4 (TLR4) to the plasma membrane which would normally induce a pro-inflammatory response [135]. CO also increases expression of interleukin-10 (IL-10) to promote an anti-inflammatory environment.

Besides these important actions of CO, heme metabolism and production of BR exerts potent antioxidant functions by sequestering ROS and NOS and undergoes cytoprotective activities by reducing lipid peroxidation, increasing NO half-life, inhibiting iNOS, and protecting against H_2O_2 toxicity [131, 132]. To prevent inflammation, BR

completely blocks leukocyte adhesion to the endothelium which is a major hallmark of the inflammatory process. Low levels of BR are highly associated with cardiovascular disease, obesity and metabolic disease [132] which further show the importance of HO1 actions. Fe^{2+} is another HO1 metabolite and free Fe^{2+} can generate toxic levels of ROS however, an increase HO1 and CO simultaneously induces ferritin which binds Fe^{2+} preventing endothelial cells from toxicity. Ferritin additionally has anti-apoptotic effects by inhibiting TNF [131].

Beyond its actions as a cytoprotective molecule, HO1 has significant roles in maintaining an angiogenic balance by promoting endothelial activation, proliferation, and tube formation. Studies show that upregulation of HO1 in microvascular endothelial cells leads to a two-fold increase in blood vessel formation [136]. In ECs, HO1 is upregulated by stromal cell-derived factor 1 (SDF-1) to regulate migration of the progenitor endothelial cells to areas of ischemic injury and assist in neovascularization. Deshane et al. found that when HO1 was silenced, SDF-1 angiogenic actions were inhibited however, exposure to CO restored SDF-1 effects, which suggest that these angiogenic actions must function through HO1 [137]. HO1-deficiencies result in poor wound healing, in part due to reduced recruitment of progenitor ECs and capillary formation in murine and *in vitro* models [138] [139]. HO1-deficient mice are shown to express higher levels of sFLT1 compared to wild-type mice however, induction of HO1 was shown to reduce sFLT1 levels in hypertensive rats [140]. HO1 may also indirectly regulate angiogenesis through increasing expression of pro-angiogenic proteins such as VEGF, monocyte chemotactic protein 1 (MCP1), TGFβ, and interleukin-8 (IL-8) while simultaneously decreasing expression of sFLT1, sEng, and CXCL10 [138].

Murine studies of HO1 further highlight the many roles of HO1 during pregnancy. Zhao et al. identified that pregnant mice who were homozygous knockout for the HO1 gene, *HMOX1*, show extremely low birth rates (2.4%) and very small litters with most HO1 deficient mice undergoing spontaneous abortion by E10.5 [141]. Heterozygous HO1 knock-out (HO1+/-) mice result in smaller litters of approximately 5 pups on average as compared to 9 pups on average in wildtype mice [141]. Mice that are heterozygous for HO1 ($HO1^{+/-}$) mice exhibit smaller placentas with an abnormal placental structure, specifically in the junctional zone with high levels of apoptosis in the spongiotrophoblast [141]. In depth analysis of the spiral artery structure of $HO1^{+/-}$ mice shows a reduction in the diameter of the uterine spiral arteries and the fetal capillaries were shown to be largely disorganized as compared to wildtype mice. Gene expression arrays of these placentas confirmed this altered vascular phenotype by showing a reduction of pro-angiogenic genes and an increase in anti-angiogenetic genes in the $HO1^{+/-}$ mice [141]. In addition, sFLT1 levels were significantly elevated in the $HO1^{+/-}$ mice compared to the wildtype mice [141] causing an increase in diastolic blood pressure, which mirrors the PE condition in humans. These factors likely contribute to the abnormal placental vasculature that is commonly observed in HO1-deficient pregnancies [142].

HO1 has a critical role of maintaining the maternal immunologic tolerance of the fetus from the start of conception which is arguably one of the most important maternal adaptions to pregnancy [2]. These actions are in-part facilitated by the balance of anti-inflammatory immune cells, such as M2 macrophages, a reduction of T effector cells and an increase of CD4+CD25+ regulatory T cells (Tregs), and the inhibited activation of dendritic cells which further lack the production of pro-inflammatory cytokines [2].

HO1 is a central component in the protection from cytotoxicity and inflammation and as well for promotes endothelial cell proliferation and migration and regulates the angiogenic balance in the placenta [126-128]. Deficiencies of HO1 enhances chronic inflammation that increases susceptibility to oxidative stress and injury in the placenta. A reduction of HO1 levels is associated with multiple pregnancy complications, including PE [29]**.** These data highlight the importance of HO1 in establishing and maintaining a successful pregnancy. HO1 deficiency is thought to cause a chronic inflammatory state, disrupt angiogenic balance and increase susceptibility to injury from oxidative stress, which in part explains how a reduction in HO1 is associated with human pregnancy complications such as infertility, miscarriage, spontaneous abortion, preeclampsia and preterm labor [2].

Indeed, the molecular processes governing the establishment of pregnancy, placental and endothelial function, and maternal adaptations to the conceptus are very complex. Several molecules must be perfectly aligned for pregnancy to occur, and their coordinated functions dictate pregnancy outcome. By understanding the roles of these proteins in healthy pregnancies, we can infer about their possible contributions to PE and further restoring their expression and functions during PE may attempt to reverse the disease.

1.6. Outlook for the research on PPARγ, preeclampsia, and the regulation of secreted proteins

PE is characterized as a multi-stage disease where abnormal placentation occurs in early pregnancy, involving shallow EVT invasion and reduced spiral artery remodeling [143]. This promotes placental malperfusion which damages fragile villous structures of the placenta leading to several pro-/anti-angiogenic and growth factor proteins that are

aberrantly secreted from the placenta [144]. The anti-angiogenic environment causes endothelial dysfunction and is thought to be the link between placental pathology and development of clinical symptoms including systemic endothelial dysfunction, leading to hypertension and proteinuria later in pregnancy. Significant research has shown the many ways that PPARγ controls trophoblast differentiation and many model systems show that PPARγ activation can improve trophoblast function during ischemic conditions. These findings position PPARγ to be an attractive placental target for the improvement of PE.

Given the large influence of the imbalance of secreted proteins on the manifestations of PE, it would be valuable to understand how placental activation of PPARγ influences protein secretion, and subsequently, how this secretory profile influences the angiogenic potential of the surrounding endothelium. To fill this gap of knowledge, this research will use healthy term and first trimester placentas, term preeclamptic placentas, and in vitro cell model systems to study how alterations in PPARγ activity effects the production and secretion of pro-angiogenic, growth factor and metabolic molecules (HO1, PIGF, FGF-2, EGF, HB-EGF, FST, Leptin) and anti-angiogenic molecules (sFLT1, Ang-2, ET-1, sEng). Moreover, this study will recapitulate the maternal response to the placental protein secretion by culturing human umbilical vein endothelial cells with conditioned medium from non-treated healthy and preeclamptic placentas, as well as preeclamptic placentas that have been treated with Rosiglitazone. These endothelial cells will be assessed for changes in their angiogenic potential, which will ultimately show the ability for placental activation of PPARγ to improve endothelial function in the disease model. These studies will advance the current field of placental biology and PE etiology by understanding mechanisms driven by PPARγ in normal and

abnormal placental development. The outcome of these works will highlight PPARγ's roles which extend beyond its direct effects in placental function to ultimately improve endothelial function in PE to reduce poor maternal-fetal outcomes.

2. CHAPTER 1. INDUCTION OF THE PPARY-GCM1 SYNCYTIALIZATION AXIS REDUCES SFLT1 IN THE PREECLAMPTIC PLACENTA

This is a non-final version of an article published in final form in [23] and can be accessed directly using the following link: https://doi.org/10.1161/HYPERTENSIONAHA.121.17267.

2.1. Introduction

The placenta serves as a critical organ during pregnancy to support fetal growth and development [1, 6, 7]. Abnormal placental development is a hallmark of several pregnancy-related complications causing significant maternal and/or fetal morbidity and mortality, especially severe fetal forms of intrauterine growth restriction and preeclampsia (sPE) that result in stillbirth or early preterm delivery [1, 145]. sPE comprises new onset of maternal hypertension after 20 weeks of gestation with systemic endothelial dysfunction and critical end-organ injury involving the kidneys, liver, brain, and coagulation system [6, 146]. In sPE, the placenta most commonly exhibits multiple histopathologic features, collectively described as maternal vascular malperfusion [32, 145]. The disease begins with reduced extravillous trophoblast invasion and transformation of the uteroplacental arteries, which results in chronic ischemia of the developing placental villi [30-32]. Patients at highest risk of sPE demonstrated bilateral abnormal uterine artery Doppler and low circulating levels of placenta growth factor (PIGF) [147] and subsequently begin to express very high levels of soluble fms-like tyrosine kinase 1 (sFLT1) [148, 149]. In combination, the high sFLT1/PlGF ratio is now an established diagnostic test for PE [150-152].

sFLT1 is a potent anti-angiogenic protein and major contributor to endothelial damage in PE [153]. sFLT1 is a splice variant of the vascular endothelial growth factor receptor 1 (VEGFR1) also known as FLT1. sFLT1 competitively binds to the receptor

domains of vascular endothelial growth factor (VEGF) [154] and its dimeric partner PIGF [155], preventing their interaction with the endothelial cell surface receptors. Our group previously found that first trimester placentas secrete higher amounts of sFLT1 by tissue weight compared to healthy term placenta, suggesting that sFLT1 has important roles in early pregnancy [80]. Increased levels of sFLT1 throughout pregnancy combined with lowered levels of PlGF largely mediates the systemic endothelial dysfunction observed in PE [156-159].

The transcription factor, Glial cell missing 1 (GCM1) regulates villous trophoblast differentiation in human placental villi [16, 160] and analogous labyrinth formation in mice [15, 69]. GCM1 thereby modulates the expression of trophoblast-derived proteins involved in the maintenance of normal pregnancy and cardiovascular function, especially the promotion of PlGF following syncytial fusion [155]. Prior reports found reduced GCM1 expression in PE placentas [17] with similar repression of the downstream fusogenic partner, syncytin, that is required for syncytiotrophoblast fusion to grow the continuous outer layer covering the placental villi. GCM1 is a strong candidate to regulate sFLT1 production in human placental villi, since a previous study identified that heterozygous Gcm1 knockout murine placentas secrete significantly higher levels of sFLT1 [161]. In further support of this hypothesis, enhanced expression of GCM1 via anti-viral drugs reduced the expression of sFLT1 in murine placentas [162].

GCM1 and the nuclear steroid receptor, peroxisome proliferator activated receptor gamma (PPARγ), are critical proteins needed for placental development and pregnancy. PPARγ and GCM1 work as sequential partners to regulate proper villous trophoblast to syncytiotrophoblast differentiation [160, 161]. PPARγ functions as an upstream

transcriptional regulator of GCM1 [69, 163] through binding at two PPARγ response elements in the GCM1 promoter [36]. Using the BeWo choriocarcinoma villous trophoblast cell line [36] and a first trimester placenta explant model [16], our group previously identified that pharmacological activation of PPARγ by Rosiglitazone led to an increase in GCM1 expression and villous trophoblast differentiation. These findings suggest that this pathway is important for normal trophoblast function and turnover.

In the past decade, PPARγ has emerged as an important player in placental development due to its regulatory roles in multiple cellular pathways including metabolism, nutrient balance, and anti-inflammatory response pathways [66-68]. Murine studies have shown that embryonic knockdown of PPARγ is lethal due to gross cardiovascular and placental abnormalities [12]. Prior studies have shown that hypoxia reduces PPARγ expression in the human placenta and murine trophoblast stem cells [164-166]. Therefore, the prolonged hypoxic/ischemic nature of the severe PE placenta is likely a cause for the reduced placenta expression of PPARγ observed in PE [167-170]. This further imposes an abnormal villous trophoblast structure and poorly-developed feto-placental vasculature observed in severely preeclamptic placentas [12]. In a rodent model of PE, decreased activity of PPARγ was found to correlate with increased sFLT1 levels [35] and re-introducing PPARγ in PPARγ$^{-/-}$ murine trophoblast stem cells rescued differentiation of the syncytiotrophoblast and labyrinthine trophoblast lineages by GCM1 upregulation [69].

While it is established that PPARγ and GCM1 are critical factors for normal placental development, the potential molecular connections between PPARγ, GCM1, and sFLT1 in the normal and diseased human placenta are unclear. In the current study, we

hypothesized that maintenance of the PPARγ-GCM1 axis in healthy developing placental villi represses the expression and secretion of the anti-angiogenic sFLT1, whereas this axis is disrupted in favor of hyper-secretion of sFLT1. We tested this hypothesis in explanted human placental villi from first trimester or from healthy and severely-preeclamptic women to determine the expression of GCM1 and production of sFLT1, under conditions that pharmacologically activated or inhibited PPARγ via the drugs Rosiglitazone and T0070907, respectively.

2.2. Methods

2.2.1. Tissue collection

First trimester (10–12 weeks of gestation) placental tissues (n = 4) were obtained with written informed consent from healthy pregnant women undergoing elective termination of pregnancy from Wayne State University in Detroit, MI between the years of 2013-2017. The Institutional Review Board of Wayne State University approved all consent forms and protocols used in this study, which abide by the NIH research guidelines. Term placental samples were obtained either by the Research Centre for Women's and Infants' Health BioBank program of Mount Sinai Hospital in Toronto, Canada, in accordance with the policies of the Mount Sinai Hospital Research Ethics Board or Women's Health Center at Spectrum Hospital in Grand Rapids, MI. All placentas collected were approved by the IRB waiver of parental consent. Term specimens were collected from age-matched idiopathic preterm without histological evidence of chorioamnionitis not complicated by PE (PTC) (n = 14; gestational age = 31-37 weeks), and pregnancies complicated by severe PE (n = 14; gestational age = 31-37 weeks) and were delivered either by Cesarean section or vaginal birth. Inclusion criteria for severe PE was in accordance with current guidelines including blood pressure > 160/110 mm Hg

on two occasions longer than 6 hr apart, evidence of end-organ damage including proteinuria, with or without fetal growth restriction [171].

2.2.2. Explant culture

For term tissues, a standardized random sampling protocol was applied dissecting random four 1cm^3 cuboidal sections to avoid sampling bias. The collected tissues were washed and transported to the laboratory in ice cold HBSS (Hank's Balanced Salt Solution) and processed within a maximum of 2 hr after delivery. On arrival, tissues were rinsed in chilled HBSS to remove residual blood and further dissected under a stereomicroscope to remove placental membranes and generate 20-30mg pieces of villous tissues for culture. First trimester explants were cultured according to our previously published floating villous explant protocol [9]. Individual clusters of villous trees were dissected under a stereomicroscope. Post dissection, the explants were cultured overnight in 500µL of Dulbecco's modified Eagle's medium/Ham's F-12 nutrient mixture (DMEM/F-12; 1:1; Life Technologies; Grand Island, NY) containing 10% fetal bovine serum (FBS; Life Technologies) and 1% Gibco™ antibiotic-antimycotic. Term explants were maintained overnight at 8% O2 with 5% CO2 at 37°C [10]. After an overnight culture, the tissues were treated with 10µM Rosiglitazone (Selleckchem) or 1µM T0070907 (R&D Systems) dissolved in dimethyl sulfoxide (DMSO, Sigma Life Sciences) for 18-24 hours. DMSO alone was used as a vehicle control. Comparison of DMSO to NT (not treated placental tissues) was performed to ensure there was not an effect from DMSO. After the culture period for each treatment, replicates were snap frozen for protein and RNA extraction and stored at -80ºC. The media was also collected, snap frozen and stored at -80ºC. In a few samples, an extra replicate was immediately fixed in 4%

paraformaldehyde for immunohistochemistry. This was included in this study as a qualitative assessment to complement RNA/Protein expression findings.

2.2.3. Protein extraction and immunoblotting

Protein extraction from tissues (20–30 mg) was performed as previously described [172]. Protein concentration was determined with BCA™ protein assay reagent (Thermo Fisher Scientific, Rockford, IL) according to the manufacturer's instructions. Equal protein amounts (35 µg) were denatured (8 min, 95°C) in Laemmli sample buffer (Bio-Rad Laboratories; Hercules, CA) and separated using sodium dodecyl sulfate-polyacrylamide gel electrophoresis, with subsequent semi-dry transfer (Trans-Blot®; Bio-Rad Laboratories) to a polyvinylidene difluoride membrane. The membranes were blocked with 5% nonfat dry milk in 1× Tris-buffered saline containing 0.05% Tween-20 and were incubated overnight at 4°C with anti-GCM1 (1:5,000; Aviva, San Diego, CA), anti-FLT1 (1:1000, Abcam), and anti-PPARγ (1:1,000; Cell Signaling Technology) primary antibodies. Subsequently, membranes were incubated with horseradish peroxidase-conjugated secondary antibodies for 1 hr at room temperature and were developed with Western Lightning® ECL Pro (PerkinElmer, Waltham, MA). Signals were visualized using a ChemiDoc™ Imaging System (Bio-Rad Laboratories) and Image Lab Version 5.1 software (Bio-Rad Laboratories). Densities of immunoreactive bands were measured as arbitrary units by the ImageJ software (NIH, Bethesda, MD). Protein levels were normalized to a housekeeping protein β-actin (1:4,000; Abcam). Protein expression values are reported as relative to β-actin.

2.2.4. ELISA

The media collected from PE, PTC, and first trimester placental explant cultures was assayed for levels of sFLT1 using the Human VEGFR1/Flt-1 DuoSet kit (R&D Systems, Minneapolis, MN) according to the manufacturer's instruction. Culture media was centrifuged at 4,500 x g for 10 minutes at 4°C to pellet all cell/tissue debris and the supernatant was used for ELISA analysis. The optical density of the final-colored reaction product was measured at 450 nm using a SoftMax Pro5 or a multispectral UV/VIS (Bio-Tek, VT) plate reader. A standard curve was used to calculate protein content, and this was normalized over wet weight of the explant to obtain the amount of protein secreted per milligram of explant tissue.

2.2.5. RNA extraction and qPCR analysis

The tissue was lysed in Qiazol and RNA was extracted using RNeasy Plus Universal Mini kit (Qiagen, Germany) as per the manufacturer's protocol. The extracted RNA was quantified using Nanodrop and 1µg was reverse transcribed using iScript RT synthesis kit (Bio-Rad Laboratories, CA). Real-time PCR was performed on the Bio-Rad CFX384 real time system in triplicates in 10µL total reaction volume containing 10 ng of template cDNA, 5µL of SYBR-green master mix (LuminoCT, Sigma-Aldrich, MO) and 500nM of primers. The primers used for assessing the expression levels of target and housekeeping genes are outlined in Table 1. Data was analyzed using the delta-delta CT method as described in [173].

Table 2.1: Chapter 1 qPCR Primer Sequences

Gene Name	Gene Symbol	Sequence
Cytochrome C1	*Cyc1*	F: 5′-CAT CAT CAA CAT CTT GAG CC-3′ R: 5′-CAG ATA GCC AAG GAT GTG TG-3′
Tyrosine 3-monooxygenase	*Ywhah*	F: 5′- CCG CCA GGA CAA ACC AGT AT -3′ R: 5′- ACT TTT GGT ACA TTG TGG CTT CAA -3’
TATA box binding protein	*Tbp*	F: 5′-CAC ATC ACA GCT CCC CAC CA-3′ R: 5′-TGC ACA GGA GCC AAG AGT GAA-3′
Glial cell missing 1	*Gcm1*	F: 5′-TGA ACA CAG CAC CTT CCT C-3′ R: 5′-CCA CTG TAA CTA CCA GGC AAT-3′
Soluble fms-like tyrosine kinase	*sFlt1*	F: 5′- CCT CAA ATG ATC CAC CTG CCT-3′ R: 5′- CAG GAA GCA CCA TAC CTC CTG -3′

2.2.6. PPARγ transcription factor assay

Nuclear proteins were isolated from first trimester tissue after treatment with Rosiglitazone (10μM), T0070907 (1μM) and DMSO using a Nuclear Extract Kit (ActiveMotif, Carlsbad, California). The assay was performed using PPARγ binding assay (TransAM, ActiveMotif, Carlsbad, California) following the manufacturer’s protocol. Briefly, 3μg of nuclear proteins from treatment and control groups were used. The proteins from each group were added to the provided 96 well plate (in triplicates) and volumes were adjusted to 10μL using the complete lysis buffer from the kit. 5μg of given positive control and complete binding buffer containing 40pmol of the consensus site (from the kit) was then added to each well. The plate was incubated for 1 hour followed by 3 washes with the 200uL of 1X wash buffer. 100uL of the supplied PPARγ antibody was then added to all wells and the plate was incubated again for 1 hour at RT. After the incubation, the wells were washed again 4 times and 100μL of developing solution was then added to each well and incubated for 5 mins. The reaction was stopped using 100μL of Stop solution and the absorbance was read at 665nm. The absorbance for the blank wells was subtracted from all the readings and then values from Rosiglitazone and T0070907

samples were normalized to the values from DMSO vehicle for comparison between the treatments.

2.2.7. Immunohistochemistry

Immunostainings of placental villi were performed as described in [174]. Briefly, the sections were deparaffinized and rehydrated, followed by antigen retrieval using Dako Target retrieval solution (Agilent-DAKO, USA). The intrinsic peroxidase activity was then quenched by incubating the sections with 3% Hydrogen peroxide (Fisher Scientific, MA) for 30 mins at RT, followed by a wash with 1X PBS. The sections were then incubated overnight at 4°C with anti-FLT1 (Santa Cruz, TX) or 10µg/ml nonimmune Rabbit IgG (Jackson Immunoresearch, PA) (used as a negative control). The following day, the slides were washed 3 times (5 minutes/wash) with 1X PBS containing 0.1% Tween 20. The samples were then incubated for 30 min with a peroxidase-conjugated polymer coupled to anti-rabbit IgG (EnVision Systems Peroxidase, Agilent-DAKO, USA). The peroxidase was visualized with 3,3-diaminobenzidine (DAB, Agilent-DAKO, USA) and hydrogen peroxide for 5 min. Tissues were counterstained with hematoxylin, dehydrated and were cover slipped. The staining was visualized using Nikon Eclipse 90i epifluorescence microscope (Nikon Inc., Japan) and the images were analyzed using ImageJ software.

2.2.8. siRNA-mediated GCM1 suppression

For silencing, Silencer™ Select Pre-Designed siRNA assays (Thermo Fischer) were used. For GCM1 specific knockdown, assay ID s16199 was used and a Cy™3-labeled scramble sequence was used a negative control (AM4621, ThermoFisher). A non-silencing control was additionally incorporated as a technical control to exclude any effects of the electroporation procedure used for silencing. The tissues were

electroporated using the P3 Primary Cell 4D-Nucleofector™ X Kit L and the Nucleofactor™ 2b device (Lonza, Switzerland) following the manufacturer's kit protocol. First trimester villous explants were cultured overnight in Dulbecco's modified Eagle's medium/Ham's F-12 nutrient mixture (DMEM/F-12; 1:1; Life Technologies; Grand Island, NY) containing 10% fetal bovine serum (FBS; Life Technologies) and 1% Gibco™ antibiotic-antimycotic at 8% O_2. On day 2, the explants were placed in the cuvette (2 explants/cuvette) along with 100uL of electroporation solution (10µL of silencing probe mix + 90µL of electroporation buffer). The program U017 was used for electroporation after which the explants were taken out and cultured in fresh media for 48 hours. After the culture period, one set of explants were processed for immunohistochemistry by fixing in 4% paraformaldehyde and another set was frozen in 700µL of Qiazol to be used for RNA expression studies. The media was collected and frozen to be used later for sFLT1 analysis using ELISA.

2.2.9. Statistical analysis

All statistical analysis was performed with GraphPad Prism 7.0 software. Raw mRNA and protein expressions were normalized to respective housekeeping genes or protein. ELISA data was normalized based on semi dry-tissue weight. Relative expression/secretion values from untreated tissues (Figure 2.1) were analyzed by student's t-test after determination if samples are normally distributed and an F-test was applied to determine variances between groups which was then used in the parameters for the t-test. Raw mRNA and protein expression values from tissues treated with either DMSO, Rosiglitazone and T0070907, or GCM1-siRNA and scramble siRNA (Figures 2.2-2.4) were normalized to respective housekeeping genes or protein. Relative expression or secretion values for each tissue sets were subsequently normalized to respective

DMSO (vehicle control, set equal to 1) or scramble siRNA control (set equal to 1) represented by a dotted line on the graphs. Groups were then analyzed by student's t-test, after determination if samples are normally distributed and an F-test was applied to determine variances between groups which was then used in the parameters for the t-test. $p<0.05$ is considered significant and is indicated with (*) on each graph. Data is reported as Mean+/-S.E.M [175]. All sample numbers are reported as per group, for example, n=6 designates 6 samples per treatment/group.

2.3. Results

2.3.1. Cultured sPE placentas show increased protein expression of FLT1, increased secretion of sFLT1 and reduced protein expression of PPARγ and GCM1 compared to PTC controls.

sFLT1 secretion into the placenta culture media was measured by ELISA after 48 hours of culture for sPE and gestational age-matched preterm control (PTC) placentas. We observed significantly higher secretion of sFLT1 from sPE placentas compared to PTC (3327±198 pg/mL vs. 2361±198 pg/mL, p=0.0067, n=5, Figure 2.1A). Placental protein expression of FLT1, PPARγ, and GCM1 were measured by western blotting. FLT1 protein expression was significantly upregulated in sPE placentas comparison to PTC (0.96±0.2 vs. 0.28±0.06 relative expression values, p=0.0167, n=6, Figure 2.1B) which mirrored representative immunohistochemical staining patterns showing enhanced localized expression of total-FLT1 (which includes all FLT1 and sFLT1 variants) in the syncytiotrophoblast layer of the sPE placenta (Figure 2.1E). sPE placentas showed a significant reduction of PPARγ protein expression (0.476±0.13 vs. 1.09±0.1, p=0.0042, n=6, Figure 2.1C, F) and a significant reduction of GCM1 protein expression (0.56±0.06 vs. 0.99±0.07, p=0.0001, n=14, Figure 2.1D, F) compared to PTC.

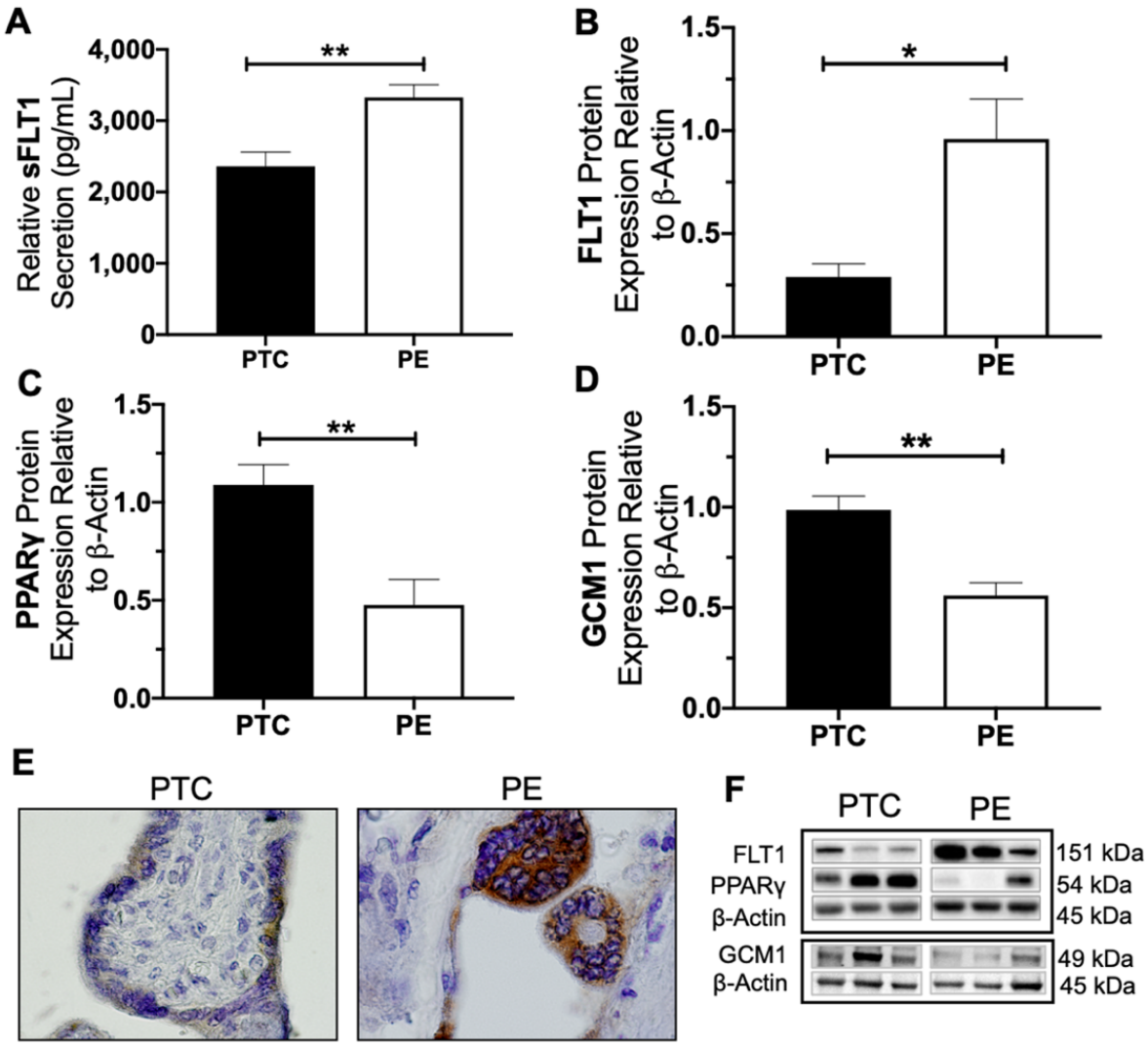

Figure 2.1: Placentas from women with sPE exhibit higher sFLT1 secretion and FLT1 expression accompanied with lower expressions of PPARγ and GCM1. sFLT1 secretion was significantly higher secreted by sPE compared to gestational-age matched control (PTC) (2361.3±198pg vs. 3326.8±178.8pg, n=5, p=0.0067) (A). This finding corresponds with higher expression of FLT1 protein in sPE compared to control (n=6, p=0.0167) (B). Immunostaining for total-FLT1 (FLT1 and sFLT1 variants) shows light staining in the syncytiotrophoblast of PTC tissues compared to a more intense signal in sPE placenta (E). Immunoblotting assessment revealed sPE placentas exhibit lower protein expression of PPARγ (n=6, p=0.0042) and GCM1 (n=14, p=0.0001) compared to PTC (C, D). Representative western blots are shown in (F). (*Relative mRNA and protein expression were determine by normalization to housekeeping genes or protein, followed by a student's t-test to determine significant differences between groups, * p<0.05, ** p<0.01, Rosi=Rosiglitazone, T007=T0070907, bar plots and data reported are presented as mean ± SEM, PE = preeclampsia, PTC = preterm healthy control)*

2.3.2. Activation of PPARγ by Rosiglitazone induces GCM1 expression and lowers placental sFLT1 secretion in first trimester placental explants.

First trimester villous placental explants were used as a model to understand how sFLT1 changes in response to modulating of the PPARγ–GCM1 axis. These tissues were cultured for 18 hours with PPARγ agonist, Rosiglitazone (10μM), or antagonist, T0070907 (1μM). Successful activation of PPARγ by Rosiglitazone was confirmed by a 28±5% increase in PPARγ global DNA-binding activity in the Rosiglitazone treated explants (128±5 vs. 100, $p<0.05$, n=3, Figure 2.2A) as measured by an ELISA-based transcription factor binding assay. There was no significance difference in PPARγ DNA-binding activity in the T0070907 treated explants (Figure 2.2A). PPARγ and GCM1 protein expressions in first trimester tissues were measured by western blotting. Rosiglitazone significantly increased PPARγ protein expression (1.3±0.09 vs 1, p=0.0446, n=4, Figure 2.2B, F) and GCM1 protein expression (1.83±0.2 vs. 1, p=0.0402, n=4, Figure 2.2C, F). Rosiglitazone significantly increased GCM1 mRNA expression (2.35±0.4 vs. 1, p=0.04, n=4) while T0070907 significantly decreased GCM1 mRNA expression (0.55±0.1 vs. 1, p=0.02, n=4, Figure 2.2D). Rosiglitazone significantly decreased sFLT1 secretion into the culture media (0.57±0.07 vs. 1, p=0.025, n=3, Figure 2.2E). Treatment with T0070907 did not result in a significant change in sFLT1 secretion from the first trimester explants (Figure 2.2E).

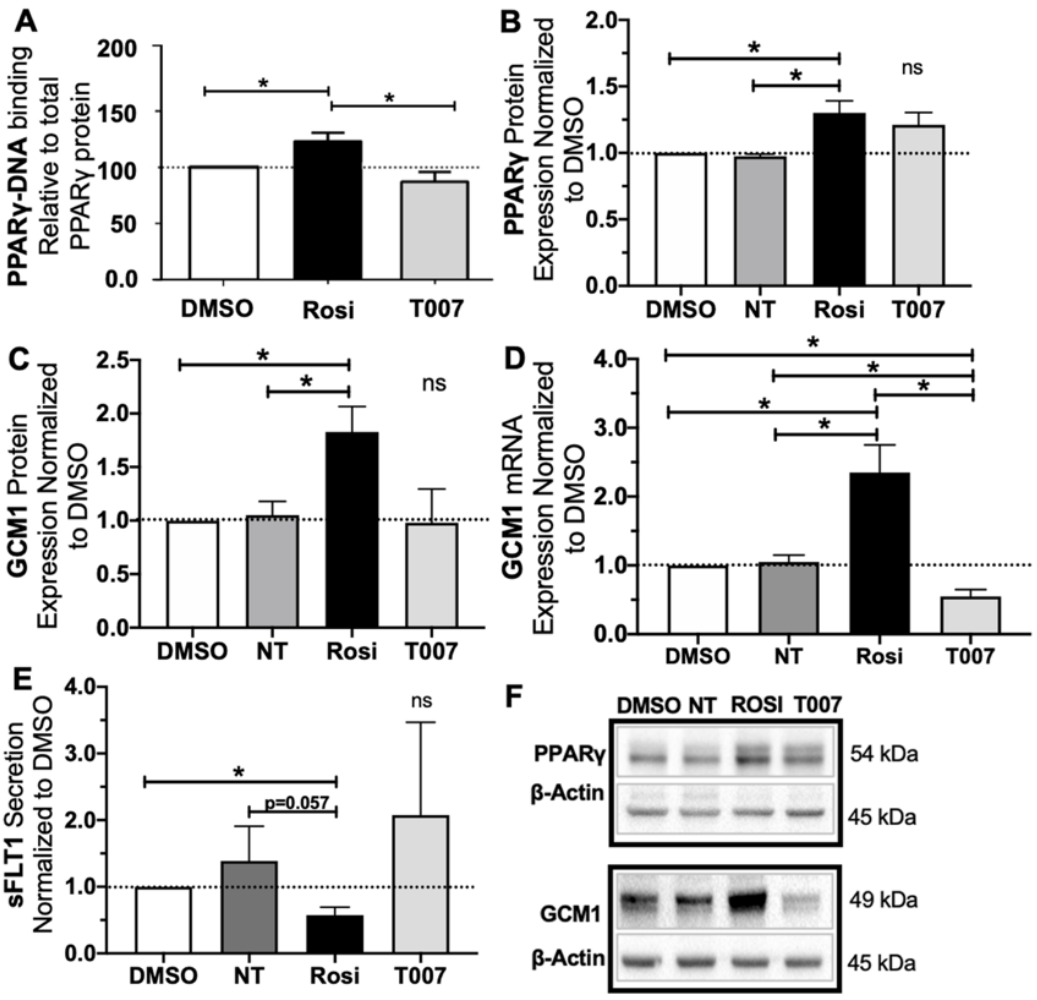

Figure 2.2: Rosiglitazone increases PPARγ activity and GCM1 mRNA expression while reducing sFLT1 secretion in the first trimester placenta. Treatment with Rosiglitazone caused a significant increase in PPARγ activity ($p<0.05$, n=3) (A). T0070907 did not cause a significant change in PPARγ activity (A). Rosiglitazone significantly upregulated PPARγ ($p=0.0446$, n=4) and GCM1 ($p=0.0402$, n=4) protein expression (B, C, F). T0070907 did not cause a significant change in PPARγ or GCM1 protein expression (B, C, F). Rosiglitazone significantly upregulated GCM1 mRNA expression ($p=0.0433$, n=4) (D). T0070907 significantly reduced GCM1 mRNA expression ($p=0.02$, n=4) (D). Rosiglitazone also caused a significant reduction in sFLT1 secretion ($p=0.025$, n=3) (E). Antagonizing PPARγ by T0070907 did not cause a statistically significant change in sFLT1 secretion (E). *(Relative mRNA and protein expression were determine by normalization to housekeeping genes or protein. Relative expression values for individual tissue sets were normalized to DMSO (vehicle control, dotted line, set equal to 1) and subsequent statistical analysis was performed by student's t-test to determine significant differences between groups,* $p<0.05$, ns=$p>0.05$, NT=not treated, Rosi=Rosiglitazone, T007=T0070907, bar plots and data reported are reported as mean ± SEM).*

2.3.3. Silencing of GCM1 upregulates FLT1 and sFLT1 in human first trimester explants

We have shown that activating PPARγ in the placenta leads to a significant induction of GCM1 mRNA and protein expression and a significant reduction of sFLT1 secretion from the first trimester placenta. Since it is already established that PPARγ acts as an upstream transcriptional regulator for GCM1 [36], we aimed to determine if GCM1 has a role in this potential pathway for regulation of sFLT1 secretion. We further used first trimester villous explants as a model for siRNA-mediated repression of GCM1. GCM1 siRNA caused a significant reduction of GCM1 mRNA expression (0.49±0.09, p=0.031, n=3, Figure 2.3A) and reduced GCM1 protein as compared to tissues transfected with the scramble siRNA (Figure 2.3C). The GCM1-silenced explants secreted significantly more sFLT1 (1.59±0.13 vs. 1, p=0.0389, n=3, Figure 2.3B). A representative immunohistochemistry staining shows higher expression of total-FLT1 protein (FLT1 and sFLT1 variants) in the syncytiotrophoblast of the GCM1-silenced explants compared to scramble siRNA and no-treatment controls (Figure 2.3D).

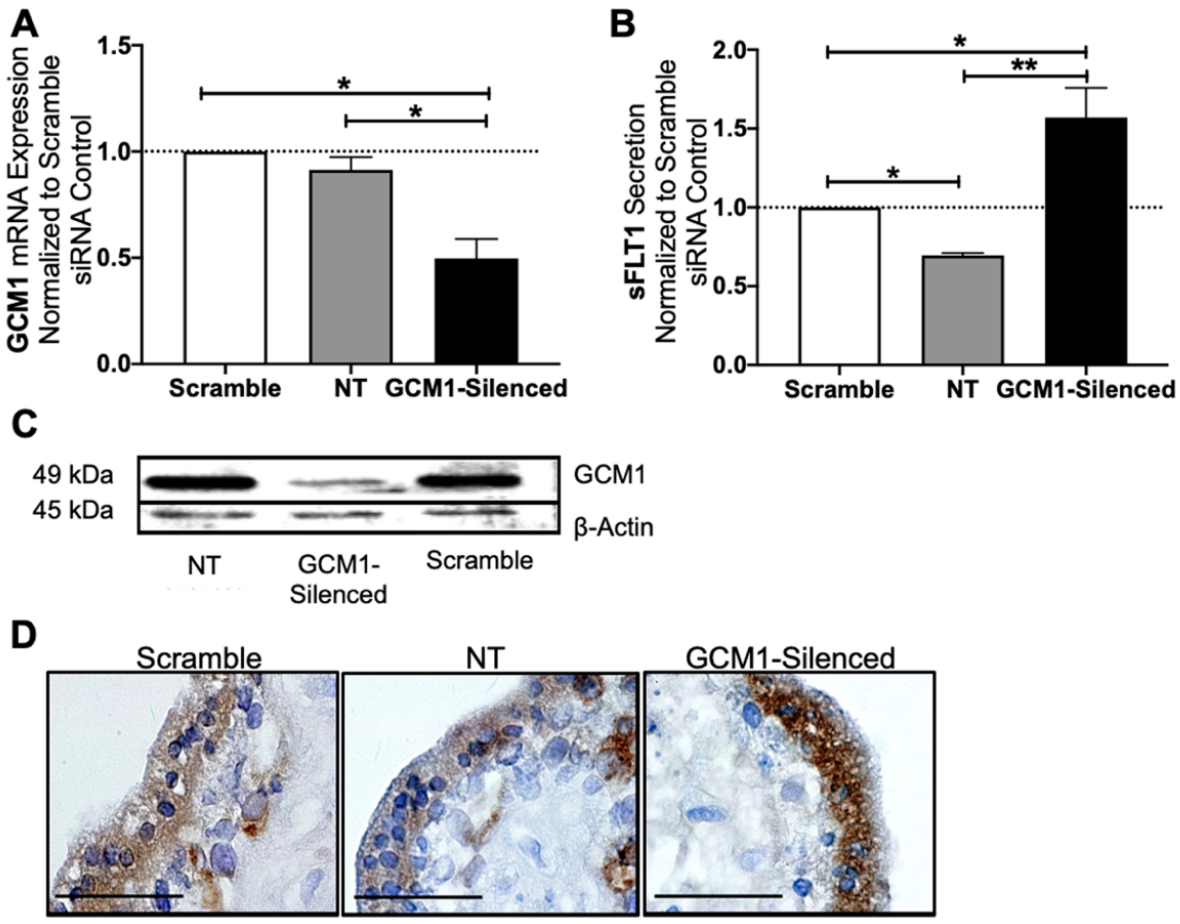

Figure 2.3: GCM1 reduction increases total-FLT1 expression and sFLT1 secretion in first trimester explants. In our first trimester explant model, siRNA-mediated silencing of GCM1 caused a significant reduction of GCM1 mRNA expression (p=0.031, n=3) **(A)**. Similarly, western blot shows GCM1 protein expression appeared to be decreased in the GCM1-silenced tissues in comparison to the scramble siRNA and no-treatment controls **(C)**. sFLT1 secretion was significantly increased in the GCM1-silenced explants (p=0.0389, n=3) **(B)**. Similarly, placental expression of total-FLT1 protein (FLT1 and sFLT1 variants) was induced in the syncytiotrophoblast of the first trimester explants, after GCM1 knockdown **(D).** *(Relative mRNA expression was normalized to housekeeping genes. sFLT1 secretion (pg/mL) data were normalized based on tissue weight. Relative expression/secretion values for individual tissue sets were normalized to the scramble siRNA control (dotted line, set equal to 1) and subsequent statistical analysis was performed by student's t-test was performed to determine significant differences between groups, NT=not treated, * p<0.05, ns= p>0.05, bar plots are reported as mean ± SEM)*.

2.3.4. Rosiglitazone restores PPARγ and GCM1 expression and downregulates sFLT1 in the severe preeclamptic placenta.

To test if the PPARγ-GCM1 axis can be modulated in the sPE placenta, we pre-treated sPE placentas with Rosiglitazone (10μM) or T0070809 (1μM) for 24 hours. Rosiglitazone significantly increased PPARγ protein expression in sPE (1.34±0.04 vs. 1, p=0.051, n=4, Figure 2.4A, B) and treatment with T0070907 did not have a significant effect on PPARγ protein expression. Rosiglitazone restored GCM1 by increasing mRNA expression the sPE placenta (1.28±0.09 vs. 1, p=0.0162, n=9, Figure 2.4C). Treatment with T0070907 caused a significant reduction of GCM1 mRNA expression in the sPE placenta (0.49±0.05 vs. 1, p=0.001, n=9, Figure 2.4C). Rosiglitazone significantly decreased sFLT1 mRNA expression in the sPE placenta (0.655±0 vs. 1, p=0.0058, n=7, Figure 2.4D). Treatment with T0070907 did not cause a significant change in sFLT1 mRNA expression in the sPE placenta (Figure 2.4D).

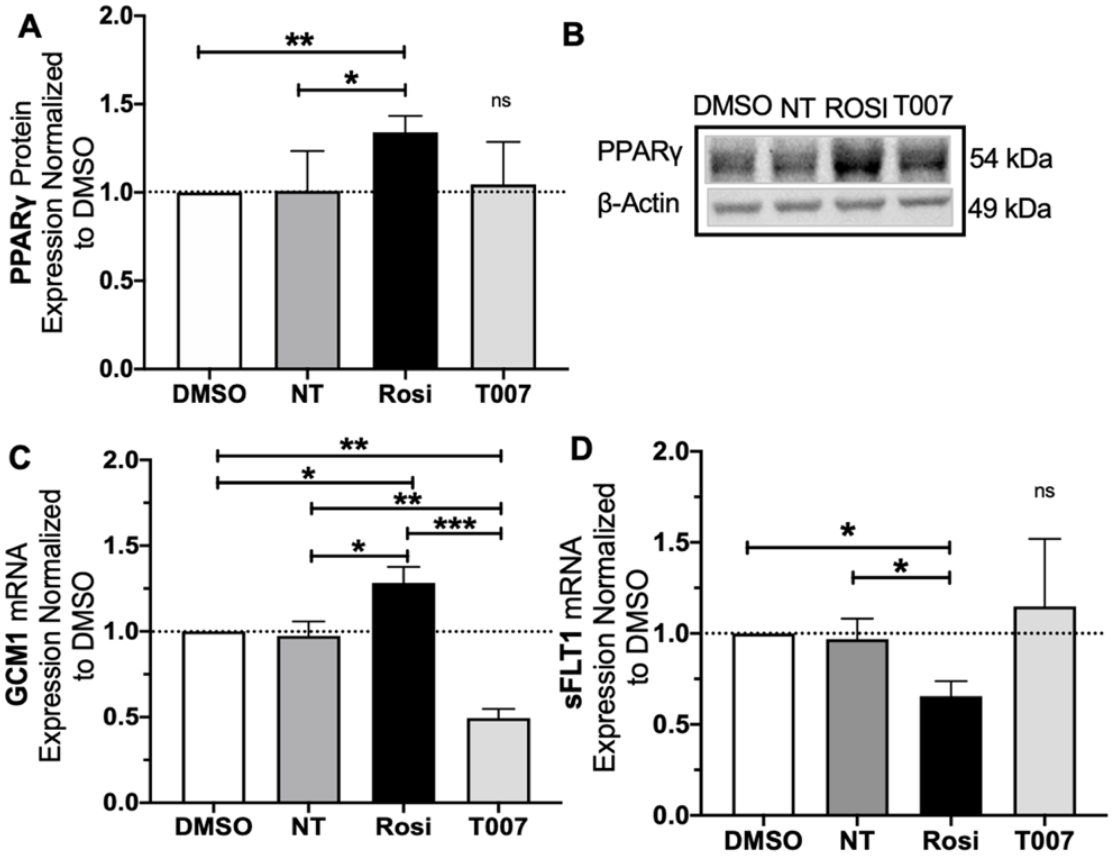

Figure 2.4: Rosiglitazone increases expression of PPARγ and GCM1 while simultaneously decreasing sFLT1 in sPE placenta. PPARγ protein expression significantly increased in sPE placenta after Rosiglitazone treatment (p=0.0051, n=4) **(A/B)**. GCM1 mRNA significantly increased in the sPE placenta by Rosiglitazone treatment (p=0.0162, n=9). GCM1 mRNA expression was significantly reduced in the sPE placenta after treatment with T0070907 (p=0.001, n=9) **(C)**. sFLT1 mRNA was significantly reduced in the sPE placenta after Rosiglitazone treatment. No significant change in sFLT1 mRNA expression was observed after exposure to T0070907 **(B)**. (*Relative mRNA/protein expressions were determined by normalization to respective housekeeping genes/protein. Relative expression values for individual tissue sets were normalized to DMSO (vehicle control, dotted line, set equal to 1) and subsequent statistical analysis was performed by student's t-test to determine significant differences between groups, *p<0.05, **p<0.01, ns=p>0.05, NT= not treated, Rosi=Rosiglitazone, T007=T0070907, bar plots are reported as mean ± SEM)*.

2.4. Discussion

In this study, we provide novel molecular evidence to demonstrate that FLT1 and its secreted splice variant, sFLT1, are regulated by a PPARγ–GCM1 axis in the trophoblast layer covering human placental villi. Under physiologic conditions, this axis

mediates orderly syncytiotrophoblast formation via asymmetric divisions of progenitor villous cytotrophoblasts [176], which in turn promotes PlGF synthesis and release into maternal blood, and in tandem, represses sFLT1 [16, 155, 160, 161]. Conversely, under sub-optimal PPARγ–GCM1 signaling, the placental villi show both structural and molecular defects characterized by defective syncytial fusion, repressed PlGF and aberrant release of sFLT1 into maternal blood [17, 167-170]. sFLT1 plays a major role in PE pathology as it promotes wide-spread endothelial dysfunction which largely contributes to the multi-organ dysfunction in the mother [31, 81, 177]. Highly secreted sFLT1 and its anti-angiogenic properties are well characterized in sPE placentas, where syncytial knot formation is one of the hallmarks of the maternal-vascular malformation disease [178, 179]. While FLT1 is known to be increased in tissues during vascular reoxygenation in response to hypoxic/ischemic insult [79] which similarly occurs in the PE placenta [33], the regulatory mechanism(s) of FLT1 and sFLT1 in the placenta remains unclear.

We observed higher sFLT1 secretion and higher protein expression of FLT1 in the PE placenta. Additionally, our immunohistochemistry staining identified that total-FLT1 protein (FLT1 and sFLT1 variants) exclusively localized to the syncytiotrophoblast in both control and sPE placenta and appears to have increased localization in the syncytial knots found in sPE tissue. Our data validates previous findings by Taché et al., who showed a correlation between high syncytiotrophoblast sFLT1 levels and PE disease severity [178]. In addition, Jebbink et al. showed syncytiotrophoblast specific localization of sFLT1 mRNA transcripts and higher sFLT1 mRNA in the PE placenta [158]. Together, these

data support the notion that the abnormal syncytiotrophoblast layer in PE may be the major source of high secretion of sFLT1.

Our data shows an inverse correlation between high FLT1 expression and sFLT1 secretion and low PPARγ and GCM1 expression in the PE placenta. This finding aligns with previous reports in the literature [17, 160, 161]. The relationship between PPARγ and sFLT1/FLT1 in the placenta was previously shown in a study by McCarthy et al., where a reduced utero-placental perfusion (RUPP) model was established to mimic PE in pregnant rats [70]. These RUPP animals showed significantly elevated levels of sFLT1 [70]. When treated with Rosiglitazone, these animals showed decreased blood pressure and decreased levels of sFLT1 [70]. In a separate study, McCarthy et al. treated pregnant rats with the PPARγ antagonist, T0070907, which caused these animals to develop PE-like symptoms such as elevated blood pressure and proteinuria accompanied by decreased VEGF and increased plasma levels of sFLT1 [35].

From this finding and our observations that PPARγ and GCM1 are inversely correlated with FLT1 expression, we hypothesized that a molecular connection exists between PPARγ, GCM1, and FLT1/sFLT1 in the human placenta, via repression of syncytin-mediated syncytial fusion. We used our first trimester placental explant model to test if this pathway can be modulated in the placenta. We used the PPARγ agonist, Rosiglitazone, and PPARγ antagonist, T0070907, to modulate this pathway. T0070907 antagonizes PPARγ by selectively binding to the PPARγ ligand binding pocket, preventing its activation by another ligand [180]. It is suggested that repressive ligands such as T0070907 do not have an effect on PPARγ protein expression levels [180], which could explain our finding that PPARγ protein expression was not significantly different in

first trimester placenta or in sePE placentas when treated with T0070907. Rosiglitazone acts as a chemical ligand for PPARγ by increasing its DNA-binding activity to influence gene expression [68] and is also shown to increase PPARγ transcription [181]. We confirmed that Rosiglitazone caused an increased in PPARγ activity in the first trimester explants and this coincided with a significant increase in PPARγ protein expression in the first trimester explants and in the sePE placenta. We observed that Rosiglitazone significantly upregulated GCM1 mRNA and significantly reduced sFLT1 secretion into placental media culture in our first trimester explant model. These results suggest that the PPARγ-GCM1 axis has a role in regulating the angiogenic environment of the placenta via sFLT1.

We further questioned whether the changes observed in sFLT1 secretion were a direct result from PPARγ activation or if GCM1 may serve as an intermediate in this pathway to modulate FLT1 expression, since PPARγ transcriptionally regulates GCM1 through two PPARγ response elements in the promoter region of GCM1 [36]. We show that siRNA mediated repression of GCM1 in our first trimester villous explants caused a significant upregulation of sFLT1 secretion, as well, caused an increase in FLT1 protein expression in the syncytiotrophoblast, observed through immunohistochemistry. Our findings align with previous studies that showed a heterozygous knockdown of Gcm1 in the mouse led to increased secretion of sFLT1 [161]. These results suggest that GCM1 may be involved in FLT1 regulation and a decrease of GCM1 expression may contribute to the anti-angiogenic state during PE through upregulation of sFLT1. We lastly show that this pathway is not unique to the first trimester placenta and can be modulated in the

diseased severely preeclamptic placenta. We found that activation of PPARγ in sPE placenta increased GCM1 and reduced sFLT1 mRNA expression.

In the current study, we show for the first time that activation of PPARγ can modulate the angiogenic environment of the human placenta by altering expression of GCM1, FLT1 and sFLT1. More studies are needed for better understanding of how this pathway impacts placental function and physiology during the second and third trimesters of pregnancy, when the high anti-angiogenic environment in PE becomes largely problematic. We acknowledge the limitations of our study, such as small sample size which necessitates follow up studies with larger cohorts. We were unable to observe an effect based on mode of delivery however this should be considered as a confounding factor in future studies. To our knowledge, we report novel findings of PPARγ, GCM1 and sFLT1 in the placenta, although we have not clearly demonstrated that a direct or indirect interaction between these molecules exist. Further studies should focus on potential direct or indirect effects of GCM1 and PPARγ at the promoter region of FLT1 to regulate FLT1, such as by interacting with promoter elements, co-factors or splicing machinery to directly influence gene expression or protein secretion of FLT1 and its splice variants. Moreover, future studies should consider how modulating this pathway could affect overall angiogenic balance, such as through increasing secretion of PIGF and VEGF from the placenta. Detailed molecular studies investigating these targets potentially using both *in vivo* and *in vitro* models with knockdown or knockout of PPARγ and GCM1 are needed to fully understand this potential mechanism and their effects on overall placental function.

3. CHAPTER 2. PPARY ACTIVATION BY ROSIGLITAZONE RESTORES HO1 IN THE PREECLAMPTIC PLACENTA VIA DIRECT TRANSCRIPTIONAL UPREGULATION

3.1. Introduction

Preeclampsia (PE), a hypertensive disorder of pregnancy, is the leading cause of maternal and fetal morbidity and mortality world-wide. Without a cure or treatment for PE, women may be required to deliver the fetus and placenta early to reduce symptoms in the mother and to prevent immediate and long-term complications in the infant [23, 182-185]. While the ultimate cause of PE remains unknown, abnormal placental development and function is thought to cause an imbalance of angiogenic proteins that are secreted from the placenta, impairing endothelial function, and ultimately causing hypertension and organ damage in the mother [24]. It would therefore be advantageous to understand how disruption of the molecular mechanisms of normal placental function contribute to PE and to further target these pathways as a method of therapeutic intervention.

The transcription factor and nuclear hormone receptor, peroxisome proliferator-activated receptor-γ (PPARγ) regulates genes in several cellular pathways including cell differentiation, oxidative stress, nutrient balance, and anti-inflammatory pathways [68]. Many studies have identified the essential roles of PPARγ in human placenta development and function, such as promoting villous trophoblast differentiation and turnover [12]. PPARγ expression is also reported to be decreased in the PE placenta and other animal-based studies have described that reduced activity and expression of PPARγ is likely implicated in development of PE [23]. Fortunately, many studies show that aberrant trophoblast differentiation and function in pathological conditions can be restored when PPARγ is activated by Rosiglitazone [18, 69, 70, 186-189].

Major disruptions to heme oxygenase 1 (HO1) expression and activity are implicated in several diseases, including cardiovascular and metabolic disease, and PE [2, 126, 129, 132, 141, 190-194]. The reduction of HO1 in PE is a major contribution to the exacerbated oxidative stress, endothelial dysfunction, high inflammation, and immune imbalances that are present in the placenta and systemically in women with PE [2, 127, 128, 132]. HO1 is an inducible cytoprotective molecule that initiates the metabolism of heme into free Fe^{2+}, CO and BV/BR [128, 131]. HO1, as well as its metabolites, have a significant impact on maintaining cytoprotection from oxidative stress, excessive inflammation, and aims to reduce blood pressure and cardiovascular disease though maintaining endothelial relaxation and vasodilation [2]. The induction of this molecule may serve an important role in decreasing the hypertension and endothelial dysfunction in the mother during pathological conditions such as PE. Hypertension is described as an imflammatory disease, with macrophages in a predominat M1 phase that induce high levels of pro-inflammatory cytokines and oxidative stress [131]. HO1 is an important target for the prevention of hypertension and reducing end organ damage based on its ability to shift the macrophage polarization towards the M2 anti-inflammatory phenotype that acts in addition to all the positive effects from the heme metabolism initiated by HO1 [131].

Several studies have highlighted the importance of targeting HO1 for restoring placental function in PE and coincidentally, the ability for PPARγ to modulate HO1 expression has been reported as well [126, 186]. PPARγ activation has been shown to upregulate HO1 and inhibit inflammation during lung injury [195] and in mouse models of asthma [196]. McCarthy et al. also show that activating PPARγ via Rosiglitazone in a

placental-hypoxia rat model reverses the 'preeclampsia phenotype' by decreasing hypertension and increasing the secretion of vasodilatory proteins, like HO1 [197].

While animal models show that PPARγ activation can increase HO1, it is not clear if this occurs in the human placenta and the mechanism behind PPARγ-driven HO1 upregulation remains unknown. In this study, we hypothesized that the PPARγ-HO1 mechanism could be enhanced in the human placenta to restore placental function and we further hypothesized that HO1 induction occurs based on direct transcrition regulation by PPARγ. To test this hypothesis, we used human placental tissues from first trimester, healthy, and preeclamptic pregnancies and treated with the PPARγ-activating drug, Rosiglitazone, to determine if this pathway is altered in the human placenta. We also developed an *in vitro* model to recapitulate the oxidative-stress conditions of the preeclamptic placenta using the human placenta-derived immortalized cell line, BeWo, that were subjected to hypoxia re-oxygenation conditions. We activated PPARγ in this model via Rosiglitazone and inhibited PPARγ via siRNA to understand how changes in PPARγ expression influenced HO1. We further employed protein:DNA binding assays to determine if PPARγ is able to bind at the HO1 promoter to regulate HO1 gene expression. This study highlights the beneficial molecular actions of PPARγ to support PPARγ-activation as a potential therapeutic intervention for women with PE.

3.2. Methods

3.2.1. Tissue collection

First trimester (10–12 weeks of gestation) placental tissues (n = 4) were obtained with written informed consent from healthy pregnant women undergoing elective termination of pregnancy. These tissues were collected and cultured between the years of 2013-2017 at Wayne State University. The Institutional Review Board of Wayne State

University approved all consent forms and protocols used in this study, which abide by the NIH research guidelines. Term placental samples were obtained either by the Research Centre for Women's and Infants' Health BioBank program of Mount Sinai Hospital in Toronto, Canada, in accordance with the policies of the Mount Sinai Hospital Research Ethics Board or Women's Health Center at Spectrum Hospital in Grand Rapids, MI. All placentas collected were approved by the IRB waiver of parental consent. Specimens were collected from age-matched idiopathic preterm without histological evidence of chorioamnionitis not complicated by PE (PTC) (n = 14; gestational age = 31-37 weeks), and pregnancies complicated by PE (n = 14; gestational age = 31-37 weeks) and were delivered either by Cesarean section or vaginal birth. Inclusion criteria for PE was in accordance with current guidelines including blood pressure > 140/90 mm Hg on two occasions longer than 6 hr apart, with or without proteinuria and fetal growth restriction [171].

3.2.2. Explant culture

Term tissues were cultured using a standardized random sampling protocol that consisted of dissecting random four 1cm^3 cuboidal sections to avoid sampling bias. The collected tissues were washed and transported to the laboratory in ice cold HBSS (Hank's Balanced Salt Solution) and processed within a maximum of 2 hr after delivery. On arrival, tissues were rinsed in chilled HBSS to remove residual blood and further dissected under a stereomicroscope to remove placental membranes and generate 20-30mg pieces of villous tissues for culture. First trimester explants were cultured according to our previously published floating villous explant protocol [9]. Individual clusters of villous trees were dissected under a stereomicroscope. Post dissection, the explants were cultured overnight in 500μL of Dulbecco's modified Eagle's medium/Ham's F-12 nutrient mixture

(DMEM/F-12; 1:1; Life Technologies; Grand Island, NY) containing 10% fetal bovine serum (FBS; Life Technologies) and 1% Gibco™ antibiotic-antimycotic. Term explants were maintained overnight at 8% O2 with 5% CO2 at 37°C [10]. After an overnight culture, the tissues were treated with 10μM Rosiglitazone (Selleckchem) dissolved in dimethyl sulfoxide (DMSO, Sigma Life Sciences) for 18-24 hours. DMSO alone was used as a vehicle control. Comparison of DMSO to NT (not treated placental tissues) was performed to ensure there was not an effect from DMSO. After the culture period for each treatment, replicates were snap frozen for protein and RNA extraction and stored at -80ºC. The media was also collected, snap frozen and stored at -80°C.

3.2.3. Human trophoblast cell culture

The BeWo choriocarcinoma cell line was cultured in Dulbecco's modified Eagle's medium/Ham's F-12 nutrient mixture (DMEM/F-12; 1:1; Life Technologies; Grand Island, NY) containing 10% fetal bovine serum (FBS; Life Technologies) and 1% Gibco™ antibiotic-antimycotic. The cell culture medium was changed every two to 3 days and cells were passaged with trypsin-ethylenediaminetetraacetic acid (EDTA) solution (Life Technologies). Cells were cultured in normal oxygen conditions (20% O_2) or hypoxia re-oxygenation (H/R; 18-hours of 1.5% O_2 in serum free media followed by 18-hours of 20% O_2). 10μM Rosiglitazone (Selleckchem) dissolved in dimethyl sulfoxide (DMSO, Sigma Life Sciences) was applied to the cells to study effects of PPARγ activation. In H/R experiments, Rosiglitazone was applied during re-oxygenation (20% O_2).

3.2.4. Protein extraction and immunoblotting

Protein extraction from tissues was performed as previously described [172]. Protein was extracted from BeWo cell culture using Pierce RIPA buffer (Thermo Fisher Scientific, Rockford, IL) supplemented with Halt Protease and Phosphatase Inhibitor

Cocktail (Thermo Fisher Scientific, Rockford, IL). Protein concentration was determined with BCA™ protein assay reagent (Thermo Fisher Scientific, Rockford, IL) according to the manufacturer's instructions. Equal protein amounts (25µg) were denatured (8 min, 95°C) in Laemmli sample buffer (Bio-Rad Laboratories; Hercules, CA) and separated using sodium dodecyl sulfate-polyacrylamide gel electrophoresis, with subsequent semi-dry transfer (Trans-Blot®; Bio-Rad Laboratories) to a polyvinylidene difluoride membrane. The membranes were blocked with 5% nonfat dry milk in 1× Tris-buffered saline containing 0.05% Tween-20 and were incubated overnight at 4°C with anti-HO1 (1:1,000; Cell Signaling Technologies) and anti-PPARγ (1:500; Santa Cruz) primary antibodies. Subsequently, membranes were incubated with horseradish peroxidase-conjugated secondary antibodies for 1 hr at room temperature and were developed with Western Lightning® ECL Pro (PerkinElmer, Waltham, MA). Signals were visualized using a ChemiDoc™ Imaging System (Bio-Rad Laboratories) and Image Lab Version 5.1 software (Bio-Rad Laboratories). Densities of immunoreactive bands were measured as arbitrary units by the ImageJ software (NIH, Bethesda, MD). Protein levels were normalized to a housekeeping protein β-actin (1:4,000; Cell Signaling Technologies). Protein expression values are reported as relative to β-actin.

3.2.5. ELISA

The media collected from PE, PTC, first trimester placental explant cultures and BeWo cell culture was assayed for levels of HO1 using the HMOX1 ELISA Kit (Aviva Systems Biology, San Diego, CA) according to the manufacturer’s instruction. Culture media was centrifuged at 4,500 x g for 10 minutes at 4°C to pellet all cell/tissue debris and the supernatant was used for ELISA analysis. The optical density of the final-colored

reaction product was measured at 450 nm using a SoftMax Pro5 plate reader. A standard curve was used to calculate protein content, and the results were normalized over protein concentration of the explant/cell culture.

3.2.6. RNA extraction and qPCR

The tissue and cells were lysed in Qiazol, and RNA was extracted using RNeasy Plus Universal Mini kit (Qiagen, Germany) as per the manufacturer's protocol. The extracted RNA was quantified using Nanodrop and 500ng of nucleic acid was reverse transcribed using iScript RT synthesis kit (Bio-Rad Laboratories, CA) according to the manufacture's instruction. Real-time PCR was performed on the Bio-Rad CFX384 real time system in triplicates in 10µL total reaction volume containing 10ng of template cDNA, 5µL of SYBR-green master mix (LuminoCT, Sigma-Aldrich, MO) and 500nM of primers. The primers used for assessing the expression levels of target and housekeeping genes are outlined in Table 2. Data was analyzed using the delta-delta CT method as previously described [173].

Table 3.1: Chapter 2 qPCR Primer Sequences

Gene Name	Gene Symbol	Sequence
Cytochrome C1	*Cyc1*	F: 5′-CAT CAT CAA CAT CTT GAG CC-3′ R: 5′-CAG ATA GCC AAG GAT GTG TG-3′
Tyrosine 3-monooxygenase	*Ywhah*	F: 5′- CCG CCA GGA CAA ACC AGT AT -3′ R: 5′- ACT TTT GGT ACA TTG TGG CTT CAA -3’
TATA box binding protein	*Tbp*	F: 5′-CAC ATC ACA GCT CCC CAC CA-3′ R: 5′-TGC ACA GGA GCC AAG AGT GAA-3′
Glial cell missing 1	*Gcm1*	F: 5′-TGA ACA CAG CAC CTT CCT C-3′ R: 5′-CCA CTG TAA CTA CCA GGC AAT-3′
Heme oxygenase 1	*Hmox1*	Hs.PT.58.45340055 Commercially available from Integrated DNA Technologies (Coralville, IA)

3.2.7. Immunohistochemistry

Immunostainings of first trimester placental villi were performed as previously described [174]. Briefly, the sections were deparaffinized and rehydrated, followed by antigen retrieval using Dako Target retrieval solution (Agilent-DAKO, USA). The intrinsic peroxidase activity was then quenched by incubating the sections with 3% Hydrogen peroxide (Fisher Scientific, MA) for 30 mins at RT, followed by a wash with 1X PBS. The sections were then incubated overnight at 4°C with anti-HO1 (Santa Cruz, TX) or 10µg/ml nonimmune Rabbit IgG (Jackson Immunoresearch, PA) which was used as a negative control. The following day, the slides were washed 3 times (5 minutes/wash) with 1X PBS containing 0.1% Tween 20. The samples were then incubated for 30 min with a peroxidase-conjugated polymer coupled to anti-rabbit IgG (EnVision Systems Peroxidase, Agilent-DAKO, USA). The peroxidase was visualized with 3,3-diaminobenzidine (DAB, Agilent-DAKO, USA) and hydrogen peroxide for 5 min. Tissues were counterstained with hematoxylin, dehydrated and were cover slipped. The staining was visualized using Nikon Eclipse 90i epifluorescence microscope (Nikon Inc., Japan).

3.2.8. siRNA-mediated PPARγ suppression

Predesigned PPARγ siRNAs (sc-29455, Santa Cruz Biotechnology, Dallas, TX) were used for PPARγ suppression and a 6-FAM-labeled scramble sequence (scramble siRNA) was used a negative control (Sigma Aldrich). siRNA experiments were performed according to manufacturer's instruction. Briefly, cells were seeded in a 6-well plate and grown to 60% confluency. DMEM-F12 media was removed, and cells were incubated with Opti-MEM Reduced Serum Media (Gibco) for 30 minutes. A solution of 50µM siRNAs were prepared using GenMute Transfection Buffer (SignaGene Laboratories, Ballenger Creek, MD) and GenMute Transfection Reagent (SignaGene Laboratories, Ballenger

Creek, MD) and added to the cells. After 5 hours of incubation with siRNAs, the medium was removed and replaced with DMEM-F12. Cells were cultured for another 72 hours before RNA and protein was collected.

3.2.9. Immunoprecipitation

Immunoprecipitation (IP) was performed using the Pierce Classic Magnetic IP/Co-IP Kit (ThermoFisher, Waltham, MA) according to the manufacture's instruction. Briefly, BeWo cells were grown to 80% confluency in a T-75 flask. Cells were removed via trypsin and counted. Two million cells were used per IP and aliquoted into 1.5mL tubes. Cells were washed with 1X PBS, then incubated in IP Lysis/Wash Buffer with the addition of 1X Protease and Phosphatase Inhibitor (ThermoFisher, Waltham, MA). Samples centrifuged at 13,000 X g for 10 minutes at 4ºC and the supernatant was incubated with 5µg of antibody overnight with mixing at 4ºC to form the antibody:protein complex. One sample was saved as the input. The following day, the Pierce Protein A/G magnetic beads were aliquoted into 1.5mL tubes and washed twice with IP Lysis/Wash Buffer. The antibody:protein mixture was added to the magnetic beads and mixed with rotation for 1 hour at room temperature. The tubes were placed on a magnetic rack and the supernatant was saved as the 'unbound' fraction. The antibody:protein:bead mixture was washed twice with IP Lysis/Wash Buffer and once with ddH_2O and finally elution buffer was added to the tube and samples were incubated for 10 minutes. The tubes were placed on a magnetic rack and the supernatant was saved as the 'bound' fraction. Neutralization buffer was added to the bound fraction. Magnetic beads were resuspended in 100uL of ddH_2O. All fractions were incubated with loading buffer at 98ºC for 8 minutes before running on a western blot.

3.2.10. Cleavage under targets and release using nuclease

CUT&RUN was performed using the CUT&RUN Assay Kit (Cell Signaling Technologies, Danvers, MA) according to the manufacture's instruction. Briefly, BeWo cells were grown in a T-25 flask to 80% confluency and removed via trypsin to generate a cell suspension. 200,000 cells were aliquoted for each sample in the CUT&RUN assay. The remaining cells were lysed in Qiazol for RNA collection. 20µL of magnetic Concalvalin A (ConA) beads were used per reaction and were aliquoted into respective tubes and washed with ConA bead activation buffer. Cells were washed in 1X Wash buffer then incubated with ConA beads at room temperature for 10 minutes with spinning. Cell:bead mixture was washed and incubated with spinning overnight at 4ºC with three different PPARγ antibodies (5µg Sc-7273, Santa Cruz, San Diego, CA; 5µg 81B8, Cell Signaling Technologies, Danvers, MA; 5µg PA3-821A ThermoFisher, Waltham, MA), H3K4Me3 antibody was used as the positive control (C42D8 Cell Signaling Technologies, Danvers, MA) and 5µL of Rabbit IgG (Cell Signaling Technologies, Danvers, MA) or 5µg Mouse IgG (Santa Cruz Biotechnology, Dallas, TX) were used as controls. The following day, the samples were washed in wash buffer and incubated with pAG-MNase enzyme at 4ºC for 1 hour with spinning. Next, the samples were incubated with calcium chloride for 30 minutes at 4ºC to activate the pAG-MNase enzyme. Stop solution was added to the solution and samples were incubated at 37ºC for 30 minutes. Samples were spun at 14,000 x g for 2 minutes at 4ºC and then incubated on a magnetic rack for 2 minutes, then the supernatant was collected which contains the enriched chromatin sample. The DNA samples were purified using the Macherey-Nagel PCR clean-up and Gel Extraction Kit according to the manufacture's instruction. The Input sample DNA was extracted using a DNeasy Kit (Qiagen, Hilden, Germany) followed by 12 rounds of 30 seconds on and 30

seconds off sonication using the Bioruptor Plus Sonication device (Diagenode, Denville, NJ). Quantitative PCR was performed to determine if there was a significant enrichment of PPARγ at the HO1, GCM1, and FABP4 promoters. Primer sequences for CUT&RUN (listed in Table 3.2) were designed based on *in silico* prediction of PPARγ putative binding sites using the LASAGNA-Search 2.0 Transcription Factor Binding search tool [198]. This bioinformatics tool uses a Length-Aware Site Alignment Guided by Nucleotide Association (LASAGNA) algorithm to search for transcription factor binding sites throughout the genome. The University of California Santa Cruz Genome Browser was then used to visualize where the predicted binding sites are occurring in the promoter region and identify if the binding sites also occur in the active promoter regions [198].

Table 3.2: CUT&RUN qPCR Primer Sequences

Gene Name	Gene Symbol	Primer Sequences
Heme oxygenase 1	*Hmox1*	F: TCCTATGGCCAGACTTTG R: GTGTGGGGTGGAGAGGAG
Glial cell missing 1	*Gcm1*	F: AGACGCTGTTCCCTATTC R: GAGTTCTGGCAATGGTCC
Fatty acid binding protein 4	*Fabp4*	F: TTCAAGGTGAGAAGGAAG R: AGGAAGTTATCTGGACTC

3.2.11. Statistical Analysis

All statistical analysis was performed with GraphPad Prism 7.0 software. Raw mRNA and protein expressions were normalized to respective housekeeping genes or protein. Relative mRNA and protein expression values from tissues or cells treated with either DMSO and Rosiglitazone or PPARγ-siRNA and scramble siRNA were normalized to respective housekeeping genes or protein, then the relative expression or secretion values for each tissue or biological replicate set were subsequently normalized to respective DMSO (vehicle control, set equal to 1) or scramble siRNA control (set equal to 1). ELISA data was normalized based on protein concentration. Groups were then

analyzed by student's t-test, after determination if samples are normally distributed and an F-test was applied to determine variances between groups which was then used in the parameters for the t-test. $p<0.05$ is considered significant and is indicated with (*) on each graph. Data is reported as Mean±S.E.M. All sample numbers are reported as per group, for example, n=6 designates 6 samples per treatment/group.

3.3. Results

3.3.1. Cultured preeclamptic placentas exhibit reduced protein expression of PPARγ and HO1 and reduced HO1 secretion compared to control placentas.

Preeclamptic and gestation-age matched controlled placentas were cultured for 48 hours and placental tissues as well as conditioned media were harvested. Placental protein expression of PPARγ and HO1 was measured by western blotting. We identified a significant reduction of PPARγ protein expression in PE placentas compared to pre-term controls (PTC) (0.47±0.13 vs. 1.03±0.11 relative expression values, p=0.01, n=7, Figure 3.1A). In addition, we observed a significant reduction of HO1 protein expression (0.79±0.1 vs. 0.34±0.06 relative expression values, p=0.0045, n=7, Figure 3.1B) and a significant reduction of HO1 secretion (as measured by ELISA) in PE compared to PTC (99±8.2 pg/mL vs. 141.0±16 pg/mL, p=0.0476, n=7, Figure 3.1C).

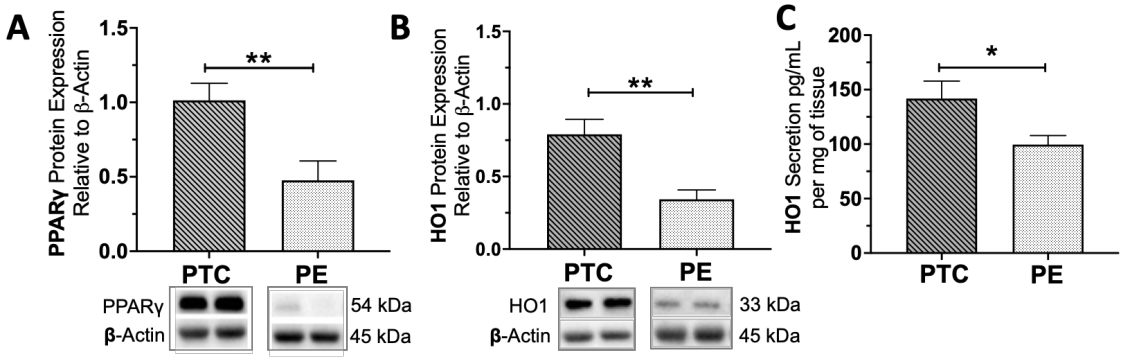

Figure 3.1: PPARγ and HO1 are reduced in the preeclamptic placenta. Cultured human preeclamptic (PE) placentas exhibit significant less protein expression of PPARγ (A) and HO1 (B) and as well secrete significantly less HO1 (C) compared to preterm controls (n=7). (*Relative protein expression was determine by normalization to β-Actin, followed by a student's t-test to determine significant differences between groups, * p<0.05, ** p<0.01, n=7, bar plots and data reported are presented as mean ± SEM, PE = preeclampsia, PTC = preterm healthy control, HO1=Heme oxygenase 1).*

3.3.2. A cell-based model of ischemia-reperfusion injury shows a reduction of PPARγ and HO1 protein expression and HO1 secretion.

BeWo cells were cultured in serum-free media in 24-hours of hypoxia (1.5% O_2) followed by 18-hours of normoxia (20% O_2) (H/R) to mimic the ischemia-reperfusion injury that occurs in PE [199]. Protein expression of PPARγ and HO1 were measured by western blotting. PPARγ protein expression was significantly reduced during H/R conditions compared to normoxia (0.37±0.12 vs. 0.9±0.08 relative expression values, p=0.026, n=5, Figure 3.2A). In addition, HO1 protein expression was significantly reduced in H/R compared to normoxia (0.54±0.09 vs. 0.9±0.09 relative expression values, p=0.045, n=7, Figure 3.2B). HO1 secretion into the cell culture media as measured by ELISA and was significantly reduced in H/R compared to normoxia (1681±129 pg/mL vs. 2666±170 pg/mL, p=0.01, n=5, Figure 3.2C). These data suggest the BeWo H/R model can recapitulate *in vitro* the reduction of PPARγ and HO1 during ischemic-reperfusion conditions.

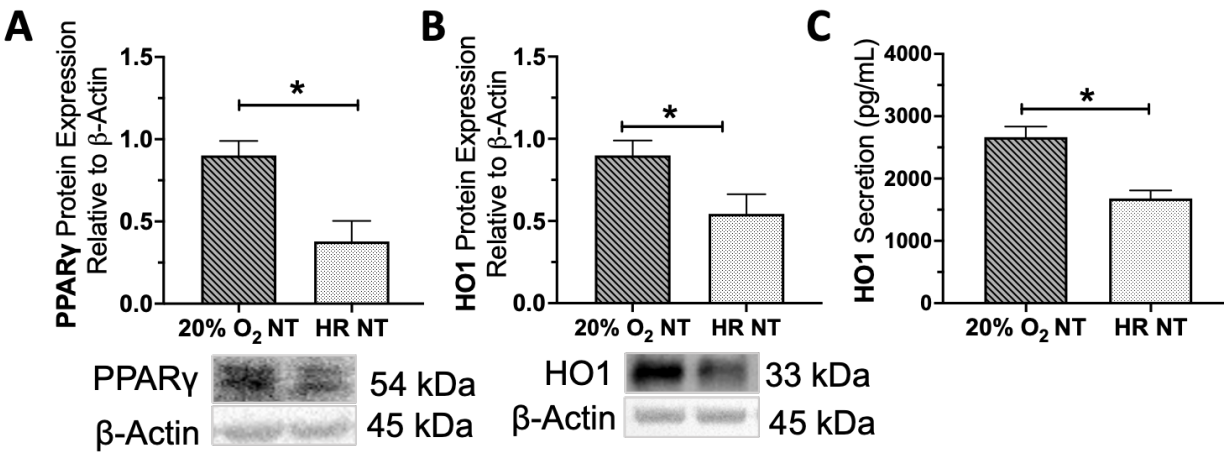

Figure 3.2: *In vitro* ischemia-reperfusion causes a reduction of PPARγ and HO1. BeWo exposed to HR mimics the reduced PPARγ (A) and HO1 protein expression (B) and HO1 secretion (C) observed in the PE placenta (n=3). *(Relative protein expression was determine by normalization to β-Actin, followed by a student's t-test to determine significant differences between groups, * p<0.05, ** p<0.01, n=7, bar plots and data reported are presented as mean ± SEM, NT=No Treatment, HR=Hypoxia Re-Oxygenation).*

3.3.3. Rosiglitazone rescues HO1 expression and secretion in the preeclamptic placenta and in a cell-based model of ischemia-reperfusion injury.

To test if PPARγ activation influences HO1 expression and secretion, we treated PE placentas, first trimester placental explants, and BeWo cells cultured in H/R conditions with Rosiglitazone or vehicle. Rosiglitazone-treated PE placentas show a significant increase of HO1 gene expression (1.213±0.17 vs. 1 relative expression values, n=6, p=0.0069, Figure 3.3A) and protein expression (1.7±0.07 vs. 1 relative expression values, n=7, p=0.01, Figure 3.3A) as well as an increase in HO1 protein secretion (1.16±0.02 vs. 1 relative expression values, n=9, p=0.017, Figure 3.3A) in comparison to the vehicle control. BeWo cultured in H/R conditions and treated with Rosiglitazone mimicked the significant increase of HO1 gene expression (2.15±0.02 vs. 1±0.03 relative expression values, n=6, p=0.004, Figure 3.3B), protein expression (1.25±0.05 vs. 1±0.02 relative

expression values, n=6, p=0.009, Figure 3.3B), and protein secretion (1.67±0.2 vs. 1±0.01 relative expression values, n=6, p=0.025, Figure 3.3B) in comparison to the vehicle control. An overnight culture of first trimester placentas treated with Rosiglitazone also caused a striking increase of HO1 protein expression (1.75±0.32 vs 1 relative expression values, n=4, $p<0.05$, Figure 3.3C) and HO1 protein secretion into the culture media (1.45±0.22 vs. 1 relative expression values, n=4, $p<0.05$, Figure 3.3C) in comparison to the vehicle control. Immunohistochemical staining of first trimester explants treated with Rosiglitazone shows an increase of HO1 production in the syncytiotrophoblast layer of the first trimester explant compared to the vehicle control (Figure 3.3D).

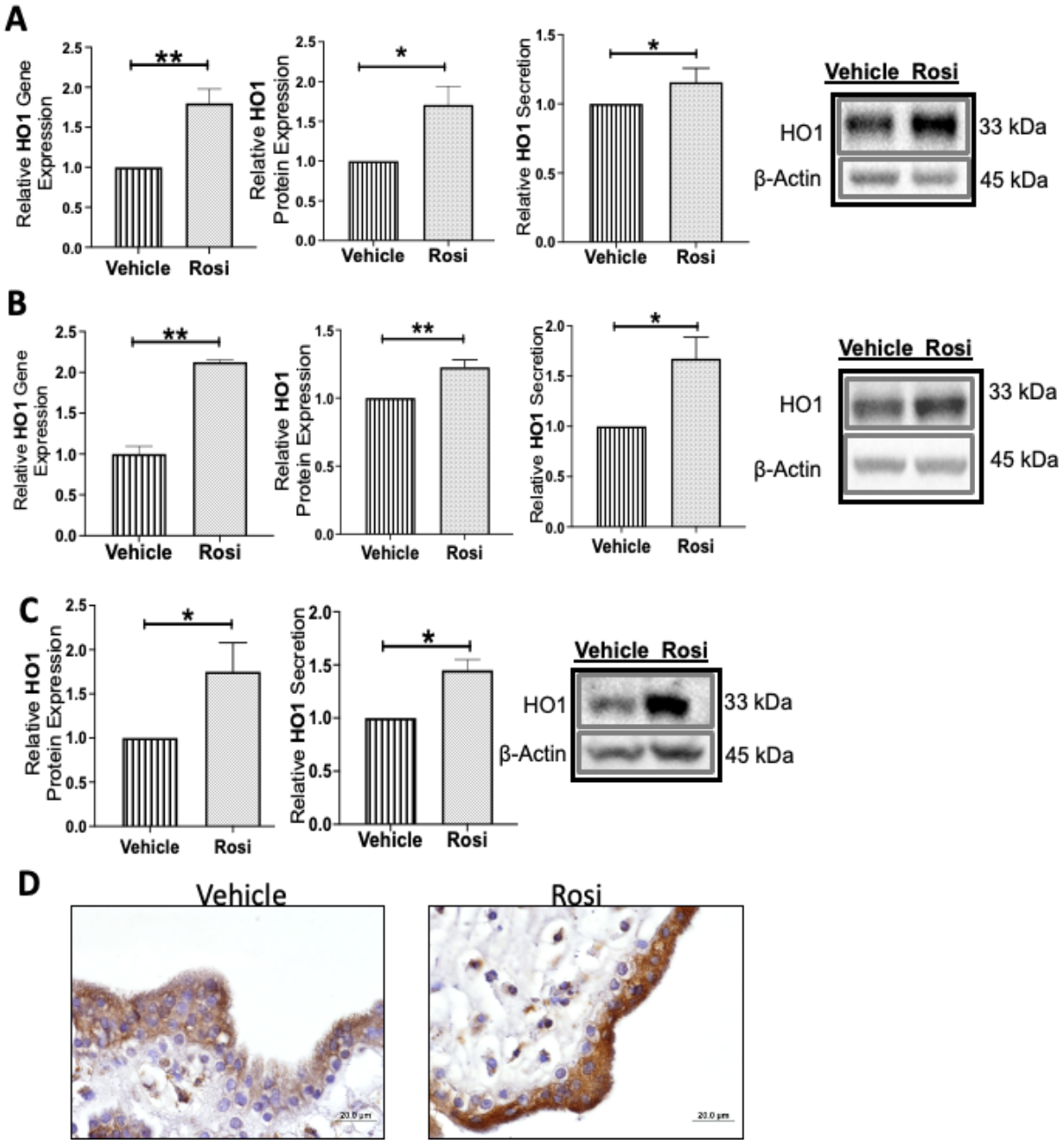

Figure 3.3: Rosiglitazone restores HO1 expression in preeclamptic placentas, first trimester placentas and during *in vitro* ischemia-reperfusion injury. PPARγ induction by Rosiglitazone causes a significant increase in HO1 gene and protein expression in the preeclamptic placenta, in addition to a significant increase in HO1 secretion (A, n=6). BeWo cultured in H/R conditions show a significant increase in HO1 gene expression, protein expression, and protein secretion when treated with Rosiglitazone (B, n=6). First trimester explants treated with Rosiglitazone also show a significant increase in HO1 protein expression and HO1 secretion into the culture media (C, n=4). Moreover, a qualitative assessment of HO1 staining revealed strong HO1 production in the syncytiotrophoblast layer of the first trimester placenta (D) when treated

Figure 3.3 (cont'd)
with Rosiglitazone. *(Relative mRNA and protein expression were determine by normalization to housekeeping genes or protein. ELISA data was normalized to total protein content or semi-dry tissue weight. Relative expression or secretion values for individual tissue or sample sets were normalized to vehicle control (DMSO, set equal to 1) and subsequent statistical analysis was performed by student's t-test to determine significant differences between groups, *p<0.05, **p<0.01, Rosi=Rosiglitazone, bar plots and data reported are reported as mean ± SEM).*

3.3.4. HO1 induction is PPARγ-dependent.

We next questioned if HO1 expression is directly influenced by PPARγ. To test this, PPARγ expression was reduced via siRNA in BeWo cells and expression of PPARγ and HO1 were measured by qPCR and western blotting. PPARγ-siRNA treatment led to a 90% reduction of PPARγ gene expression (0.09±0.01 vs. 1 relative expression values, n=3, p<0.0001, Figure 3.4A) and a 53% reduction of PPARγ protein expression (0.47±0.01 vs. 1 relative expression values, n=3, p=0.0004, Figure 3.4A) when compared to the scramble siRNA control. The siRNA-mediated reduction of PPARγ led to a 44% reduction of HO1 gene expression (0.56±0.06 vs. 1 relative expression values, n=3, p=0.0029, Figure 3.4B) and a 40% reduction of HO1 protein expression (0.6±0.1 vs. 1 relative expression values, n=3, p=0.0285, Figure 3.4B) when compared to the scramble siRNA control.

We next treated the PPARγ-silenced cells with Rosiglitazone to determine if the prior observed upregulation of HO1 by Rosiglitazone occurs in a PPARγ-dependent manner. In the scramble-siRNA control cells, Rosiglitazone significantly increased HO1 protein expression compared to vehicle-treated scramble-siRNA cells (1.17±0.13 vs 0.77±0.02 relative expression values, n=3, p=0.0416, Figure 3.4C). In the PPARγ-siRNA treated cells, Rosiglitazone did not change HO1 expression in comparison to the vehicle control (0.43±0.03 vs 0.56±0.07 relative expression values, n=3, p=0.17, Figure 3.4C).

HO1 protein expression was significantly reduced in the PPARγ siRNA-Rosiglitazone treated cells in comparison to the scramble-siRNA control cells which were treated with DMSO (0.43±0.03 vs 0.77±0.02 relative expression values, n=3, p=0.011, Figure 3.4C) and Rosiglitazone (0.43±0.03 vs 1.17±0.13 relative expression values, n=3, p=0.0053, Figure 3.4C).

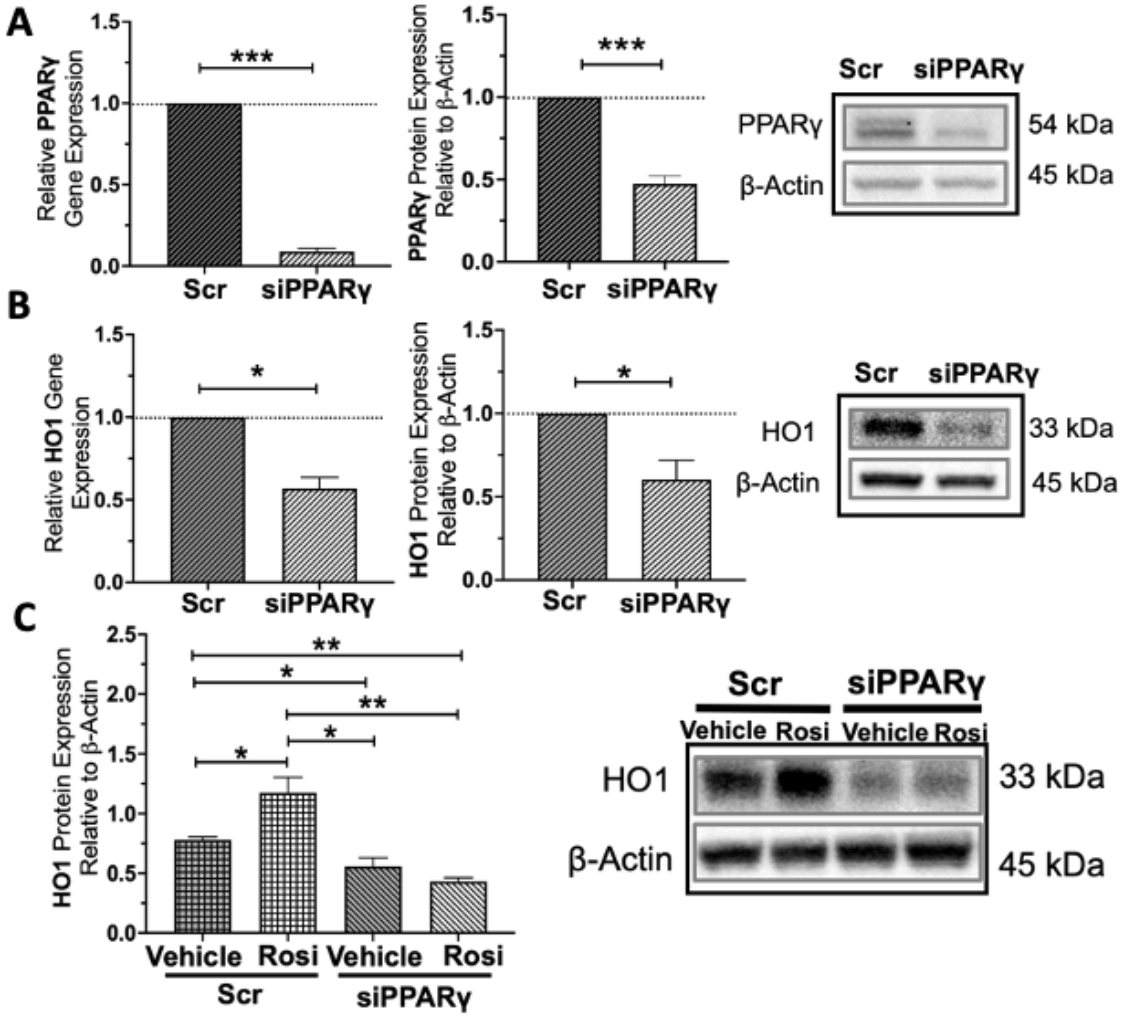

Figure 3.4: siRNA-mediated reduction of PPARγ significantly decreased HO1 expression that were not rescued by Rosiglitazone. PPARγ siRNA caused a significant reduction of PPARγ gene and protein expression (A, n=3) and HO1 gene and protein expression (B, n=3) when compared to the scramble siRNA control. Scramble-siRNA treated cells were simultaneously treated with Rosiglitazone and caused a significant increase in HO1 protein expression in comparison to the scramble-siRNA treated vehicle control (C, n=3). In the PPARγ-silenced cells, Rosiglitazone could not

Figure 3.4 (cont'd)
increase HO1 protein expression when compared to vehicle-treated PPARγ-silenced cells (C, n=3). HO1 protein expression was significantly reduced in both vehicle and Rosiglitazone treated PPARγ-silenced cells in comparison to the Rosiglitazone and vehicle-treated scramble siRNA-treated cells, which collectively suggests a PPARγ-dependent mechanism for HO1 regulation. (*Relative mRNA and protein expression were determine by normalization to housekeeping genes or protein. Relative expression values for sample sets were normalized to scramble siRNA control (set equal to 1) and subsequent statistical analysis was performed by student's t-test to determine significant differences between groups, *p<0.05, **p<0.01, ***p<0.0001, Rosi=Rosiglitazone, Scr=scramble siRNA, siPPARγ=PPARγ siRNA, bar plots and data reported are reported as mean ± SEM).*

3.3.5. *In silico* analysis reveals putative PPARγ binding site in HO1 promoter region

To test the hypothesis that HO1 induction be completed by direct transcriptional upregulation by PPARγ, we first performed *in silico* analysis to identify if any PPRE sites exist in the promoter region of HO1 using the LASAGNA-Search 2.0 Transcription Factor Binding search tool [198]. Our search results show one PPRE site in the active HO1 promoter, that contains 11 statically significant overlapping nucleotides in the promoter and with the known PPARγ binding sequence (Figure 3.5A,B). With this knowledge, one set of primers were designed for qPCR to amplify the DNA flanking where PPARγ is predicted to bind (Figure 3.5C).

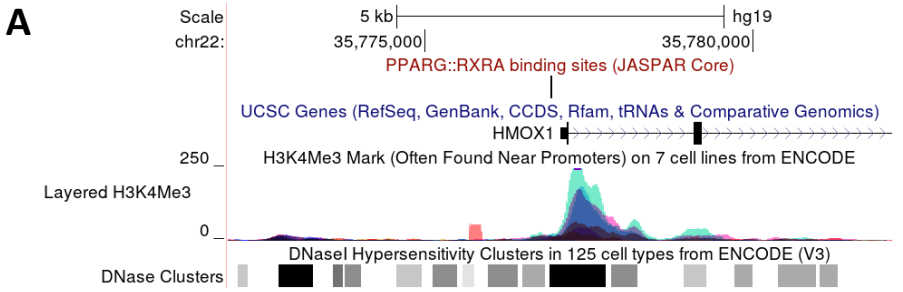

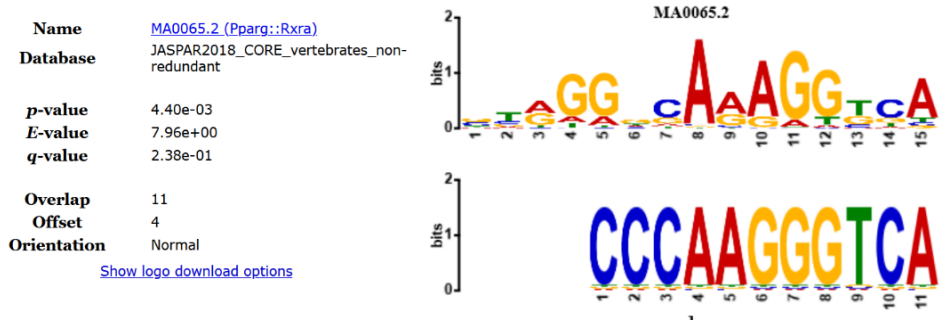

C

```
TATAAGTCAGACCTGAATGTGCCTGGAAGAGTGTCCCACGCATTCCAGCAGGGAAGCAGTTTGTATGACAGGTGTCCCAGTCCAGGCGGATA
CCAGGTGCTGCCAGAGTGTGGAGGAGGCAGGCGGGGACTTAGTCTCCTCCCTGGGTTTGGACACTGGCATCCTGCTTTATGTGTGACACCAC
TGCACCCCTCTGAGCCTCGGTTTCCCCATCTGTAAAATAGAAGCGATCTACCCTCACAGGTCAGTTGTAGGGATGAACCATGAAAATACTAG
AGTCTCTGTTTTTTGACAGGAACTCAAAAAACAGATCCTAAATGTACATTTAAAGAGGGTGTGAGGAGGCAAGCAGTCAGCAGAGGATTCCA
GCAGGTGACATTTTAGGGAGCTGGAGACAGCAGAGCCTGGGGTTGCTAAGTTCCTGATGTTGCCCACCAGGCTATTGCTCTGAGCAGCGCTG
CCTCCCAGCTTTCTGGAACCTTCTGGGACGCCTGGGGTGCATCAAGTCCCAAGGGGACAGGGAGCAGAAGGGGGGGCTCTGGAAGGAGCAAA
ATCACACCCAGAGCCTGCAGCTTCTCAGATTTCCTTAAAGGTTTTGTGTGTGTGTGTGTGTGTGTGTGTGTATGTGTGTGTGTGTGTG
TGTGTGTGTGTGTTTTCTCTAAAAGTCCTATGGCCAGACTTTGTTTCCCAAGGGTCATATGACTGCTCCTCTCCACCCCACACTGGCCCGGG
GCGGGCTGGGCGCGGGCCCCTGCGGGTGTTGCAACGCCCGGCCAGAAAGTGGGCATCAGCTGTTCCGCCTGGCCCACGTGACCCGCCGAGCA
TAAATGTGACCGGCCGCGGCTCCGGCAGTCAACGCCTGCCTCCTCTCGAGCGTCCTCAGCGCAGCCGCCGCCCGCGGAGCCAGCACGAACGA
GCCCAGCACCGGCCGGATGGAGCGTCCGCAACCCGACAGGCAAGCGCGGGGCGCGGGACGCGGGACGGGCGCCTTTCTCTCCCAACCCTGCT
TGCGTCCTAGCCCCACCCCGGGACACTGCCACACAGCGACAGAGCCCAGGAGCCAGAAACTTGGGCTCTGGAGTCAGGAGGTGCGGGGTTCT
GATCCTGCCTGTGCCCGTAGGGTAGTTGGAGGGAGGAACGGTAATTTACATGCCTGGCACCCTGGTATGCGGTTGGTGACCAAGATGGGAGT
GTCCCTAGAGTATCCAGTCTTTGAGGTAGCCAATTTTTTTTTTAATCCTACTTTCGAGGTGTGTTTGGAGTTGCTCTCTGCTGAATCTAGAT
CTCTGGGGCTCTGCCAGCCTGGGGGAGCATGCTTGGTTCTCTTGGTGGCATCTGTCCCTCACTAGCTACGGAGGACCTGAGCCAGACATCAC
CCTGGCTGCGGTGTTCCATGTC
```

PPARγ Target Binding Site

Forward Primer Sequence	Reverse Primer Sequence	
pHMOX1: TCCTATGGCCAGACTTTG	pHMOX1: GTGTGGGGTGGAGAGGAG	SIZE: 58 bp

Figure 3.5: Putative PPARγ binding site occurs in the HO1 promoter. *In silico* analysis of putative PPARγ binding sites in the HO1 promoter was performed with the LASAGNA-Search 2.0 Transcription Factor Binding search tool [198] and visualized using the UCSC genome browser. There appears to be one putative binding site for PPARγ in the active HO1 promoter region (A) with 11 nucleotides in the promoter region found to significantly overlap with known DNA sequence for PPARγ binding sites (B). Based on this information, quantitative PCR primers shown in gray and blue highlight were designed for CUT&RUN experiments (C).

Two additional known downstream PPARγ target genes, glial cell missing 1 (GCM1) and fatty acid binding protein 4 (FABP4) were also analyzed with the LASAGNA-

Search 2.0 Transcription Factor Binding search tool [198]. There is one PPRE site found in the GCM1 promoter region that has 20 statistically significantly overlapping nucleotides in the GCM1 promoter region and known PPARγ binding sequence (Figure 3.6).

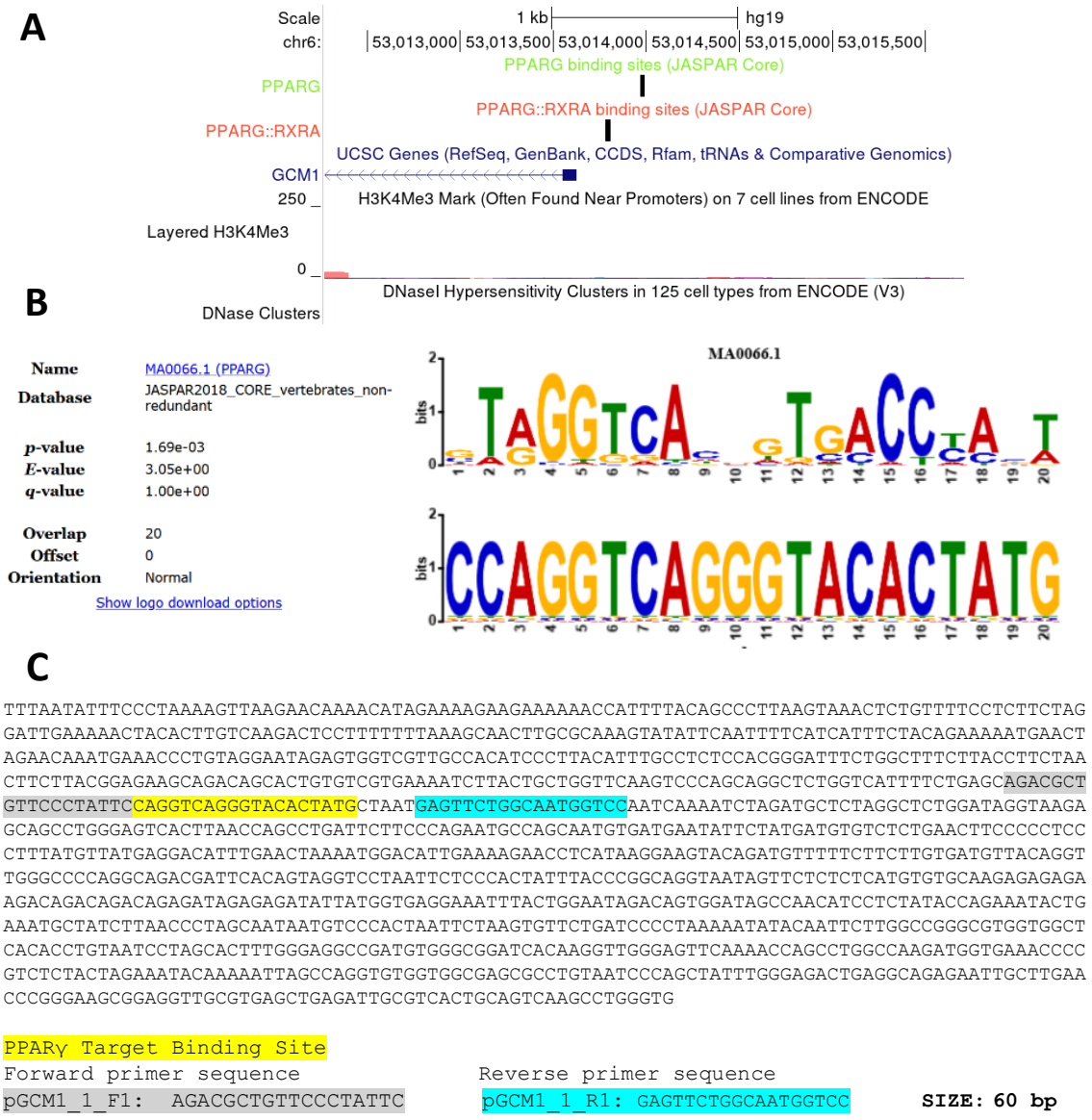

Figure 3.6: Putative PPARγ binding site occurs in the GCM1 promoter. *In silico* analysis of putative PPARγ binding sites in the GCM1 promoter was performed with the LASAGNA-Search 2.0 Transcription Factor Binding search tool [198] and visualized using the UCSC genome browser. There appears to be one putative binding sites for PPARγ in the active GCM1 promoter region (A) with 20 nucleotides in the promoter region found to significantly overlap with the known PPARγ DNA binding sequence (B). Based on this

Figure 3.6 (cont'd)
information, quantitative PCR primers shown in gray/blue highlight were designed for CUT&RUN experiments (C).

There was one PPRE site found in the FABP4 promoter region that has 20 statistically significantly overlapping nucleotides in the FABP4 promoter region and known PPARγ binding sequence (Figure 3.7). Primer sequences are listed in Figure 3.7 and were generated in accordance with the predicted PPARγ binding sites.

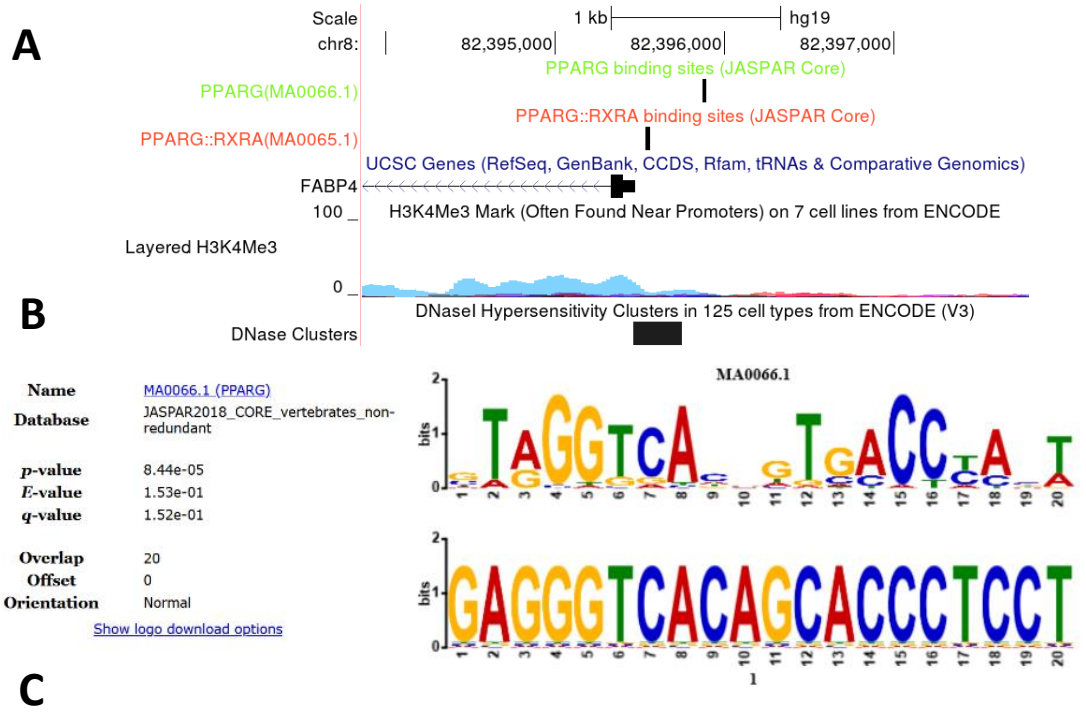

Figure 3.7: Putative PPARγ binding site occurs in the FABP4 promoter. *In silico* analysis of putative PPARγ binding sites in the FABP4 promoter was performed with the LASAGNA-Search 2.0 Transcription Factor Binding search tool [198] and visualized using the UCSC genome browser. There appears to be two putative binding sites for PPARγ in the active FABP4 promoter region (A) with 20 and 18 nucleotides, respectively, in the promoter region found to significantly overlap with the known PPARγ DNA binding sequence (B). Based on this information, quantitative PCR primers shown in gray/blue and pink/green highlight were designed for CUT&RUN experiments (C).

3.3.6. The regulatory role of PPARγ for HO1 remains uncertain.

CUT&RUN was performed to identify if PPARγ is present at the HO1 promoter to transcriptionally regulate HO1 transcription. Because this assay relies on a high-quality antibody that can bind to the native form of PPARγ, three antibodies were tested by immunoprecipitation to identify if there is sufficient pulldown (Figure 3.8). While all three antibodies were shown to bind PPARγ, the ThermoFisher (PPARγ TH) and Santa Cruz antibodies (PPARγ SC) were able to bind PPARγ to a higher degree compared to the Cell Signaling Technology antibody (PPARγ CST), with the Santa Cruz antibody showing the most amount of target protein in the bound versus unbound fraction (Figure 3.8).

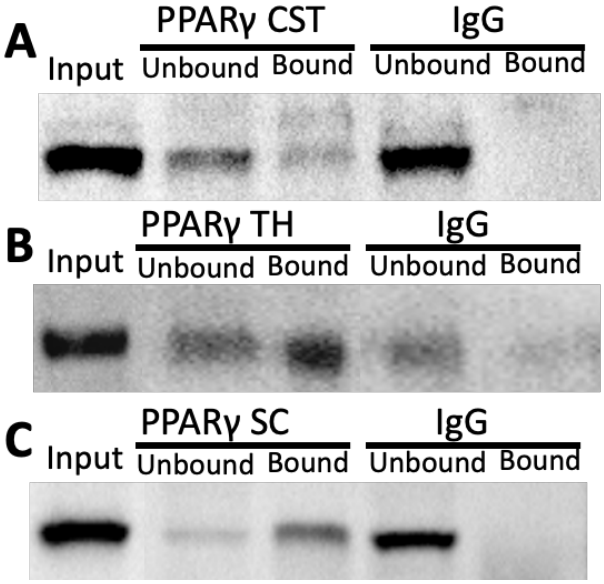

Figure 3.8: Immunoprecipitation reveals three PPARγ antibodies can bind to PPARγ target protein. The Cell Signaling Technology PPARγ antibody (PPARγ CST) shows small amount of PPARγ binding in the bound fraction (A). The ThermoFisher PPARγ antibody (PPARγ TH) shows increased amount of PPARγ binding in the bound fraction (B). The Santa Cruz PPARγ antibody (PPARγ SC) shows very little PPARγ antibody present in the unbound fraction (C).

Each PPARγ antibody was also performed in separate CUT&RUN experiments along with a positive control antibody, H3K4Me3 (Figure 3.9). The PPARγ TH antibody

was the only antibody that showed a statistically significant enrichment of PPARγ presence at the promoter of GCM1 (3.7±0.17 vs 1 fold enrichment, n=3, p=0.0014, Figure 3.9A), FABP4 (5.4±0.7 vs 1-fold enrichment, n=3, p=0.0082, Figure 3.9B), and HO1 (7.4±0.34 vs 1-fold enrichment, n=3, p=0.001, Figure 3.9C) when compared to the IgG control. As an additional confirmation that this experiment worked, the H3K4Me3 antibody shows a statistically significant enrichment at the RPL30 promoter compared to the IgG control (124±12 vs 1-fold enrichment, n=3, p=0.0032, Figure 3.9D).

The PPARγ SC antibody resulted in a statistically significant reduction of PPARγ enrichment compared to the IgG control at the promoter region for GCM1 (0.53±0.28 vs 1-fold enrichment, n=3, p=0.046, Figure 3.9E), FABP4 (0.49±0.25 vs 1-fold enrichment, n=3, p=0.0279, Figure 3.9F), and HO1 (0.43±0.2 vs 1-fold enrichment, n=3, p=0.012, Figure 3.9G). However, the positive control H3K4Me3 antibody showed statistically significant enrichment at the RPL30 promoter (33±6 vs 1-fold enrichment, n=3, p=0.01, Figure 3.9H), confirming the success of this CUT&RUN experiment.

The PPARγ CST antibody did not show a significant change of PPARγ enrichment compared to the IgG control for the promoter regions of GCM1 (0.76±0.13 vs 1-fold enrichment, n=3, p=0.09, Figure 3.9I), FABP4 (0.98±0.26 vs 1-fold enrichment, n=3, p=0.9, Figure 3.9J), and HO1 (1.28±0.43 vs 1-fold enrichment, n=3, p=0.36, Figure 3.9K). The positive control suggests the experiment worked correctly due to a statistically significant enrichment of H3K4Me3 at the RPL30 promoter (179±42 vs 1-fold enrichment, n=3, p=0.01, Figure 3.9L).

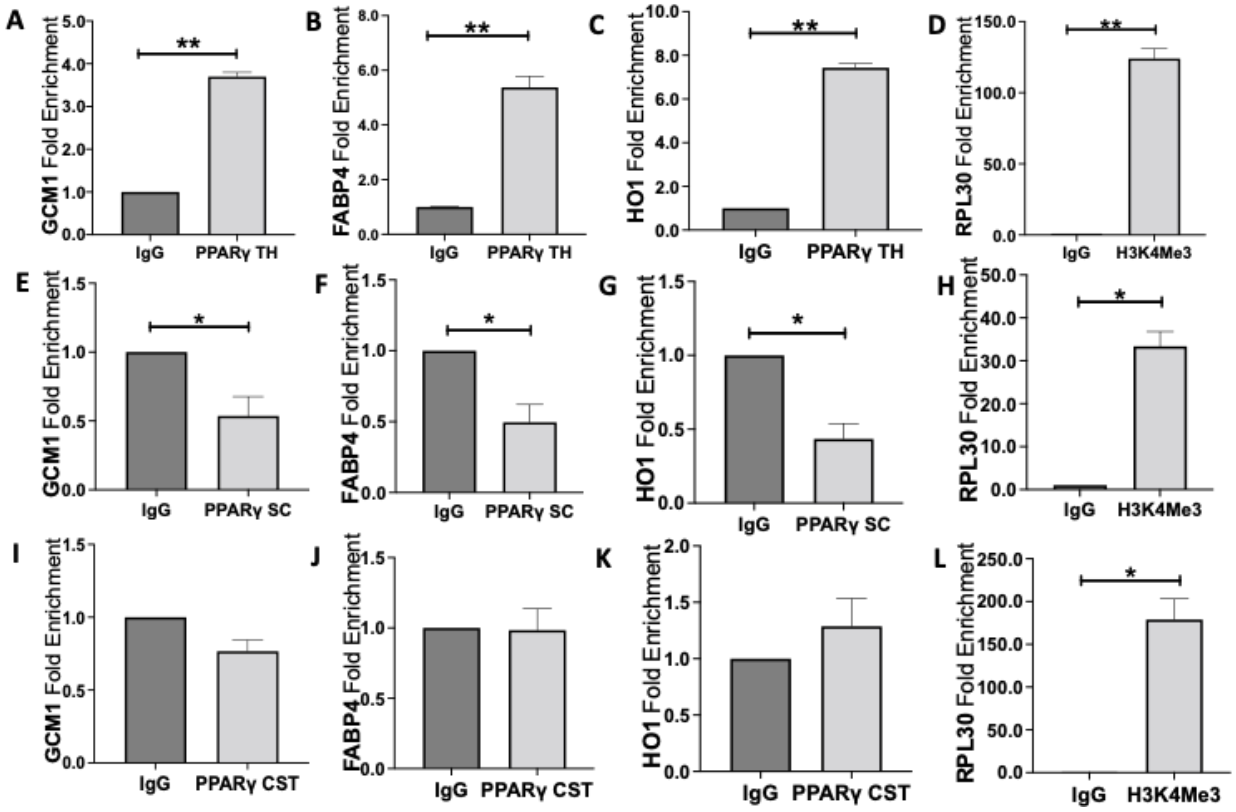

Figure 3.9: The ThermoFisher PPARγ antibody captures PPARγ presence at downstream target genes. PPARγ antibodies from ThermoFisher (PPARγ TH), Santa Cruz (PPARγ SC), and Cell Signaling Technology (PPARγ CST) were tested in CUT&RUN reactions. qPCR was performed to test if PPARγ showed increased enrichment at the promoter region of two known PPARγ downstream targets, GCM1 and FABP4, as well as HO1. The H3K4Me3 positive control antibody was also tested in each CUT&RUN assay and its presence at the RPL30 promoter confirmed each reaction was executed properly. PPARγ TH antibody shows high enrichment of PPARγ at the GCM1 (A), FABP4 (B), and HO1 (C) promoters. As well, the high enrichment of H3K4Me3 at the RPL30 promoter confirmed the accuracy of the assay (D). PPARγ SC antibody shows reduced PPARγ enrichment at the GCM1 (E), FABP4 (F), and HO1 (G) promoters however, there was significant enrichment of H3K4Me3 at the RPL30 promoter (H). The PPARγ CST antibody did not show any significant enrichment of PPARγ at the GCM1 (**I**), FABP4 (J), and HO1 (K) promoters however, similar to the PPARγ SC results, there was significant enrichment of H3K4Me3 at the RPL30 promoter (L). *(All experiments were performed in triplicate (n=3). Relative fold enrichment of PPARγ or H3K4Me3 was determined by the delta-delta CT value relative to the IgG control and subsequent statistical analysis was performed by student's t-test to determine significant differences between PPARγ or H3K4Me3 and IgG control, *p<0.05, **p<0.01, ***p<0.0001, IgG=IgG control, PPARγ TH=ThermoFisher PPARγ antibody, PPARγ SC=Santa Cruz PPARγ antibody, PPARγ CST=Cell Signaling Technology PPARγ antibody, H3K4Me3=H3K4Me3 antibody, bar plots and data reported are reported as mean ± SEM).*

The PPARγ TH antibody was used in additional CUT&RUN assays to test if Rosiglitazone treatment causes a significant enrichment of PPARγ at the promoter region of downstream targets. In non-treated cells, the PPARγ TH antibody produced a statistically significant increase of PPARγ enrichment at the GCM1 promoter (3.3±0.27 vs 1-fold enrichment, n=3, p=0.014, Figure 3.10A) however, there was no significant enrichment of PPARγ at the FABP4 promoter (3.0±0.6 vs 1-fold enrichment, n=3, p=0.07, Figure 3.10B) and the HO1 promoter (3.0±0.73 vs 1-fold enrichment, n=3, p=0.11, Figure 3.10C). In vehicle treated cells, there was a statistically significant increase of PPARγ enrichment at the HO1 promoter (2.1± vs 1-fold enrichment, n=3, p=0.01 Figure 3.10G) however, there was no significant enrichment of PPARγ at the GCM1 promoter (1.7±0.6 vs 1-fold enrichment, n=3, p=0.07, Figure 3.10E) and the FABP4 promoter (1.8±0.2 vs 1-fold enrichment, n=3, p=0.06, Figure 3.10F). In Rosiglitazone treated cells, there was no significant enrichment of PPARγ at the GCM1 promoter (0.9±0.25 vs 1-fold enrichment, n=3, p=0.82, Figure 3.10H), FABP4 promoter (1.6±0.95 vs 1-fold enrichment, n=3, p=0.58, Figure 3.10I), and the HO1 promoter (2.1±0.5 vs 1-fold enrichment, n=3, p=0.15 Figure 3.10J) compared to the IgG. There was significant enrichment of H3K4Me3 at the RPL30 promoter (73±1.7 vs 1-fold enrichment, n=3, p=0.0006, Figure 3.10D) which confirms that there was no technical error of the assay.

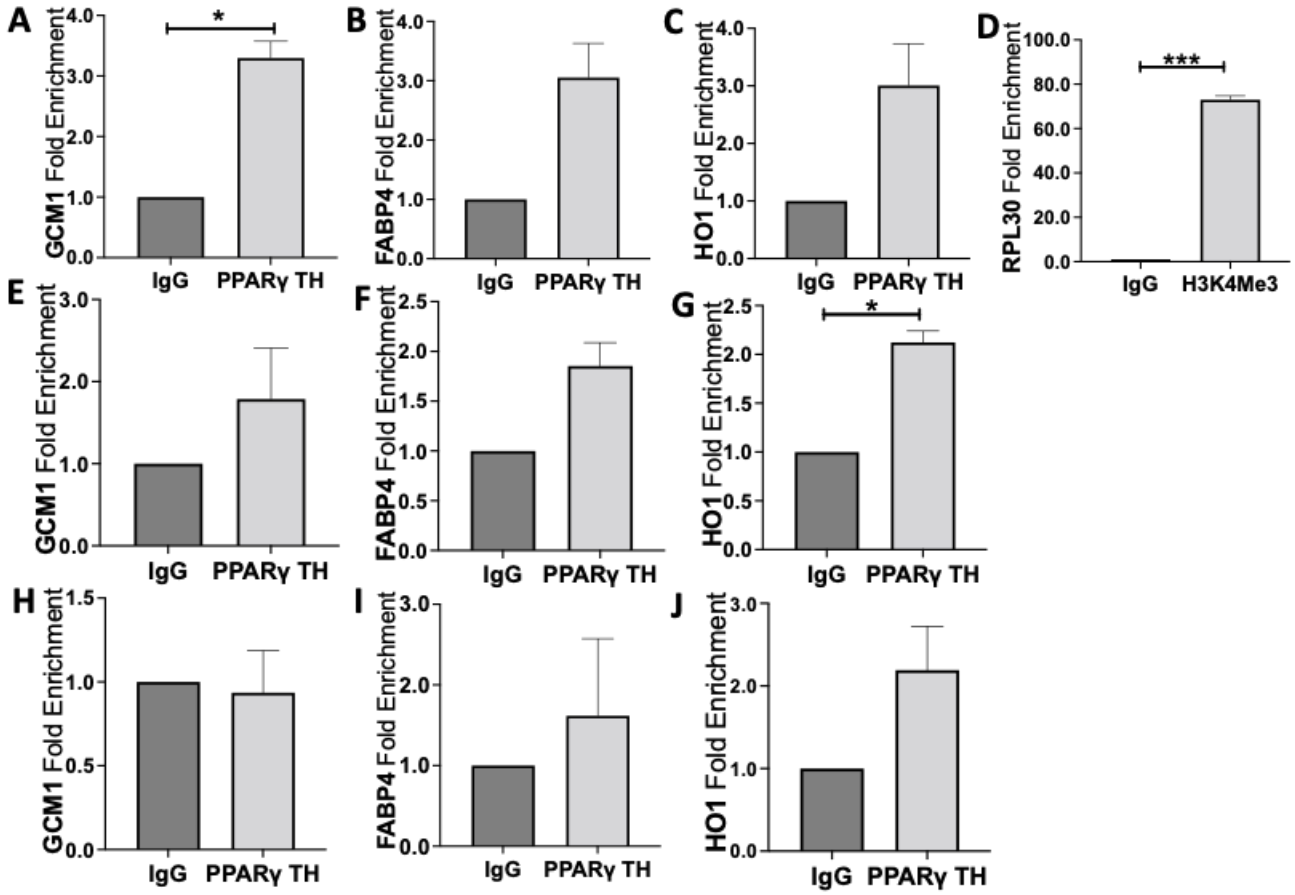

Figure 3.10: There is significant enrichment of PPARγ at the promoter of downstream target genes in cells treated with Rosiglitazone. Non-treated cells show a significant enrichment of PPARγ at the GCM1 promoter (A) but not at the FABP4 promoter (B) and the HO1 promoter (C) compared to IgG control. Non-treated cells show significant enrichment for the H3K4Me3 positive control at the RPL30 promoter (D). Vehicle-treated cells show a significant enrichment of PPARγ at the HO1 promoter (G) however there was no significant enrichment at the GCM1 promoter (E) and FABP4 promoter (F) when compared to IgG control. Rosiglitazone-treated cells show no significant enrichment of PPARγ at the GCM1 (H), FABP4 (I) and HO1 (J) promoters when compared to IgG control. *(All experiments were performed in triplicate (n=3). Relative fold enrichment of PPARγ or H3K4Me3 was determined by the delta-delta CT value relative to the IgG control and subsequent statistical analysis was performed by student's t-test to determine significant differences between PPARγ or H3K4Me3 and IgG control, *p<0.05, **p<0.01, ***p<0.0001, IgG=IgG control, PPARγ TH=ThermoFisher PPARγ antibody, H3K4Me3=H3K4Me3 antibody, bar plots and data reported are reported as mean ± SEM).*

Gene expression of HO1 and GCM1 were also measured in the same cells used for CUT&RUN assay to validate the Rosiglitazone treatment. We observed a significant

enrichment of GCM1 gene expression when cells were treated with Rosiglitazone in comparison to the vehicle (1.6±0.1 vs 1-fold changes, n=3, p=0.0095, Figure 3.11A) and no-treatment (1.6±0.1 vs 1.01±0.12-fold changes, n=3, p=0.01, Figure 3.11A). HO1 was also significantly increased in cells treated with Rosiglitazone in comparison to the vehicle (3.3±0.2 vs 1-fold changes, n=3, p=0.0075, Figure 3.12B) and no-treatment (3.3±0.2 vs 0.9±0.05-fold changes, n=3, p=0.0003, Figure 3.12B).

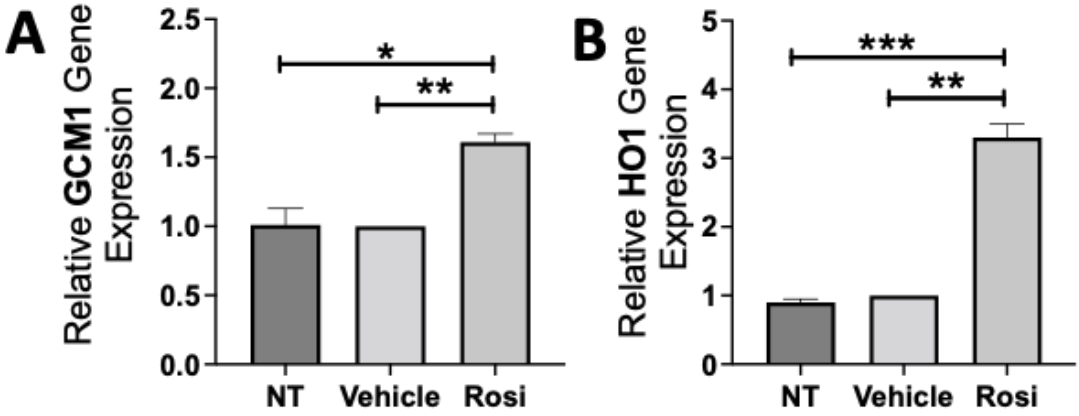

Figure 3.11: Rosiglitazone treatment increases GCM1 and HO1 gene expression in the same cells used for CUT&RUN. GCM1 and HO1 gene expression was measured in the same cells used for the CUT&RUN with non-treated, vehicle-treated, and Rosiglitazone-treated cells. GCM1 gene expression was significantly increased from Rosiglitazone treatment in comparison to vehicle and non-treated cells (A). HO1 gene expression was also significantly increased from Rosiglitazone treatment in comparison to vehicle and non-treated cells (B). *(Relative mRNA expression was determine by normalization to housekeeping genes. Relative expression values for individual sample sets were normalized to vehicle control (DMSO, set equal to 1) and subsequent statistical analysis was performed by student's t-test to determine significant differences between groups, *p<0.05, **p<0.01, Rosi=Rosiglitazone, bar plots and data reported are reported as mean ± SEM).*

3.4. Discussion

A major contribution to the manifestation of PE is the abnormal secretion of proteins that are released from the placenta into maternal circulation and cause damage to the maternal endothelium leading to high blood pressure and organ damage. PPARγ expression and activity normally regulates VT differentiation in the placenta and its

perturbations in PE are thought to directly contribute to the aberrant secretion of proteins, such as HO1, that lead to the endothelial dysfunction. HO1 has critical roles in regulating cytoprotection from oxidative stress, excessive inflammation, and maintaining endothelial relaxation and vasodilation [2], which are all perturbed in PE. Targeting the upstream pathways that regulate these abnormally secreted proteins, such as HO1, may serve as an opportunity for therapeutic intervention that can restore placental function and dampen maternal sequalae.

It was previously known that PPARγ can increase HO1 in a variety of model systems [126, 186] including animal models of PE [70]. Until now, it was unclear if this pathway occurs in the human placenta and the mechanism by which PPARγ upregulates HO1 has not been fully elucidated. Our *in-silico* analysis of PPARγ-DNA binding sites identified a putative binding site for PPARγ in the active HO1 promoter. These data led to our hypothesis that PPARγ could be responsible for HO1 induction through direct transcriptional regulation.

Our data shows that PPARγ and HO1 are reduced in the preeclamptic placenta, as well during *in vitro* ischemia, which supports similar data reported in the literature [23, 35, 36, 68-71, 163, 165, 166]. These data further confirms that our *in vitro* model recapitulates placental oxidative stress and was therefore used to study the molecular relationship between PPARγ and HO1. Induction of PPARγ by Rosiglitazone is shown to increase HO1 expression in human preeclamptic tissues, as well as during *in vitro* ischemia and in first trimester placental explants. The immunohistochemical staining of HO1 in the first trimester placenta revealed greater HO1 production in Rosiglitazone-treated explants compared to the vehicle, specifically in the syncytiotrophoblast layer of

the first trimester explant, which suggests that these cells are largely responsible for the increased production of HO1 in the placenta. The use of the first trimester explants is an important alternative to using healthy term control placentas due to the higher abundance of villous trophoblast and syncytiotrophoblast cells that are present in the first trimester placentas. The siRNA-mediated reduction of PPARγ led to a significant decrease in HO1 expression and Rosiglitazone-treatment during PPARγ siRNA could not rescue HO1 expression. Collectively, these data reveal that the PPARγ-HO1 pathway can be modulated in the human placenta during PE and that PPARγ likely regulates HO1 through a direct mechanism.

Cleavage Under Targets and Release Using Nuclease (CUT&RUN) assay was performed to identify PPARγ-specific binding in the active promoter of HO1, and at the promoter of GCM1 and FABP4, which are two known downstream targets of PPARγ. CUT&RUN is used to profile protein:DNA binding sites throughout the genome using an antibody targeted approach similar to that of Chromatin Immunoprecipitation (ChIP) studies. CUT&RUN requires that cells are maintained alive in solution throughout the entire assay and there is no cross-linking involved. The experiment begins with binding the cells to magnetic beads and then the cells are gently permeabilized with Digitonin buffer, allowing reagents to flow in and out of the cell while still maintaining the integrity of the cells [200, 201]. An antibody for the protein of interest is added to solution. Following the antibody binding, a Micrococcal nuclease (MNase) enzyme coupled to Protein A and Protein G (pAG-MNase) is added to solution. The pAG-MNase will bind to the antibody which is bound to the protein of interest and upon activation with calcium chloride, the MNase will cleave the DNA adjacent to the bound protein targets. This assay

produces small DNA fragments which flow out of the cell and then purified, and this enriched chromatin fraction can be either saved for PCR analysis or sequenced.

Prior to carrying out the CUT&RUN assay, we had worked through several steps of optimization for the highest chance of success for the assay. This experiment relies on live cells binding to the Concalvalin-A magnetic beads and enough digitonin in the buffer, which is used to permeabilize the cells so that the reagents can flow freely in and out of the live cells. The amount of digitonin was optimized based on a 10-minute cell incubation, then the cells were incubated with trypan-blue staining and counted to determine the percent of dead (permeabilized) cells. This step was validated twice to confirm enough digitonin was added to the buffer to permeabilize >95% of the cells. We also tested the number of cells needed to provide a clear result for the assay using the positive control H3K4Me3 antibody. We observed 200,000 cells could provide reliable CT values for the H3K4Me3 antibody and IgG controls (CT values in the range of 24-30, respectively) as compared to using 100,000 cells which is the starting material suggested by the CUT&RUN assay kit.

One of the most important factors of the CUT&RUN assay is an efficient antibody that can target the protein of interest in its native form. There previously was not an antibody for PPARγ that was produced specifically for this assay, therefore we searched the literature and information online to identify antibodies for PPARγ that are known to be either ChIP-grade or used for immunofluorescence (IF), since IF antibodies are known to bind their target protein in a similar manner as the CUT&RUN assay. We identified three antibodies that fit these criteria, and we began with testing them with immunoprecipitation. We tested variable amounts of the antibody per IP, ranging from 2µg to 10µg, with 2

million cells per reaction and we identified that 5ug produced sufficient results. While all three antibodies were shown to pull down PPARγ, the antibodies from ThermoFisher and Santa Cruz showed the highest amount of PPARγ isolation.

All three antibodies were tested in the CUT&RUN reaction however, the ThermoFisher antibody proved to show statistically significant enrichment of PPARγ at the promoter of all downstream targets. Based on this result, the ThermoFisher antibody was used in the next CUT&RUN reaction, which was performed on non-treated, vehicle-treated, and Rosiglitazone-treated cells. While there was evidence that the CUT&RUN assay was executed properly based on the positive control H3K4Me3 antibody, there was not a consistent pattern of significant enrichment of PPARγ at the promoter region of downstream target genes. Moreover, there was no increased enrichment in the Rosiglitazone treated cells in comparison to the vehicle treated cells. Both findings were unexpected due to prior establishment of the PPARγ TH antibody binding at the HO1 promoter. As well, it is known that Rosiglitazone acts as a chemical ligand for PPARγ to increase PPARγ DNA-binding activity and thus we anticipated that PPARγ would have significantly higher enrichment at the target promoters in the cells that were treated with Rosiglitazone.

By using the positive control H3K4Me3 antibody, we could ensure each assay was a success. The increased gene expression of GCM1 and HO1 from Rosiglitazone confirmed that our treatment worked as expected. Moreover, the assay optimization steps were carried out in the exact same manner for each of the remaining experiments to reduce levels of variability between each experiment. Given these measures, we don’t

have a clear explanation for why our first experiment with the PPARγ TH antibody worked accordingly in the first assay but was unable to be repeated.

In attempt to further explain these results, we considered some of the limitations of the assay. Performing CUT&RUN qPCR relies on an accurate estimation of where PPARγ will bind in the target DNA region. While *in-silico* analysis can identify potential binding sites, we are not completely certain this is the exact location where PPARγ will bind, and we are limited with qPCR to only examine the regions of DNA in which we design primers for. Moreover, we can only estimate that the MNase enzyme will cut the DNA to produce approximately 200bp-sized DNA fragments, without knowing exactly the location of the cleaved DNA. These factors pose a significant challenge to designing qPCR primers to amplify a small DNA sequence (60-80bp) which may or may not contain the PPARγ enriched chromatin.

Many of the experiments yielded inconclusive results due to the raw qPCR CT values from the IgG control being only slightly higher than the PPARγ antibodies (0.2-0.7 CT value difference in most experiments). This is concerning, because the IgG should undergo non-specific binding and permit the MNase to cut randomly in the genome. In comparison to the PPARγ antibody, this suggests that the antibody yields just slightly higher than a random chance for amplifying the target regions by qPCR. This observation revels two possible explanations for the inconclusive results – either the PPARγ antibodies are not sufficiently targeting the native form of PPARγ to then bind with the MNase enzyme for sufficient assay execution, or there are possibly other regions in the DNA where PPARγ is binding that cannot be measured due to the qPCR primers. The

only way to truly identify the reason behind our unclear result is to perform next generation sequencing on the enriched chromatin fragments.

Based on the information at hand, we can still confirm that there is a molecular relationship between PPARγ and HO1 in the human placenta. We show that Rosiglitazone can rescue the reduction of HO1 during ischemia reperfusion and in the sick preeclamptic placenta, which must occur directly though PPARγ. We can confirm that PPARγ is able to bind to the HO1 promoter regions however more studies are required to confirm the ability for PPARγ to cause direct transcriptional upregulation of HO1. In addition to sequencing the enriched chromatin fragments from the PPARγ CUT&RUN assay, overlaying this data from RNA-sequencing will identify globally where PPARγ binds throughout the genome to influence gene expression. The sequencing data will identify even more pathways governed by PPARγ in the placenta that are currently unknown and may serve as further evidence to support placental activation of PPARγ as a method for therapeutic intervention of PE. While this data is still forth-coming, we still point the focus towards the several beneficial effects of PPARγ-mediated induction of HO1, where several studies point that HO1 can help regulate the angiogenic balance of the placenta, reduce inflammation, restore the maternal-placental immunologic tolerance, and prevent injury from oxidative stress in the placenta. All these factors highlight the importance of this study and the potential for improving placental function and pregnancy outcome in women with preeclampsia.

4. CHAPTER 3. IDENTIFYING THE ROLE OF PPARY IN PLACENTAL ANGIOGENIC PROTEIN SECRETION IN NORMAL PREGNANCY AND PREECLAMPSIA

4.1. Introduction

Preeclampsia (PE) is the leading cause of maternal-fetal morbidity and mortality worldwide [28]. PE diagnosis is based on new-onset of maternal hypertension, wide-spread maternal endothelial dysfunction, and proteinuria in most cases [2]. Severe cases or early-onset PE clinically manifests around 20 weeks of gestation and often requires preterm delivery (<37 weeks) as the only treatment option. This poses a significant risk to a newborn's health and is associated with extensive neonatal intensive care costs [25]. If untreated, PE can involve the hepatic and coagulation systems, causing seizures, brain damage, or maternal death. The PE placenta exhibits multiple histopathologic features, described as maternal vascular malperfusion [145, 202] which can be caused from reduced transformation of the maternal spiral arteries impairing blood flow to the placenta and causing chronic hypoxia of the developing placental villi [23, 31]. This results in defects in the structure and molecular regulation of villous trophoblast (VT) differentiation and turnover. Simultaneously, the syncytiotrophoblast (STB) abnormally secretes anti-angiogenic proteins causing an anti-angiogenic environment to further enhance maternal systemic endothelial dysfunction.

The anti-angiogenic environment in sePE poses life-long maternal complications, as nearly half of all women with PE have high blood pressure through 12 weeks post-partum [43, 44] and are at risk of developing chronic hypertension within a few years after giving birth [6]. PE poses a greater risk for cardiovascular disease than smoking [6] and women in the United States who have PE have a 9.4 fold increased risk for

cardiovascular-related deaths when the newborn is born within a 34 weeks of gestation [45]. Thus, there is a great need to identify mechanisms of the placental contribution to PE and establish interventions to dampen maternal sequalae.

The transcription factor, peroxisome proliferator activated receptor-γ (PPARγ) has been widely studied for its roles in promoting trophoblast differentiation, especially through directing VT differentiation [23, 36, 68, 70]. Beyond this, PPARγ acts upstream of several pathways that regulate cell metabolism, anti-inflammatory pathways, and oxidative stress response. PPARγ expression and activity is significantly reduced in the PE placenta, and is therefore thought to contribute to PE pathogenesis [23]. Studies have also suggested that activating PPARγ can restore placental function as a potential treatment for PE [197]. There could be a connection between the aberrant VT differentiation and imbalance of secreted proteins from the placenta in PE since PPARγ has a large role in regulating VT differentiation and thus it may contribute to maintaining the angiogenic balance in the placenta. This claim is supported by previous reports which show placental activation of PPARγ improved the placental angiogenic environment by downregulating the anti-angiogenic molecule, Soluble fms-like tyrosine kinase 1 (sFLT1) [23] and through the upregulation of the pro-angiogenic heme oxygenase 1 (HO1).

This study aims to investigate the connection between PPARγ-driven trophoblast differentiation and the secretion of angiogenic/growth factor proteins from the placenta that subsequently impact the endothelium. To investigate this, we measured expression of several angiogenic, metabolic, and growth factor proteins (Angiopoeitin-2 (Ang-2), soluble Endoglin (sEng), and Endothelin-1 (ET-1), Placental growth factor (PlGF), Fibroblast growth factor-2 (FGF-2), Epidermal growth factor (EGF), Heparin-binding

growth factor (HB-EGF), Follistatin, and Leptin) from the healthy and preeclamptic placenta, as well from preeclamptic placentas that have been treated with Rosiglitazone, a PPARγ agonist. To better understand if placental activation of PPARγ exerts an effect on the surrounding endothelium, we recapitulated the maternal endothelial response to the placental protein secretion by culturing human umbilical vein endothelial cells (HUVECs) with placental conditioned media. By uncovering the broader roles of PPARγ's effect on placental protein secretion, we will add greater knowledge to the roles of PPARγ within the placenta. Moreover, this study will discover the important indirect effects of placental activation of PPARγ on the maternal endothelium that could prove to be beneficial for women with PE.

4.2. Methods

4.2.1. Tissue collection

Term placental samples were obtained either by the Research Centre for Women's and Infants' Health (RCWIH) BioBank program of Mount Sinai Hospital in Toronto, Canada, in accordance with the policies of the Mount Sinai Hospital Research Ethics Board or Women's Health Center at Spectrum Hospital in Grand Rapids, MI. All placentas collected were approved by the IRB waiver of parental consent. Specimens were collected from age-matched idiopathic preterm without histological evidence of chorioamnionitis not complicated by PE (Control) (n = 10; gestational age = 34-39 weeks), and pregnancies complicated by pre-term PE (n=10, gestational age 31-37 weeks) or sPE (n=4; gestational age = 37-39 weeks) and were delivered either by Cesarean section or vaginal birth. Inclusion criteria for PE/sPE was in accordance with current guidelines including blood pressure > 140/90 mm Hg on two occasions longer than 6 hr apart, with or without proteinuria and fetal growth restriction [171].

4.2.2. Explant culture

Placental tissues were cultured using a standardized random sampling protocol that consisted of dissecting random four 1cm^3 cuboidal sections to avoid sampling bias. The collected tissues were washed and transported to the laboratory in ice cold HBSS (Hank's Balanced Salt Solution) and processed within a maximum of 2 hr after delivery. On arrival, tissues were rinsed in chilled HBSS to remove residual blood and further dissected under a stereomicroscope to remove placental membranes and generate 20-30mg pieces of villous tissues for culture. Post dissection, the explants were cultured overnight in 500uL of Dulbecco's modified Eagle's medium/Ham's F-12 nutrient mixture (DMEM/F-12; 1:1; Life Technologies; Grand Island, NY) containing 10% fetal bovine serum (FBS; Life Technologies) and 1% Gibco™ antibiotic-antimycotic. Explants were maintained overnight at 8% O2 with 5% CO2 at 37°C [10]. After an overnight culture, the tissues were treated with 10μM Rosiglitazone (Selleckchem) dissolved in dimethyl sulfoxide (DMSO, Sigma Life Sciences) for 18-24 hours. DMSO alone was used as a vehicle control. After the culture period for each treatment, the placental conditioned media was collected, snap frozen and stored at -80ºC. Separate conditioned media controls were generated by culturing DMEM/F-12 media overnight at 8% O2 with 5% CO_2 at 37°C with or without 10μM Rosiglitazone or DMSO. These conditioned media controls are used for controls in the tube formation assay.

4.2.3. Luminex Assay

The angiogenesis Luminex assay (HAGP1MAG, Millipore Sigma, Burlington, MA) is a multiplex antibody-coated bead based fluorescent assay that allows for quantitative assessment of several proteins using only 25μL of placental conditioned media. The assay was performed according to manufacturer’s instruction. Briefly, the placental

conditioned media was centrifuged at 4,500 x g at 4ºC to pellet any tissue/cell debris. The individual antibody-bead vials were all combined into one solution and pipetted into a 96-well plate and incubated with the conditioned media samples, internal control standard or analyte standards overnight with rotation at 4ºC. The following day, the supernatant contents were removed (analyte:antibody:bead mixtures were contained in the 96-well plate with a plate magnet). The plate was washed 3 times with wash buffer and then the plate was incubated with the detection antibodies for 1 hour at room temperature with rotation. Following this, Streptavidin-phycoerythrin was added to each well and incubated for another 30 minutes at room temperature with rotation. The plate was washed 3 times with wash buffer then the sheath fluid was added to each well and the plate was inserted into the Luminex 200 machine. The machine detects the median fluorescent intensity (MFI) of each analyte to detect how much maternal is present in each sample (provided in the form of pg/mL). The Luminex 200 software performs a 5-point logistic curve analysis of each sample which is compared relative the standard curve. Data from the internal controls were compared to the expected values provided by the kit to ensure the assay was performed properly.

4.2.4. Human umbilical vein endothelial cell culture and tube formation assay

Human umbilical vein endothelial cells (HUVECs) were purchased from American Type Culture Collection (ATCC, Manassas, VA) and cultured according to manufacture instruction. Briefly, frozen cells were thawed and seeded in a T-75 flask with F-12K medium (ATCC, Manassas, VA) containing 10% fetal bovine serum (FBS; Life Technologies), 1% Gibco™ antibiotic-antimycotic, 0.1mg/mL Heparin and 30µg/mL Endothelial Cell Growth Supplement. Cell culture medium was changed every 2 days and

cells were passaged at 60-70% confluency using 0.25% Trypsin-EDTA solution and 1e5 cells were re-seeded into a new flask. The Tube formation assay was performed based on published protocols [203]. Briefly, the HUVECs were serum-starved for 6 hours prior to the tube formation assay and 2 x 96-well plates were coated with 50µL of Growth-Factor Reduced Matrigel (Corning) per well and incubated at 37ºC for a minimum of 30 minutes. HUVECs were removed from the cell culture flasks with trypsin and counted. A 7mL solution was generated which contained 500,000 cells per mL. 200uL of this cell suspension was added to 27 separate 1.5mL Eppendorf tubes, each tube corresponded to a different treatment, listed in Table 4.1. 800uL of the control medium or placental conditioned medium was added to the 1.5mL Eppendorf tubes that each contained 100,000 HUVECs. 100uL of the HUVEC:conditioned media solution was added to the 96-well plate. There was a minimum of 7 technical replicates for each treatment. This produced a total of 189 wells that contained the HUVEC:conditioned media solution. These plates were incubated for 18 hours in 20% O_2 with 5% CO_2 at 37°C then phase contrast images were captured on an inverted microscope using the 4X objective and were imported into the ImageJ software [204] and the images were analyzed using the Angiogenesis Analyzer macros plugin [203]. The images were segmented and skeletonized, and the trees were analyzed to provide quantitative assessment of the number of nodes, junctions, meshes and total branching length present in the HUVECs.

Table 4.1: Experimental Conditions and Controls for HUVEC Tube Formation Assay

Experimental treatment	**Culture Conditions**
HUVEC Positive Control	F-12K media containing 10% FBS, 1% Anti-Anti, heparin, and endothelial cell growth supplement
DMEM/F-12 + DMSO Control	Plain placental DMEM/F-12 media cultured with DMSO overnight

Table 4.1 (cont'd)

DMEM/F-12 + Rosi Control	Plain placental DMEM/F-12 media culture with Rosi overnight
Placental conditioned media from 6 non-treated preeclamptic placentas	Non-treated PE placentas were cultured for 24 hours in DMEM/F-12 media with 10% FBS and 1% anti-anti
Placental conditioned media from 6 non-treated control placentas	Non-treated healthy control placentas were cultured for 24 hours in DMEM/F-12 media with 10% FBS and 1% ant-anti
Placental conditioned media from 6 matching DMSO-treated preeclamptic placentas	DMSO-treated PE placentas were cultured for 24 hours in DMEM/F-12 media with 10% FBS and 1% anti-anti
Placental conditioned media from 6 matching Rosi-treated preeclamptic placentas	Rosi-treated PE placentas were cultured for 24 hours in DMEM/F-12 media with 10% FBS and 1% anti-anti

4.2.5. Statistical Analysis

All statistical analysis was performed with GraphPad Prism 7.0 software. Raw expressions were analyzed by student's t-test, after determination if samples are normally distributed and an F-test was applied to determine variances between groups which was then used in the parameters for the t-test. $p<0.05$ is considered significant and is indicated with (*) on each graph. Data is reported as Mean±S.E.M. All sample numbers are reported as per group, for example, n=6 designates 6 samples per treatment/group.

4.3. Results

4.3.1. Rosiglitazone has a significant impact on angiogenic and growth factor protein secretion from the preeclamptic placenta.

To test if placental activation of PPARγ influences angiogenic protein secretion, preeclamptic placentas treated with or without Rosiglitazone and vehicle, as well as non-treated healthy placentas were cultured for 24-hours, and the conditioned medium was used for Luminex analysis. We observed no significant differences in Ang-2 secretion

levels between in the control and PE placentas (2532±517.6 vs. 2365±303.7 pg/mL, n>10, p>0.05, Figure 4.1A). However, we observed a significant reduction in Ang-2 secretion in Rosiglitazone-treated PE placentas when compared to the vehicle (1671±223 vs. 3086±407pg/mL, n=14, p=0.04, Figure 4.1A).

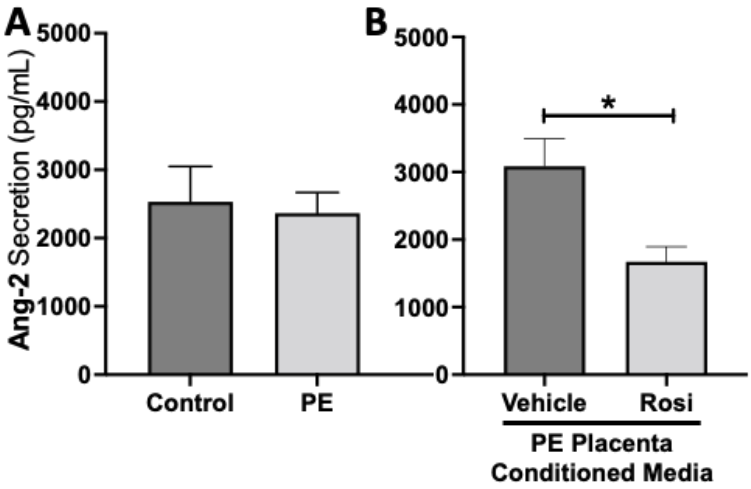

Figure 4.1: Angiopoeitin-2 secretion is reduced in Rosiglitazone-treated preeclamptic placentas. Angiopoeitin-2 (Ang-2) levels were measured via Luminex assay from conditioned media from non-treated control and preeclamptic (PE) placentas (A) and vehicle- or Rosiglitazone (Rosi)-treated PE placentas (B). There was no significant difference in Ang-2 secretion between PE and control placentas (A, n>10). Rosi-treated PE placentas show a significant reduction of Ang-2 secretion in comparison to the vehicle control (B, n=14). (*Protein secretion was measured by a Luminex assay where experimental values were determined relative to a standard curve. Statistical analysis was performed by student's t-test to determine significant differences between groups, *p<0.05, PE=Preeclampsia, Ang-2=Angiopoietin-2, Rosi=Rosiglitazone, bar plots and data reported are reported as mean pg/mL values ± SEM)*.

Our Luminex data shows that there is a significant upregulation of sEng from the preeclamptic placentas in comparison to the healthy control placentas (2017±364 vs. 836±135 pg/mL, n>10, p=0.0164, Figure 4.2A). We also observed a reduction of sEng in the Rosiglitazone-treated PE placentas in comparison to the vehicle control however it was not statistically significant (745±161.5 vs. 1242±179 pg/mL, n=14, p=0.0537, Figure 4.2B).

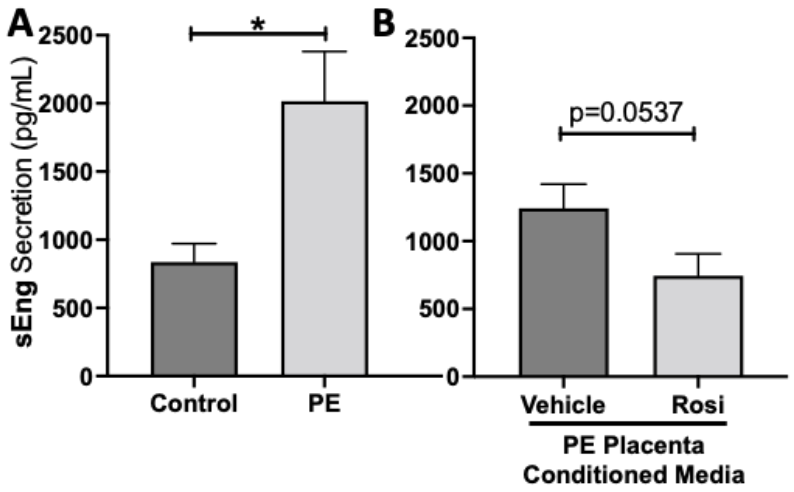

Figure 4.2: Soluble Endoglin secretion is increased in the preeclamptic placenta but reduced after Rosiglitazone treatment. Soluble Endoglin (sEng) levels were measured via Luminex assay from conditioned media from non-treated control and preeclamptic (PE) placentas (A) and vehicle- or Rosiglitazone (Rosi)-treated PE placentas (B). There was a significant upregulation of sEng secretion in PE compared to control placentas (A, n>10). Rosi-treated PE placentas show a reduction of sEng secretion however this was not statistically significant when compared to the vehicle control (B, n=14). (*Protein secretion was measured by a Luminex assay where experimental values were determined relative to a standard curve. Statistical analysis was performed by student's t-test to determine significant differences between groups, *p<0.05, PE=Preeclampsia, sEng=Soluble Endoglin, Rosi=Rosiglitazone, bar plots and data reported are reported as mean pg/mL values ± SEM)*.

We did not observe a significant difference in ET-1 secretion from control compared to preeclamptic placentas (2.2±0.2 vs. 1.9±0.25, n>10, p>0.05, Figure 4.3A). Further, there was no change in ET-1 secretion from Rosiglitazone-treated PE placentas compared to the vehicle control (1.83±0.15 vs. 1.74±0.19 pg/mL, n=14, p>0.05, Figure 4.3B).

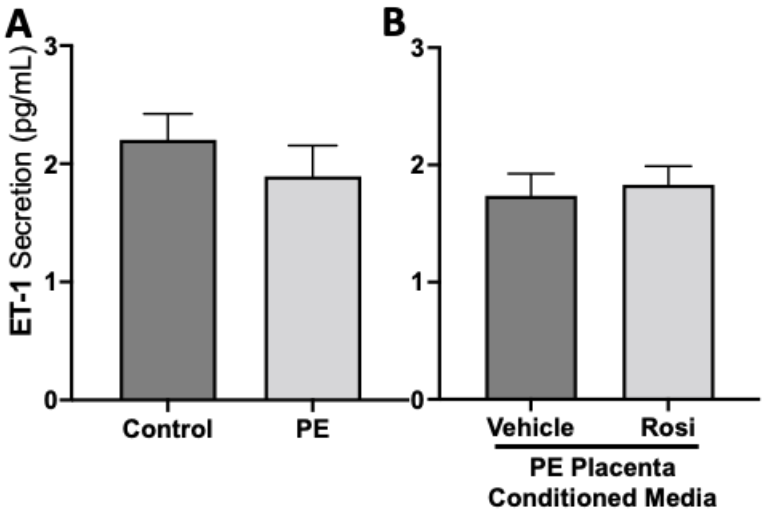

Figure 4.3: There are no significant differences in Endothelin-1 secretion from healthy or preeclamptic placentas with or without drug treatment. Secretion of Endothelin-1 was measured via Luminex assay from conditioned media from non-treated control and preeclamptic (PE) placentas (A) and vehicle- or Rosiglitazone-treated PE placentas (B). There was no significant change in ET-1 secretion between PE and control placentas (A, n>10) and between vehicle and Rosiglitazone-treated PE placentas in the PE compared to control placentas however this was not statistically significant (B, n=14). *(Protein secretion was measured by a Luminex assay where experimental values were determined relative to a standard curve. Statistical analysis was performed by student's t-test to determine significant differences between groups, PE=Preeclampsia, ET-1=Endothelin-1, Rosi=Rosiglitazone, bar plots and data reported are reported as mean pg/mL values ± SEM).*

We observed a decreasing trend of PIGF secretion from PE placentas however, this was not statistically significant in comparison to the control placentas (2.913±0.82 vs 7.12±2.3, n>10, p=0.13, Figure 4.4A). We observed an increase of PIGF secretion in the Rosiglitazone-treated PE placentas however, it was not statistically significant in comparison to the vehicle (4.765±1 pg/mL vs. 2.668±0.6 pg/mL, n=14, p=0.07, Figure 4.4B).

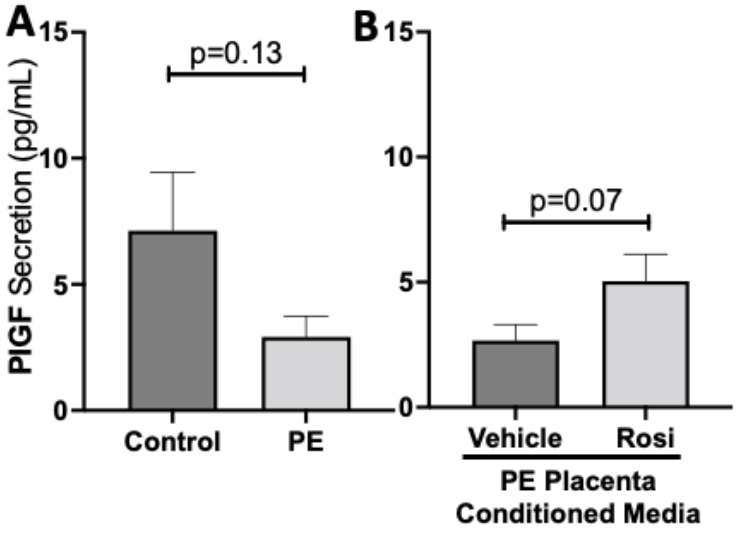

Figure 4.4: There is a decreasing trend in placental growth factor secretion in the preeclamptic placenta that is partially rescued by Rosiglitazone treatment. Secretion of Placental growth factor (PIGF) were measured via Luminex assay from conditioned media from non-treated control and preeclamptic (PE) placentas (A) and vehicle- or Rosiglitazone (Rosi)-treated PE placentas (B). There was a trending decrease of PIGF secretion in the PE compared to control placentas however this was not statistically significant (A, n>10). Rosi-treated PE placentas show an increasing of PIGF secretion however this was not statistically significant when compared to the vehicle control (B, n=14). (*Protein secretion was measured by a Luminex assay where experimental values were determined relative to a standard curve. Statistical analysis was performed by student's t-test to determine significant differences between groups, PE=Preeclampsia, PIGF=Placental growth factor, Rosi=Rosiglitazone, bar plots and data reported are reported as mean pg/mL values ± SEM)*.

While we observed a decreasing of FGF-2 secretion from preeclamptic placentas, this was not statistically significant change in FGF-2 secretion in preeclamptic compared to healthy control placentas (977±266 pg/mL vs. 646±96 pg/mL, n>10, p=0.12, Figure 4.5A). However, Rosiglitazone caused a significant increase of FGF-2 secretion in PE placentas compared to vehicle treatment (1041±121 pg/mL vs. 649±97 pg/mL, n=14, p=0.04, Figure 4.5B).

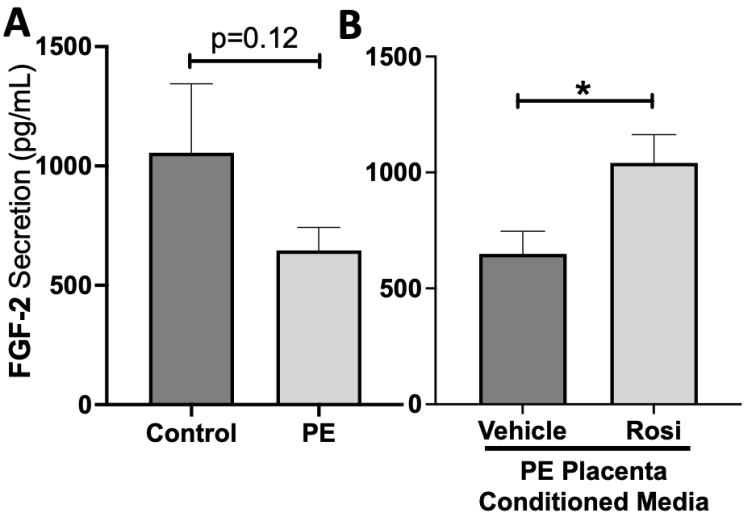

Figure 4.5: Fibroblast Growth Factor 2 shows reduced secretion from the preeclamptic placenta that is reversed by Rosiglitazone treatment. Secretion of Fibroblast Growth Factor 2 was measured via Luminex assay from conditioned media from non-treated control and preeclamptic (PE) placentas (A) and vehicle- or Rosiglitazone (Rosi)-treated PE placentas (B). FGF-2 secretion appears to be reduced in preeclamptic placenta however this decrease isn't statistically different from control placentas (A, n>10). Rosiglitazone-treated PE placentas show a significant increase in FGF-2 secretion compared to the vehicle control (B, n=14). (*Protein secretion was measured by a Luminex assay where experimental values were determined relative to a standard curve. Statistical analysis was performed by student's t-test to determine significant differences between groups, PE=Preeclampsia, FGF-2=Fibroblast Growth Factor 2, Rosi=Rosiglitazone, bar plots and data reported are reported as mean pg/mL values ± SEM)*.

There was no significant change in EGF secretion between preeclamptic and control placentas (1.38±0.15 pg/mL vs. 1.84±0.27 pg/mL, n>10 p>0.05, Figure 4.6A). There were also no measurable changes of EGF secretion from Rosiglitazone-treated PE placentas in comparison to vehicle-treated PE placentas (2.1±0.25 pg/mL vs. 1.8±0.22 pg/mL, n=14, p>0.05, Figure 4.6B).

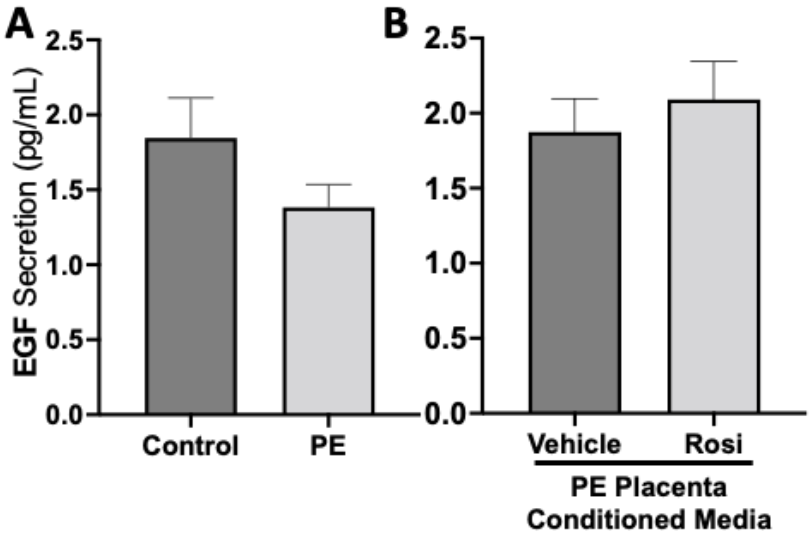

Figure 4.6: There are no significant changes in Epidermal Growth Factor secretion between healthy and preeclamptic placentas treated with or without Rosiglitazone. Secretion of Epidermal Growth Factor (EGF) was measured via Luminex assay from conditioned media from non-treated control and preeclamptic (PE) placentas (A) and vehicle- or Rosiglitazone-treated PE placentas (B). There was no significant change in EGF secretion between PE and control placentas (A, n>10) and between vehicle and Rosiglitazone-treated PE placentas in the PE compared to control placentas however this was not statistically significant (B, n=14). *(Protein secretion was measured by a Luminex assay where experimental values were determined relative to a standard curve. Statistical analysis was performed by student's t-test to determine significant differences between groups, PE=Preeclampsia, EGF=Epidermal Growth Factor, Rosi=Rosiglitazone, bar plots and data reported are reported as mean pg/mL values ± SEM).*

Our data indicates that secretion of HB-EGF is significantly reduced in the PE placenta in comparison to controls (46.5±6.4 pg/mL vs. 119±38 pg/mL, n>10, p=0.05, Figure 4.7A) however HB-EGF secretion was restored when treated with Rosiglitazone in comparison to the vehicle control (71.6±4.9 pg/mL vs. 44.8±6 pg/mL, n=14, p=0.0027, Figure 4.7B).

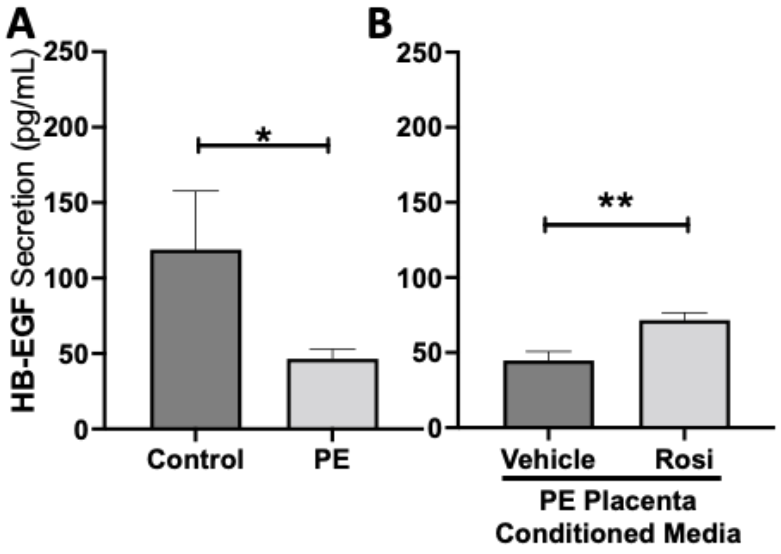

Figure 4.7: Heparin-Binding Epidermal Growth Factor shows reduced secretion from the preeclamptic placenta but is reversed by Rosiglitazone treatment. Secretion of Heparin-Binding Epidermal Growth Factor (HB-EGF) was measured via Luminex assay from conditioned media from non-treated control and preeclamptic (PE) placentas (A) and vehicle- or Rosiglitazone (Rosi)-treated PE placentas (B). There was a significant reduction of HB-EGF secretion from the PE placenta compared to control (A, n>6). Rosiglitazone-treated PE placentas show a significant increase in HB-EGF secretion compared to the vehicle control (B, n=10). (*Protein secretion was measured by a Luminex assay where experimental values were determined relative to a standard curve. Statistical analysis was performed by student's t-test to determine significant differences between groups, PE=Preeclampsia, HB-EGF=Heparin-Binding Epidermal Growth Factor, Rosi=Rosiglitazone, bar plots and data reported are reported as mean pg/mL values ± SEM)*.

Our data shows a significant reduction of Follistatin (FST) secretion from the PE placenta in comparison to control (89±9 vs. 63±6 pg/mL, n>10, p=0.034, Figure 4.8A). Rosiglitazone caused a significant increase in FST secretion from the PE placenta in comparison to the vehicle control (89±10 vs. 63±5 pg/mL, n=14, p=0.044, Figure 4.8B).

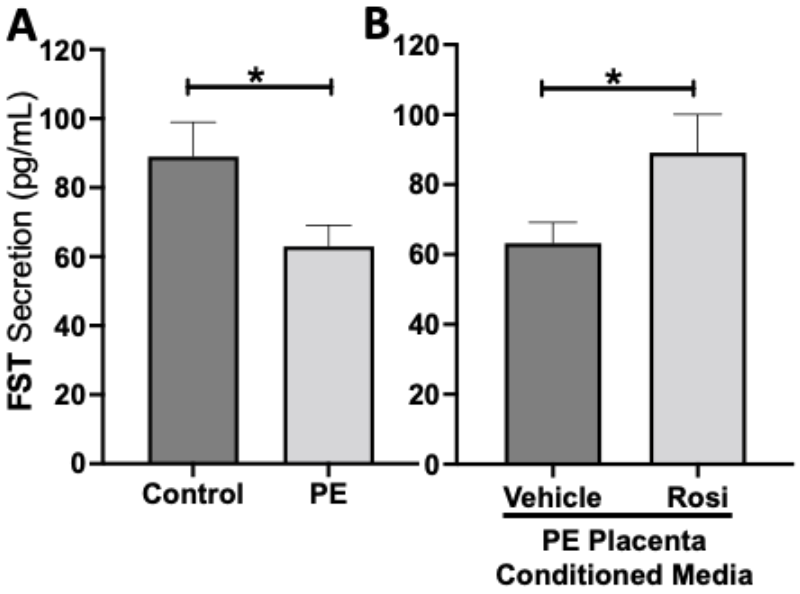

Figure 4.8: Follistatin shows reduced secretion from the preeclamptic placenta but is reversed by Rosiglitazone. Secretion of Follistatin (FST) was measured via Luminex assay from conditioned media from non-treated control and preeclamptic (PE) placentas (A) and vehicle- or Rosiglitazone-treated PE placentas (B). FST secretion was significantly reduced in the PE placenta compared to control placentas (A, n>10) however, Rosiglitazone treatment led to a significantly increased secretion of FST from the PE placenta compared to vehicle-treated PE placentas (B, n=14). (*Protein secretion was measured by a Luminex assay where experimental values were determined relative to a standard curve. Statistical analysis was performed by student's t-test to determine significant differences between groups, PE=Preeclampsia, Rosi=Rosiglitazone, FST=Follistatin, bar plots and data reported are reported as mean pg/mL values ± SEM)*.

There appeared to be a greater secretion of Leptin from the PE placenta in comparison to the control placentas although this was not statistically significant (2889±1047 vs. 1517±514 pg/mL, n>10, p>0.05, Figure 4.9A). Rosiglitazone-treated PE placentas did not show a significant change in Leptin secretion in comparison to the vehicle-treated PE placentas (4146±1320 vs. 3376±1651 pg/mL, n=14, p>0.05, Figure 3.9B).

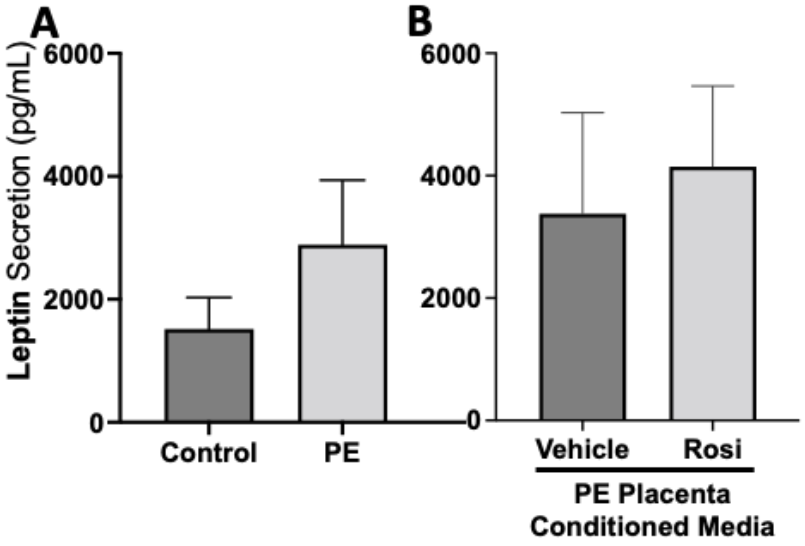

Figure 4.9: There are no significant changes in Leptin secretion between healthy and preeclamptic placentas with or without drug treatment. Secretion of Leptin was measured via Luminex assay from conditioned media from non-treated control and preeclamptic (PE) placentas (A) and vehicle- or Rosiglitazone-treated PE placentas (B). Although there was an increasing trend of Leptin secretion from PE placentas, this was not statistically different from the control placentas (A, n>10). There were no significant changes in Leptin secretion between vehicle and Rosiglitazone-treated PE placentas (B, n=14). (*Protein secretion was measured by a Luminex assay where experimental values were determined relative to a standard curve. Statistical analysis was performed by student's t-test to determine significant differences between groups, PE=Preeclampsia, Rosi=Rosiglitazone, bar plots and data reported are reported as mean pg/mL values ± SEM)*.

4.3.2. Tube formation assays reveals a pro-angiogenic effect of Rosiglitazone on the preeclamptic placenta.

The endothelial tube formation is an assessment of angiogenesis through the measurement of nodes, junctions, meshes, and total branching length of the HUVECs when cultured with placental conditioned media or control media. We observed a significant reduction in the number of nodes present in the HUVECs treated with PE conditioned media compared to control (165±15 vs. 243±14 nodes, n=6, p=0.0004, Figure 4.10A). However, there was a statistically significant increase in the number of nodes present in the HUVECs cultured with Rosiglitazone-treated placental conditioned media

in comparison to the vehicle control (271±30 vs. 165±17 nodes, n=6, p=0.0032, Figure 4.10B). We observed no significant changes in the number of nodes produced from the HUVEC positive control when compared to the HUVECs cultured with the vehicle and Rosiglitazone conditioned media controls (139±8 vs. 167±20 vs. 169±12 nodes, n=6, p>0.05, Figure 4.10C).

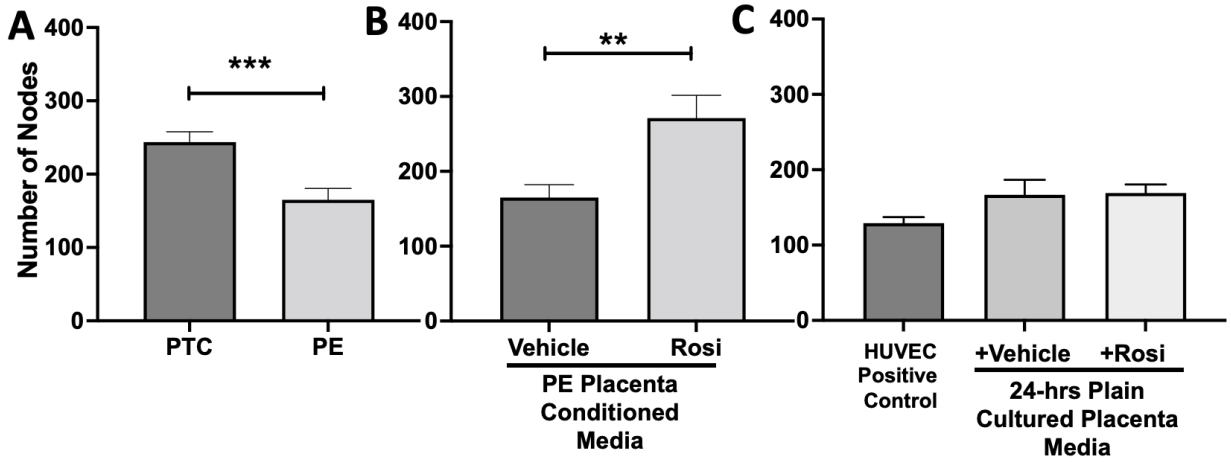

Figure 4.10: There is a significant reduction in the number of nodes present in the HUVECs cultured with preeclamptic conditioned media, but this is reversed in Rosiglitazone-treated placentas. HUVECs were cultured with conditioned media on matrigel, and the number of nodes present was calculated by the Image J Angiogenesis Analyzer tool [203]. Conditioned media from preeclamptic placentas show significantly reduced number of nodes as compared to healthy control placentas (A, n=6). Conditioned media from Rosiglitazone-treated preeclamptic placentas led to a significant increase in the number of nodes present in the HUVECs compared to the conditioned media from the vehicle-treated preeclamptic placentas (B, n=6). Rosiglitazone and vehicle were cultured in placental media without any tissues for 24-hours then applied to the HUVECs. Additionally, HUVECs cultured with standard full-serum media all served as controls for this experiment. There were no significant changes in the number of nodes present among the HUVEC positive control and Rosiglitazone and vehicle conditioned media controls (**C**, n=6). *(Statistical analysis was performed by student's t-test to determine significant differences between groups, PTC=Preterm Control, PE=Preeclampsia, Rosi=Rosiglitazone, bar plots and data reported are reported as numerical values ± SEM).*

The number of junctions among the HUVECs was also measured and is shown to be significantly reduced in conditioned media from PE compared to PTC placentas (50±4

vs. 64±3 junctions, n=6, p=0.02, Figure 4.11A). There was a significant increase in the number of junctions in the HUVECs after culture with conditioned media from Rosiglitazone-treated PE placentas as compared to vehicle-treated PE placentas (87±8 vs. 45±4 junctions, n=6, p<0.0001, Figure 4.11B). There were no significant differences in the number of junctions shown in the HUVEC positive control compared to the vehicle and Rosiglitazone conditioned media controls (37±3 vs. 47±6 vs. 46±3 junctions, n=6, p>0.05, Figure 4.11C).

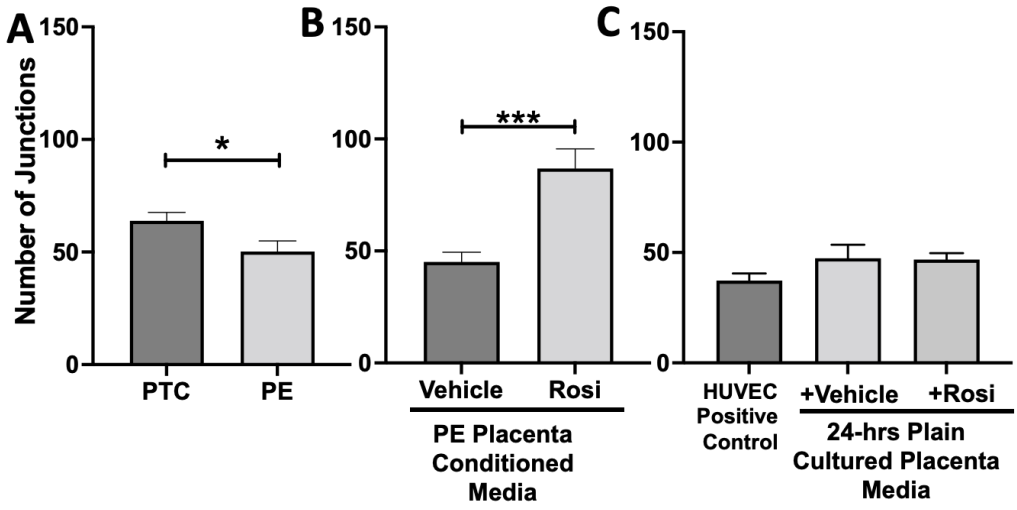

Figure 4.11: There is a reduction of junctions present in HUVECs cultured with preeclamptic placental conditioned media and this was significantly increased after culture with Rosiglitazone-treated preeclamptic placentas. HUVECs were cultured with conditioned media on matrigel, and the number of junctions present was calculated by the Image J Angiogenesis Analyzer tool [203]. Conditioned media from preeclamptic placentas show significantly reduced number of junctions as compared to healthy control placentas (A, n=6). Conditioned media from Rosiglitazone-treated preeclamptic placentas led to a significant increase in the number of junctions present in the HUVECs compared to the conditioned media from the vehicle-treated preeclamptic placentas (B, n=6). Rosiglitazone and vehicle were cultured in placental media without any tissues for 24-hours then applied to the HUVECs. Additionally, HUVECs cultured with standard full-serum media all served as controls for this experiment. There were no significant changes in the number of nodes present among the HUVEC positive control and Rosiglitazone and vehicle conditioned media controls (C, n=6). *(Statistical analysis was performed by student's t-test to determine significant differences between groups, PTC=Preterm Control, PE=Preeclampsia, Rosi=Rosiglitazone, bar plots and data reported are reported as numerical values ± SEM).*

Our data shows that HUVECs cultured with conditioned media from PE placentas show significantly reduced total branching length in comparison to the conditioned media from the control placentas (5085±414 vs. 6074±257 relative pixel values, n=6, p=0.03, Figure 4.12A). However, the conditioned medium from the Rosiglitazone-treated PE placentas led to a significant increase in the total branching length as compared to the conditioned media from the vehicle-treated PE placentas (7994±662 vs. 5538±337 relative pixel values, n=6, p=0.0013, Figure 4.12B). There was no significant difference in total branching length between the HUVEC positive control, the vehicle conditioned media, and Rosiglitazone conditioned media controls (5238±621, 6401±554, 5885±336 relative pixel values, n=6, p>0.05, Figure 4.12C).

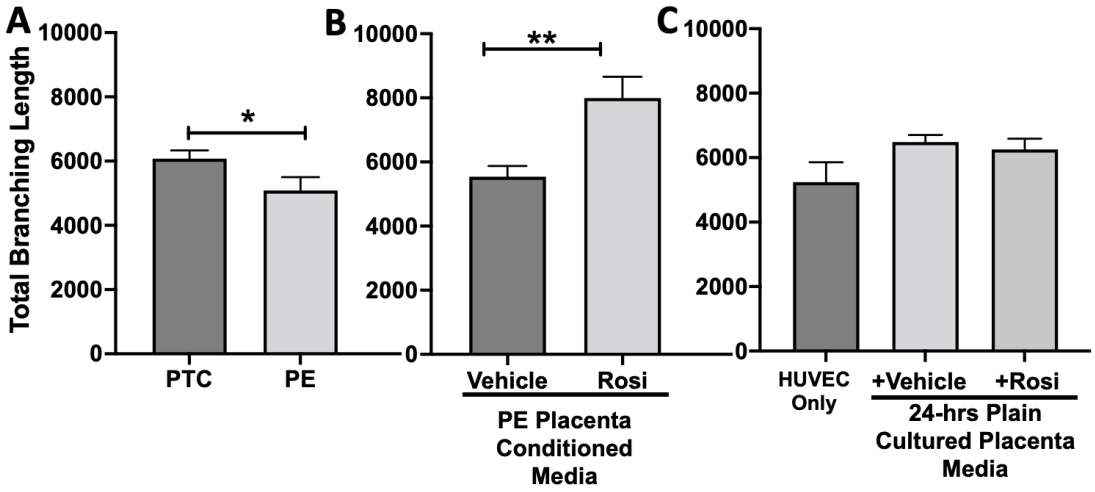

Figure 4.12: There is a reduction of the total branching length present in HUVECs cultured with preeclamptic placental conditioned media, but this was significantly increased after culture with Rosiglitazone-treated preeclamptic placentas. HUVECs were cultured with conditioned media on matrigel, and the total branching length was calculated by the Image J Angiogenesis Analyzer tool [203]. Conditioned media from preeclamptic placentas show significantly reduced total branching length as compared to healthy control placentas (A, n=6). Conditioned media from Rosiglitazone-treated preeclamptic placentas led to a significant increase in the total branching length present in the HUVECs compared to the conditioned media from the vehicle-treated preeclamptic placentas (B, n=6). Rosiglitazone and vehicle were cultured in placental media without any tissues for 24-hours along with HUVECs cultured with standard full-serum media all

Figure 4.12 (cont'd)
served as controls for this experiment. There were not any significant changes in the total branching length among the HUVEC positive control and Rosiglitazone and vehicle conditioned media controls (C, n=6). *(Statistical analysis was performed by student's t-test to determine significant differences between groups, PTC=Preterm Control, PE=Preeclampsia, Rosi=Rosiglitazone, bar plots and data reported are reported as numerical values ± SEM).*

The number of meshes appear to be significantly reduced when HUVECs were cultured with conditioned media from PE placentas as compared to the conditioned media from control placentas (10±1.5 vs. 15.5±1.6 meshes, n=6, p=0.0165, Figure 4.13A). Conditioned media from Rosiglitazone-treated PE placentas led to a remarkable increase in the number of meshes present in the HUVECs, as compared to the conditioned media from the vehicle-treated PE placentas (24.5±4 vs. 9.6±1.7 meshes, n=6, p=0.0032, Figure 4.13B). There were no significant changes in the number of meshes present in the among the HUVEC positive control and the vehicle and Rosiglitazone conditioned media controls (7±2.5, 7±3, 9.7±2.3 meshes, n=6, p>0.05, Figure 4.13C).

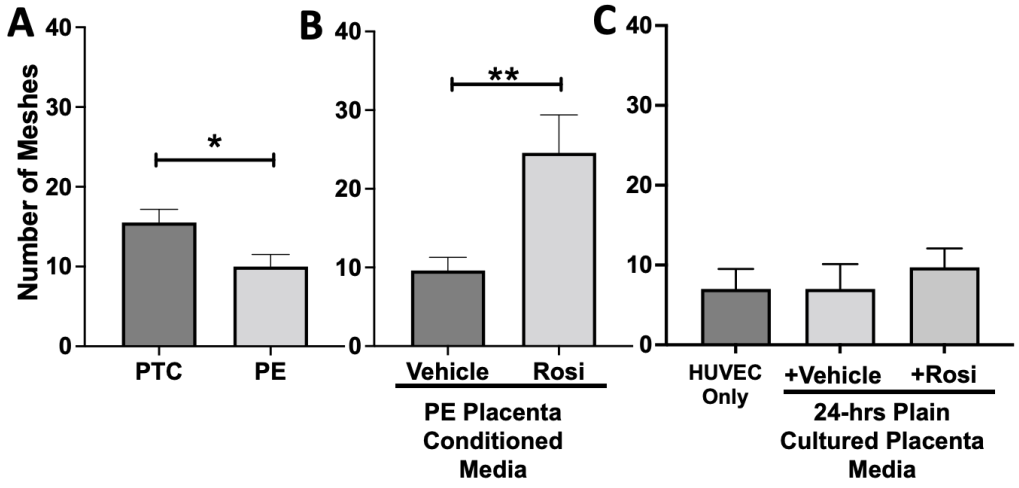

Figure 4.13: There is a reduction of the total number of meshes present in HUVECs from culture with conditioned media from preeclamptic placentas, but this was significantly increased after culture with Rosiglitazone-treated preeclamptic placentas. HUVECs were cultured with conditioned media on matrigel, and the number of meshes was calculated by the Image J Angiogenesis Analyzer tool [203]. Conditioned

Figure 4.13 (cont'd)
media from preeclamptic placentas show significantly reduced the number of meshes as compared to healthy control placentas (A, n=6). Conditioned media from Rosiglitazone-treated preeclamptic placentas led to a significant increase in the number of meshes present in the HUVECs compared to the conditioned media from the vehicle-treated preeclamptic placentas (B, n=6). Rosiglitazone and vehicle were cultured in placental media without any tissues for 24-hours along with HUVECs cultured with standard full-serum media all served as controls for this experiment. There were not any significant changes in the number of meshes among the HUVEC positive control and Rosiglitazone and vehicle conditioned media controls (C, n=6). *(Statistical analysis was performed by student's t-test to determine significant differences between groups, PTC=Preterm Control, PE=Preeclampsia, Rosi=Rosiglitazone, bar plots and data reported are reported as numerical values ± SEM).*

Representative images of the HUVECs with each treatment correlate with the reduction of angiogenic potential that was observed in the cells incubated with the conditioned media from PE placentas (Figure 4.14B). There is a visible increase of tube formation observed in the HUVECs that were cultured with conditioned media from Rosiglitazone-treated PE placentas (Figure 4.14D) as compared to HUVEC culture with conditioned media from vehicle-treated PE placentas (Figure 4.14C). There appears to be no visible differences in tube formation in the positive control HUVECs (Figure 4.14E) or in the HUVECs cultured with either the vehicle-conditioned media control (Figure 4.14F) or Rosiglitazone-conditioned media control (Figure 4.14G).

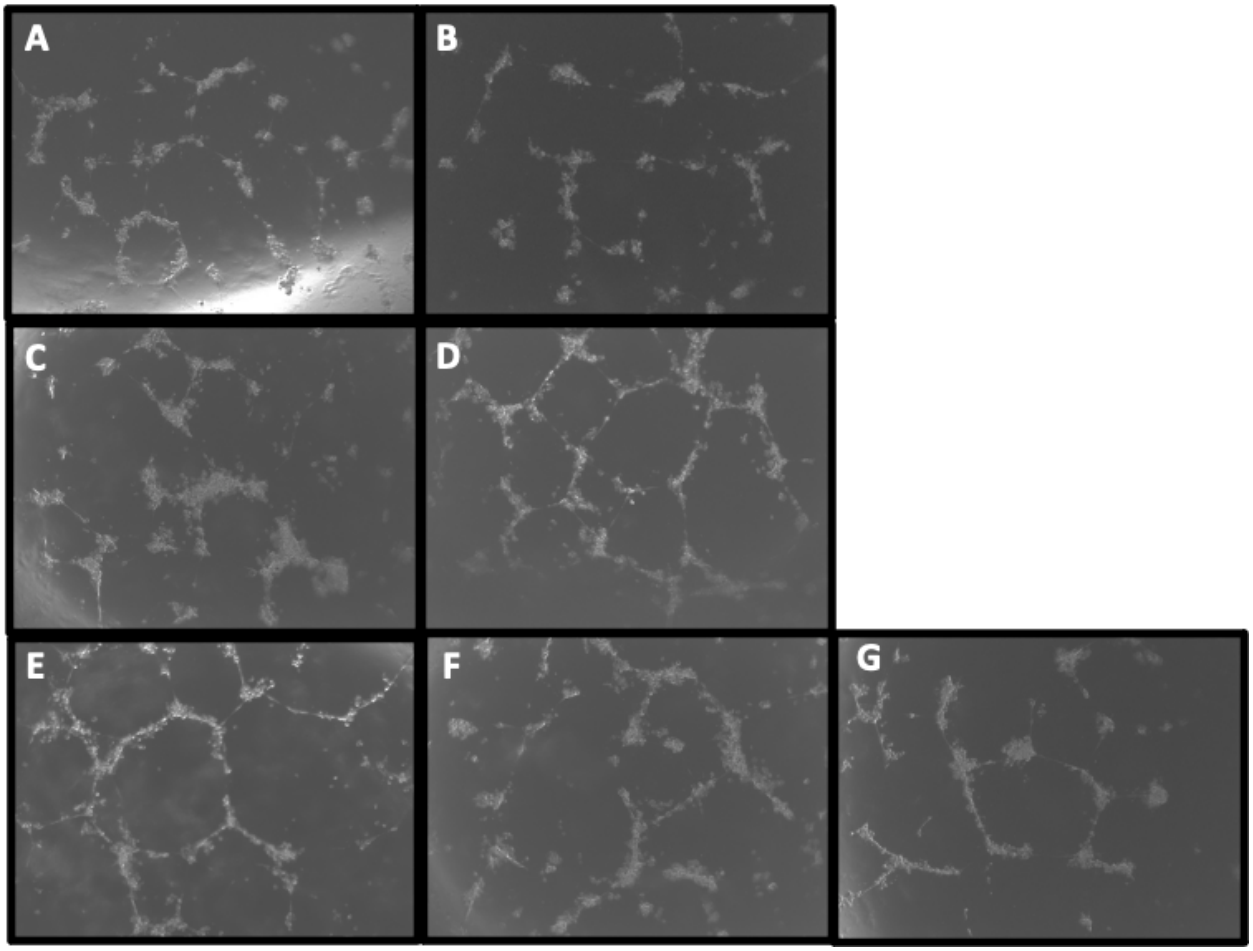

Figure 4.14: Representative images of HUVEC tube formation assays. Conditioned media from placenta culture (A-D), HUVEC positive control (E) and Rosiglitazone and vehicle conditioned media controls (F, G) were cultured with HUVECs on matrigel and images were captured after 18 hours of culture. Images were uploaded to the ImageJ Angiogenesis Analyzer to measure various parameters of tube formation to indicate which conditions permit the greatest angiogenic potential of the HUVECs. Qualitative data suggests that the control placentas (A) show greater angiogenic/tube formation as compared to the preeclamptic placentas (B). However, the preeclamptic placentas treated with Rosiglitazone show improved angiogenic potential (D) as compared to the vehicle control-treated preeclamptic placentas (C). There doesn't appear to be measurable differences in angiogenic potential in the HUVEC positive control (E) compared to the vehicle conditioned media (F) and Rosiglitazone conditioned media controls (G).

4.4. Discussion

Endothelial dysfunction is the major hallmark of PE which causes significant symptoms in the mother that pose long-term risk of cardiovascular disease. In early-onset PE and severe PE, the hypoxic and ischemic nature of the placenta is hypothesized to

be a major contribution to the aberrant secretion of angiogenic and growth factor proteins that result in endothelial dysfunction. There has been considerable evidence to show that PPARγ not only improves trophoblast function in ischemic placentas, but it also it can influence the secretion of proteins that are important for maintaining an angiogenic balance, such as sFLT1 and HO1.

In cases of placental dysfunction where PPARγ activity and expression is altered, we questioned whether this drives aberrant placental protein secretion that leads to an overall anti-angiogenic state in the surrounding endothelium. We hypothesized through restoring placental expression of PPARγ, this could rescue the imbalance of angiogenic/growth factor proteins secreted from the PE placenta to subsequently lead to improved angiogenesis in the endothelium. To study this, we measured multiple angiogenic/growth factor proteins from healthy control and PE placentas as well as PE placentas that were treated with Rosiglitazone or vehicle to understand the secretory profile in control versus PE placentas and to learn how these factors are influenced from placental activation of PPARγ. We further cultured human umbilical vein endothelial cells with conditioned media from these pregnancies to understand the overall 'angiogenic potential' of the secreted factors.

Our Luminex data shows there is not much change in Ang-2 secretion between control and PE placentas, which does not clarify prior reports in the literature measuring Ang-2 in healthy and preeclamptic placentas which show conflicting results. One study showed Ang-2 mRNA expression is significantly higher in the PE placenta [93, 205] and that maternal plasma Ang-2 levels are higher in PE compared to healthy pregnancies

[93], while some studies show that maternal blood plasma Ang-2 levels are decreased in PE [92].

Prior to this study, there has been little investigation on the role for PPARγ in regulating the expression of Ang-2 It was shown in a porcine model, that activation of PPARγ led to an upregulation of hypoxia-inducible factors 1a and 2a, VEGF and Ang-1 as well increased placental porcine angiogenesis [206]. Other studies show that PPARγ targets the PPARγ angiopoietin-related gene (PARG) which belongs in the angiopoietin family and is involved in lipid metabolism, energy homeostasis and angiogenesis [207]. However, there is minimal investigation on the role for PPARγ to regulate Ang-2 or other angiopoietin proteins. Our study is the first to report that placental activation of PPARγ by Rosiglitazone leads to a significant reduction of Ang-2 protein secretion. While this may seem as an exciting result, some studies have shown that intrauterine growth restricted (IUGR) pregnancies are associated with reduced Ang-2 levels, which could potentially interfere with placental angiogenesis [88]. More research is needed to determine healthy versus pathologic expression of Ang-2 in pregnancy.

Endothelial vasodilation is a crucial aspect to maintaining a steady and low-pressure flow of maternal blood to the implantation site that, when disrupted, can contribute to placental ischemia [34]. sEng significantly impair vasodilation and our Luminex data is in accordance with the literature in showing that there is a significant upregulation of sEng from the preeclamptic placentas in comparison to the healthy control placentas [26, 42]. We excitedly found that sEng secretion is dampened in the PE placenta through PPARγ activation. This could be very beneficial in PE due to the significant contributions of sEng on endothelial dysfunction in PE.

Endothelin-1 is another potent vasoconstrictive molecule that is known to be elevated in PE and contribute to endothelial dysfunction in multiple cardiovascular diseases [84, 208, 209]. We surprisingly did not observe a significant difference in ET-1 secretion from control placentas compared to preeclamptic placentas. One explanation for a lack of increased secretion in PE could be due to the placental not serving as the primary source of ET-1 during pregnancy. Due to Rosiglitazone-treated PE placentas not showing any change in ET-1 levels, this result could suggest that placental PPARγ activation does not affect ET-1 secretion. There is little research that has investigated PPARγ regulation of ET-1 in the human placenta. However, there are reports in the literature that suggest in endothelial cells, PPARγ can regulate upstream pathways of ET-1 such as though increasing the expression of ET-1-inhibiting miRNAs, which result in reduced ET-1 expression [85]. It has also been shown that treatment with PPARγ agonists led to inactivation of the Activating Protein-1 (AP1) pathway which then led to transcriptional inactivation of ET-1 and subsequent reduction of ET-1 secretion [210]. It is possible that PPARγ activation could affect ET-1 at the transcript levels, but this may not be great enough to measure changes in protein secretion.

Placental growth factor (PIGF) is another major factor in the regulation of angiogenesis [75]. While our data is not statically significant, it does follow a pattern of reduced PIGF secretion from the PE placenta and in increased in PE placentas treated with Rosiglitazone. Our data supports findings in the literature that discuss PIGF being downregulated in PE [211]. There is considerable evidence to suggest PPARγ may be able to indirectly regulate PIGF, due to the role for PPARγ to regulate the expression of GCM1 which acts directly upstream of PIGF to induce transcription [155, 212, 213].

Fibroblast growth factor-2 has significant roles in regulating angiogenesis both in the endothelium and in the placenta [98]. FGF-2 has a direct role in the production of NO, which is very important due to NO being the main vasodilatory agent in the placenta that contributes to regulation of trophoblast invasion, uterine vascular remodeling, and placental perfusion [99]. Our data shows that FGF-2 is decreased in PE. Although this result was not statistically significant, it does correlate with reports in the literature stating that women with sPE are shown to have significantly reduced blood serum levels of FGF-2 compared to women of healthy pregnancies [101]. PPARγ activation by Rosiglitazone led to a significant increase in FGF-2 secretion. Given the many roles of FGF-2 in the placenta and endothelium, increasing its production in PE would likely have many beneficial effects. Previous studies have shown that other PPARγ agonists in the TZD drug-family are shown to increase FGF-2 secretion from osteoblasts [214], however our study still brings novel information from the upregulation of FGF-2 secretion in the placenta from Rosiglitazone treatment.

Placental function is also mediated through epidermal growth factor (EGF) and heparin-binding epidermal growth factor (HB-EGF) which both act on EGF receptors on the trophoblast and in the decidua [113, 114, 116, 118]. There were no significant changes in EGF secretion between PE and control placentas, which is contradictory to reports in the literature that state EGF is decreased in PE [112]. It is however possible that the placenta may not be the main source of EGF production which could explain our results. We did observe significant reductions of HB-EGF from the PE placenta which is in accordance with reports in the literature [113, 118]. The reduction of HB-EGF in term PE placentas can contribute to the enhanced trophoblast apoptosis. Fortunately, our data

shows that Rosiglitazone treatment significantly increase HB-EGF secretion from the placenta, which could help to promote trophoblast cell survival in the PE placenta. This is an exciting finding can also confirm data reported by Kushwaha et al., who previously found that Rosiglitazone can increase HB-EGF in astrocytes [215].

Follistatin (FST) has important roles throughout the menstrual cycle such as by preventing hormone release to prevent follicular development. Throughout pregnancy, FST levels generally increase then decrease towards normal levels within a few days following parturition [121]. We observed a significant reduction of FST from the PE placenta. While there is little data to show FST levels in during PE, it is known that FST levels are reduced during miscarriages [123, 124] and implantation failure in IVF [125]. We observed a significant increase in FST levels when the PE placenta was treated with Rosiglitazone. This was a surprising finding, due to reports starting that PPARγ activation downregulates FST in intestinal epithelial cells [216]. The potential for PPARγ-upregulation of follistatin should be further investigated not only in the PE placenta, but also in the first trimester based on the known importance of FST functions in early pregnancy.

Leptin is an important metabolic molecule that is known to be increased throughout healthy pregnancy [103]. We did not observe significant changes in leptin expression between PE and control placentas. Reports of leptin measurements in PE pregnancies do not all follow one pattern. Some studies mention there is an increase of leptin in women with late on-set PE, while others mention that early on-set PE have greater leptin expression even compared to late on-set PE [110]. There were no significant changes for leptin secretion based on Rosiglitazone treatment, which is surprising because other

studies have reported that PPARγ and leptin can both enact on each other to reduce each other's expressions in chondrocytes. [217]

Collectively, the Luminex assay results confirm that the PE placenta exhibits greater secretions of anti-angiogenic proteins compared to controls, evidenced by the increase in sEng secretion and the decrease in PIGF, FGF-2 and HB-EGF secretion. We can confirm that placental activation of PPARγ has an overall beneficial effect on the angiogenic profile through the reduction of Ang-2 and sEng and the upregulation of PIGF, FGF-2, HB-EGF and FST. To greater understand the impact of the angiogenic secretory profile influenced by placental activation of PPARγ, we used the conditioned medium from these placentas in culture with HUVECs.

Endothelial cells undergo angiogenesis to form new blood vessels from existing blood vessels which occur in multiple conditions, such as hypoxia and during wound healing [203]. The angiogenesis must be initiated by a stimulus, often VEGF-A, which causes endothelial activation, degradation of the basement membrane, proliferation, and migration of the cells to form into tube-like structures. Using the Angiogenesis Analyzer tool [203], the phase contrast images captured from the tube formation assay are transformed and characteristic points and elements from the images are extracted and quantified. The nodes from the HUVEC structure represent the location of two branches. Junctions are determined when a node has three or more branches that are intersecting. The total branching length is quantified as the sum of all the branch lengths per image. The 'mesh' is used to describe the general HUVEC structure and is measured by the areas enclosed by the branches.

In total, these measurements can relate to the potential for the HUVECs to undergo tube formation, which we refer to as ‘angiogenic potential’. Our data shows a very clear pattern of reduced number of nodes, junctions, total branching length and meshes in the HUVECs which were cultured with conditioned media from preeclamptic placentas. These data are not a surprise and confirm the clams presented in the literature that state the preeclamptic placenta causes an overall anti-angiogenic state. Remarkably, we saw that the Rosiglitazone-treated PE placentas cause overall greater number of nodes, junctions, total branching length and meshes, in comparison to the vehicle-treated PE placentas. This finding further validated our Luminex findings which had suggested an increase towards pro-angiogenic state of the PE placenta when treated with Rosiglitazone.

To our knowledge, we report novel findings of PPARγ actions in the placenta which have dramatic indirect effects on the endothelium. Future studies should follow up on the ability for PPARγ to modulate secreted proteins from the placenta such as Ang-2, sEng, PlGF, FGF-2, HB-EGF and FST. While VEGF-A was in our panel of markers to investigate, we did not obtain data that was within the standard curve from the Luminex assay. Due to the significant impacts of VEGF-A on the endothelium and initiation of angiogenesis, it would be helpful to know if placental activation of PPARγ effects VEGF-A secretion. Moreover, more detailed studies investigating the overall impact on the endothelial cells are warranted. For example, performing RNA-sequencing of the HUVEC cells would provide significant detail on the molecular mechanisms that are altered in these cells to permit the increased angiogenic potential.

5. DISCUSSION & CONCLUSIONS

The placenta has a significant role in establishing and securing a healthy pregnancy. It functions as an exchange organ between the mother and fetus to supply nutrients and remove waste. The placenta will anchor into the uterus, securing blood flow and acts as a protective barrier to prevent fetal infections and maternal immune rejection. In addition, the placenta will secrete hormones and peptides that can be helpful to the maternal adaptations during pregnancy (Figure 5.1). These processes can be disrupted at any time during pregnancy and result in pregnancy complications. Preeclampsia (PE) is known for causing maternal high blood pressure during pregnancy and is diagnosed after week 20 of gestation. PE has been reported in ancient civilizations through the observations of eclampsia, which occurs when PE has progressed to cause maternal seizures. Since the late 20th century, we have now established that the placenta has a significant part in causing PE. While PE is considered a heterogenous condition and not all causes of PE directly occur from abnormal placental function, the dysfunctional placenta affects most of the women who are diagnosed with severe PE (sPE) and early onset PE, especially when their pregnancy complications result in preterm delivery. Generally, it is thought that localized areas of intermitted placental perfusion or prolonged hypoxia leads to overwhelming levels of reactive oxygen species which result in aberrant trophoblast differentiation and increased apoptosis (Figure 5.1). Many molecules are dysregulated during this process, including the transcription factor, peroxisome proliferator activated receptor γ (PPARγ).

PPARγ has been shown to be essential for placental development. Murine embryos lacking PPARγ die in utero from placental and cardiovascular abnormalities [12].

PPARγ initiates villous trophoblast differentiation and without PPARγ, murine trophoblast stem cells preferentially differentiate to the extra villous trophoblast subtype [69]. Antagonizing PPARγ during rat model of pregnancy produces PE-like phenotypes, such as hypertension and proteinuria [35]. Conversely, activating PPARγ via Rosiglitazone (PPARγ agonist) in a placental-hypoxia rat model reverses these effects by decreasing hypertension and increasing the secretion of vasodilatory proteins, like HO1 [70]. PPARγ is repressed during PE and may contribute to abnormal features identified in the PE placenta. The underlying mechanisms linking PPARγ in shallow EVT invasion, molecular dysregulation of STB formation and the anti-angiogenic state in PE are not understood, but offer potential therapeutic pathways to reverse the disease, extend pregnancy duration and reduce maternal burden from disease. This study aimed to close the gap on the role for PPARγ to regulate the production and secretion of angiogenic proteins from that placenta which happen to be dysregulated during PE.

In our first study, we observed that there were significantly high protein expression of the vascular endothelial growth factor receptor 1 (VEGFR1/FLT1) present in the syncytial knots in the PE placenta. Due to VT differentiation being under the control of PPARγ, which acts subsequently on glial cell missing 1 (GCM1) to promote STB formation, we hypothesized that the disruption of VT differentiation by the PPARy-GCM1 axis could be contributed to the enhanced expression of FLT1 and sFLT1 in PE. We used severe PE, age-matched control placentas as well as first trimester human placentas to modulate this pathway. We were able to show that by PPARy-GCM1 expression and activity could be increased in the human placenta by Rosiglitazone while FLT1 and sFLT1 were significantly reduced. Through siRNA-mediated reduction of GCM1, we show that

sFLT1 expression inversely correlated with GCM1 expression and thus GCM1 likely acts as the intermediate of this pathway. These findings show crucial evidence for the first time that sFLT1 can be reduced by activating the mediations that regulate normal trophoblast differentiation.

We aimed to expand on this study to the investigation of PPARγ regulation for another important molecule, heme oxygenase 1 (HO1). PE is compromised by reductions of HO1, which significantly impairs pro-angiogenic, cytoprotective and response to oxidative stress in the placenta. We show in our first trimester and term healthy/sPE placentas that PPARγ activation can restore HO1 levels. Moreover, we established an *in vitro* model system using the BeWo choriocarcinoma cell line, during ischemic conditions that mimicked these results from the PE placenta. Through siRNA-mediated PPARγ reduction, we could show that HO1 expression is at least partially dependent on PPARγ and that Rosiglitazone-mediated upregulation of HO1 occurs directly through PPARγ. While we aimed to investigate the mechanism of PPARγ-mediated HO1 upregulation, there is more work that is needed to show the direct transcriptional upregulate of HO1 by PPARγ.

We lastly aimed to discover more broadly a panel of angiogenic, metabolic and growth factor proteins that are secreted from the placenta and their expressions are disrupted in PE. We further aimed to uncover the angiogenic potential of the PE placenta and how this is changed through placental activation of PPARγ. We discovered that PPARγ could reduce anti-angiogenic proteins (Ang-2 and sEng) while increasing pro-angiogenic and growth factor proteins (PIGF, FGF-2, HB-EGF, Follistatin) which all have critical functions in the surrounding endothelium and in the placenta and point that PPARγ

can partially restore the angiogenic balance in the placenta (Figure 5.1). Our final investigation on the indirect angiogenic potential of PPARγ activation in the PE placenta, was performed by culturing human umbilical vein endothelial cells (HUVECs) with placental conditioned media from healthy and PE placentas, and PE placentas that have been treated with Rosiglitazone. Based on this tube formation assay, we could see a very clear overall decreased angiogenic potential in the HUVECs cultured with the conditioned media from the PE placentas when compared to the HUVECs cultured with control placental conditioned media. There was however a remarkable increase in the tube formation based on Rosiglitazone treatment in the PE placenta. These findings could confirm the pattern which we had begun to see based on measuring the secreted proteins. Overall, the Rosiglitazone has a favorable effect towards increasing angiogenic/growth factor proteins to impact endothelial and placental function. While these novel studies discover new avenues for PPARγ function in the placenta, more work is needed to fully understand how PPARγ can modulate these proteins. Studies that investigate how PPARγ effects the global transcriptome and coupled with genome-wide PPARγ-DNA binding assay (such as ChIP or CUT&RUN) will fully define how PPARγ acts in the human placenta. One critical limitation of this study was the use of Rosiglitazone to activate PPARγ. While the overall long-term goal is to translate these finds to establish treatment for women with PE, Rosiglitazone is not a safe drug to use in pregnancy due to its significant off target effects. Establishment of new drugs that are either safe to consume during pregnancy, or directly target placental cells, is required, and warranted based on the significant beneficial effects of PPARγ in the placenta and its ability to reverse many aspects of placental dysfunction in PE.

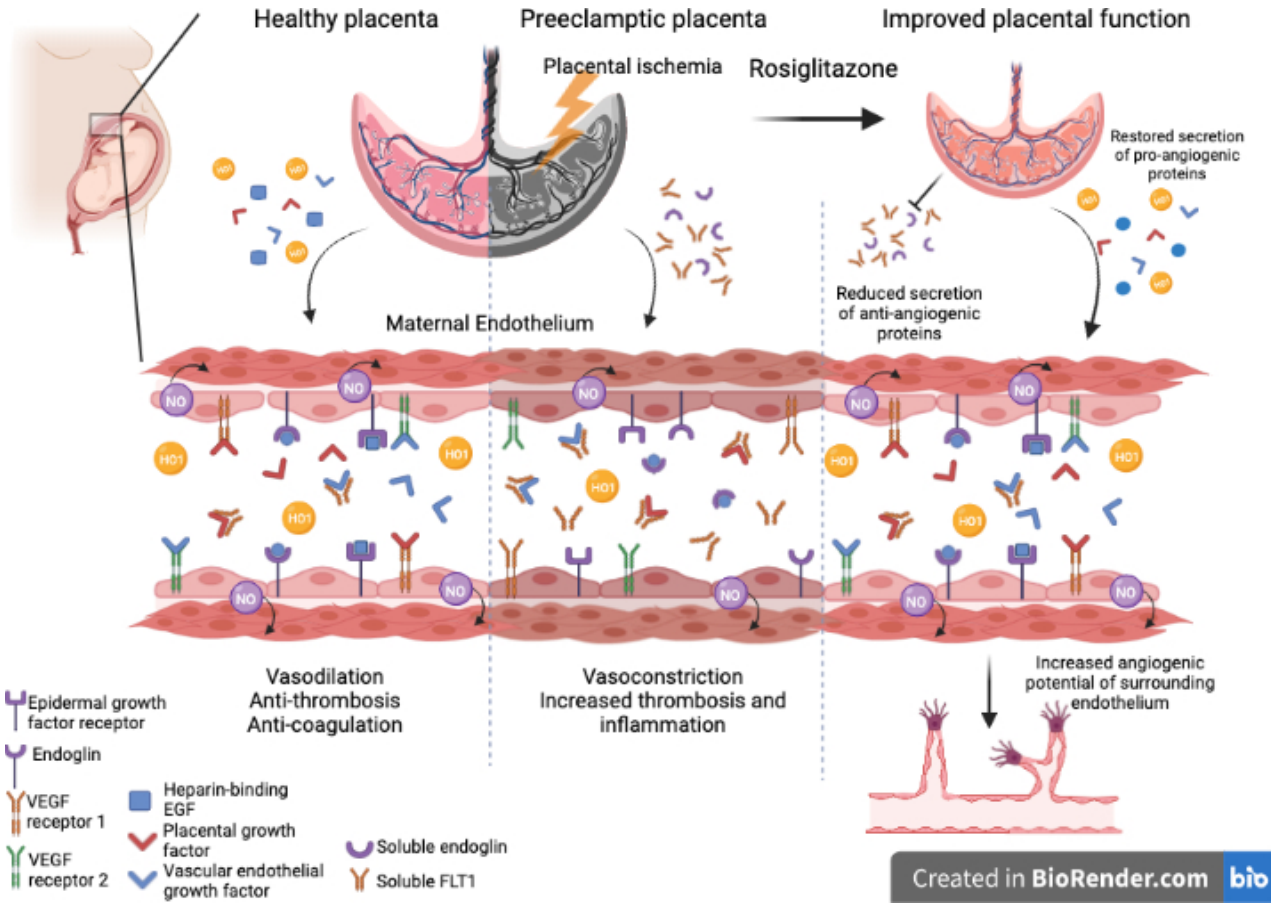

Figure 5.1: Rosiglitazone can attenuate preeclampsia phenotypes in placental and angiogenic model systems. Preeclampsia is burdened with excessive production of anti-angiogenic factors such as soluble endoglin and soluble FLT1 and a reduction of pro-angiogenic molecules such as heme oxygenase 1. Treatment of preeclamptic placentas with the PPARγ-activating molecule, Rosiglitazone, leads to significant reduction of anti-angiogenic proteins and restored secretion of pro-angiogenic proteins from the placenta. This subsequently causes increased angiogenic potential of the surrounding endothelium.

REFERENCES

REFERENCES

1. Armistead, B., et al., *Placental Regulation of Energy Homeostasis During Human Pregnancy.* Endocrinology, 2020. **161**(7).

2. Ozen, M., et al., *Heme oxygenase and the immune system in normal and pathological pregnancies.* Front Pharmacol, 2015. **6**: p. 84.

3. Mor, G., *Inflammation and pregnancy - The role of toll-like receptors in trophoblast-immune interaction.* Assessment of Human Reproductive Function, 2008. **1127**: p. 121-128.

4. Mor, G., et al., *Inflammation and pregnancy: the role of the immune system at the implantation site.* Ann N Y Acad Sci, 2011. **1221**: p. 80-7.

5. Mor, G. and J.Y. Kwon, *Trophoblast-microbiome interaction: a new paradigm on immune regulation.* Am J Obstet Gynecol, 2015. **213**(4 Suppl): p. S131-7.

6. Lindheimer, M.D., *CHESLEY'S HYPERTENSIVE DISORDERS IN PREGNANCY THIRD EDITION Preface.* Chesley's Hypertensive Disorders in Pregnancy, 3rd Edition, 2009: p. Ix-X.

7. Knofler, M., et al., *Human placenta and trophoblast development: key molecular mechanisms and model systems.* Cellular and Molecular Life Sciences, 2019. **76**(18): p. 3479-3496.

8. *Chesley's Hypertensive Disorders in Pregnancy, 3rd Edition.* Chesley's Hypertensive Disorders in Pregnancy, 3rd Edition, 2009: p. 1-431.

9. Baczyk, D., et al., *Bi-potential behaviour of cytotrophoblasts in first trimester chorionic villi.* Placenta, 2006. **27**(4-5): p. 367-74.

10. Chang, C.W., A.K. Wakeland, and M.M. Parast, *Trophoblast lineage specification, differentiation and their regulation by oxygen tension.* J Endocrinol, 2018. **236**(1): p. R43-R56.

11. Kohan-Ghadr, H.R., et al., *Potential role of epigenetic mechanisms in regulation of trophoblast differentiation, migration, and invasion in the human placenta.* Cell Adh Migr, 2016. **10**(1-2): p. 126-35.

12. Barak, Y., et al., *PPAR gamma is required for placental, cardiac, and adipose tissue development.* Mol Cell, 1999. **4**(4): p. 585-95.

13. Barak, Y., et al., *Effects of peroxisome proliferator-activated receptor delta on placentation, adiposity, and colorectal cancer.* Proceedings of the National Academy of Sciences of the United States of America, 2002. **99**(1): p. 303-308.

14. Borel, V., et al., *Placental implications of peroxisome proliferator-activated receptors in gestation and parturition.* PPAR Res, 2008. **2008**: p. 758562.

15. Anson-Cartwright, L., et al., *The glial cells missing-1 protein is essential for branching morphogenesis in the chorioallantoic placenta.* Nature Genetics, 2000. **25**: p. 311.

16. Baczyk, D., et al., *Glial cell missing-1 transcription factor is required for the differentiation of the human trophoblast.* Cell Death and Differentiation, 2009. **16**(5): p. 719-727.

17. Chen, C.P., et al., *Decreased Placental GCM1 (Glial Cells Missing) Gene Expression in Pre-eclampsia.* Placenta, 2004. **25**(5): p. 413-421.

18. Kadam, L., et al., *Rosiglitazone blocks first trimester in-vitro placental injury caused by NF-kappaB-mediated inflammation.* Sci Rep, 2019. **9**(1): p. 2018.

19. Pollheimer, J., et al., *Regulation of Placental Extravillous Trophoblasts by the Maternal Uterine Environment.* Frontiers in Immunology, 2018. **9**.

20. Geva, E., et al., *Human placental vascular development: vasculogenic and angiogenic (branching and nonbranching) transformation is regulated by vascular endothelial growth factor-A, angiopoietin-1, and angiopoietin-2.* J Clin Endocrinol Metab, 2002. **87**(9): p. 4213-24.

21. Lyall, F., S.C. Robson, and J.N. Bulmer, *Spiral artery remodeling and trophoblast invasion in preeclampsia and fetal growth restriction: relationship to clinical outcome.* Hypertension, 2013. **62**(6): p. 1046-54.

22. Bardin, N., P. Murthi, and N. Alfaidy, *Normal and pathological placental angiogenesis.* Biomed Res Int, 2015. **2015**: p. 354359.

23. Armistead, B., et al., *Induction of the PPARγ (Peroxisome Proliferator-Activated Receptor γ)-GCM1 (Glial Cell Missing 1) Syncytialization Axis Reduces sFLT1 (Soluble fms-Like Tyrosine Kinase 1) in the Preeclamptic Placenta.* Hypertension, 2021. **78**(1): p. 230-240.

24. Benton, S.J., et al., *The clinical heterogeneity of preeclampsia is related to both placental gene expression and placental histopathology.* Am J Obstet Gynecol, 2018. **219**(6): p. 604.e1-604.e25.

25. Croke, L., *Gestational Hypertension and Preeclampsia: A Practice Bulletin from ACOG.* Am Fam Physician, 2019. **100**(10): p. 649-650.

26. Ahmed, A., *New insights into the etiology of preeclampsia: identification of key elusive factors for the vascular complications.* Thromb Res, 2011. **127 Suppl 3**: p. S72-5.

27. Roberts, J.M., et al., *Subtypes of Preeclampsia: Recognition and Determining Clinical Usefulness.* Hypertension, 2021. **77**(5): p. 1430-1441.

28. Jeyabalan, A., *Epidemiology of preeclampsia: impact of obesity.* Nutrition Reviews, 2013. **71**: p. S18-S25.

29. Levytska, K., et al., *Heme oxygenase-1 in placental development and pathology.* Placenta, 2013. **34**(4): p. 291-298.

30. Armistead, B., et al., *The Role of NFkappaB in Healthy and Preeclamptic Placenta: Trophoblasts in the Spotlight.* Int J Mol Sci, 2020. **21**(5).

31. Rana, S., et al., *Preeclampsia: Pathophysiology, Challenges, and Perspectives.* Circ Res, 2019. **124**(7): p. 1094-1112.

32. Ho, A.E.P., et al., *T2* Placental Magnetic Resonance Imaging in Preterm Preeclampsia: An Observational Cohort Study.* Hypertension, 2020. **75**(6): p. 1523-1531.

33. Aouache, R., et al., *Oxidative Stress in Preeclampsia and Placental Diseases.* Int J Mol Sci, 2018. **19**(5).

34. Myatt, L. and R.P. Webster, *Vascular biology of preeclampsia.* J Thromb Haemost, 2009. **7**(3): p. 375-84.

35. McCarthy, F.P., et al., *Evidence Implicating Peroxisome Proliferator-Activated Receptor-gamma in the Pathogenesis of Preeclampsia.* Hypertension, 2011. **58**(5): p. 882-U447.

36. Levytska, K., et al., *PPAR-gamma Regulates Trophoblast Differentiation in the BeWo Cell Model.* Ppar Research, 2014.

37. O'Brien, M., D. Baczyk, and J.C. Kingdom, *Endothelial Dysfunction in Severe Preeclampsia is Mediated by Soluble Factors, Rather than Extracellular Vesicles.* Scientific Reports, 2017. **7**.

38. Reynolds, L.P. and D.A. Redmer, *Angiogenesis in the placenta.* Biol Reprod, 2001. **64**(4): p. 1033-40.

39. Maynard, S.E. and S.A. Karumanchi, *Angiogenic factors and preeclampsia.* Semin Nephrol, 2011. **31**(1): p. 33-46.

40. Azliana, A., et al., *Vascular endothelial growth factor expression in placenta of hypertensive disorder in pregnancy.* Indian Journal of Pathology and Microbiology, 2017. **60**(4): p. 515-520.

41. Kornacki, J., et al., *Endothelial Dysfunction in Pregnancy Complications.* Biomedicines, 2021. **9**(12).

42. Huynh, D.T.N. and K.S. Heo, *Therapeutic targets for endothelial dysfunction in vascular diseases.* Arch Pharm Res, 2019. **42**(10): p. 848-861.

43. Goel, A., et al., *Epidemiology and Mechanisms of De Novo and Persistent Hypertension in the Postpartum Period.* Circulation, 2015. **132**(18): p. 1726-33.

44. Ditisheim, A., et al., *Prevalence of Hypertensive Phenotypes After Preeclampsia: A Prospective Cohort Study.* Hypertension, 2018. **71**(1): p. 103-109.

45. Mongraw-Chaffin, M.L., P.M. Cirillo, and B.A. Cohn, *Preeclampsia and cardiovascular disease death: prospective evidence from the child health and development studies cohort.* Hypertension, 2010. **56**(1): p. 166-71.

46. Wang, S., E.J. Dougherty, and R.L. Danner, *PPARγ signaling and emerging opportunities for improved therapeutics.* Pharmacol Res, 2016. **111**: p. 76-85.

47. Brunmeir, R. and F. Xu, *Functional Regulation of PPARs through Post-Translational Modifications.* Int J Mol Sci, 2018. **19**(6).

48. Janani, C. and B.D. Ranjitha Kumari, *PPAR gamma gene--a review.* Diabetes Metab Syndr, 2015. **9**(1): p. 46-50.

49. Grygiel-Górniak, B., *Peroxisome proliferator-activated receptors and their ligands: nutritional and clinical implications--a review.* Nutr J, 2014. **13**: p. 17.

50. Hu, E., et al., *Inhibition of adipogenesis through MAP kinase-mediated phosphorylation of PPARgamma.* Science, 1996. **274**(5295): p. 2100-3.

51. Zhang, B., et al., *Insulin- and mitogen-activated protein kinase-mediated phosphorylation and activation of peroxisome proliferator-activated receptor gamma.* J Biol Chem, 1996. **271**(50): p. 31771-4.

52. Adams, M., et al., *Transcriptional activation by peroxisome proliferator-activated receptor gamma is inhibited by phosphorylation at a consensus mitogen-activated protein kinase site.* J Biol Chem, 1997. **272**(8): p. 5128-32.

53. Reginato, M.J., et al., *Prostaglandins promote and block adipogenesis through opposing effects on peroxisome proliferator-activated receptor gamma.* J Biol Chem, 1998. **273**(4): p. 1855-8.

54. Picard, F., et al., *Sirt1 promotes fat mobilization in white adipocytes by repressing PPAR-gamma.* Nature, 2004. **429**(6993): p. 771-6.

55. Banks, A.S., et al., *An ERK/Cdk5 axis controls the diabetogenic actions of PPARγ.* Nature, 2015. **517**(7534): p. 391-5.

56. Choi, J.H., et al., *Anti-diabetic drugs inhibit obesity-linked phosphorylation of PPARgamma by Cdk5.* Nature, 2010. **466**(7305): p. 451-6.

57. Armistead, B., et al., *The Role of NFκB in Healthy and Preeclamptic Placenta: Trophoblasts in the Spotlight.* Int J Mol Sci, 2020. **21**(5).

58. Qiang, L., et al., *Brown remodeling of white adipose tissue by SirT1-dependent deacetylation of Pparγ.* Cell, 2012. **150**(3): p. 620-32.

59. Han, L., et al., *SIRT1 is regulated by a PPAR{γ}-SIRT1 negative feedback loop associated with senescence.* Nucleic Acids Res, 2010. **38**(21): p. 7458-71.

60. van Beekum, O., et al., *The adipogenic acetyltransferase Tip60 targets activation function 1 of peroxisome proliferator-activated receptor gamma.* Endocrinology, 2008. **149**(4): p. 1840-9.

61. Wang, I.K., et al., *Subsequent risk of gout for women with hypertensive disorders in pregnancy: a retrospective cohort study.* Journal of Hypertension, 2016. **34**(5): p. 914-919.

62. Ryan, K.K., et al., *A role for central nervous system PPAR-γ in the regulation of energy balance.* Nat Med, 2011. **17**(5): p. 623-6.

63. Lu, M., et al., *Brain PPAR-γ promotes obesity and is required for the insulin-sensitizing effect of thiazolidinediones.* Nat Med, 2011. **17**(5): p. 618-22.

64. Guan, Y., et al., *Thiazolidinediones expand body fluid volume through PPARgamma stimulation of ENaC-mediated renal salt absorption.* Nat Med, 2005. **11**(8): p. 861-6.

65. Ahmadian, M., et al., *PPARγ signaling and metabolism: the good, the bad and the future.* Nat Med, 2013. **19**(5): p. 557-66.

66. Liu, L., et al., *ANGPTL4 mediates the protective role of PPAR. activators in the pathogenesis of preeclampsia.* Cell Death & Disease, 2017. **8**.

67. Abdelrahman, M., A. Sivarajah, and C. Thiemermann, *Beneficial effects of PPAR-gamma ligands in ischemia-reperfusion injury, inflammation and shock.* Cardiovascular Research, 2005. **65**(4): p. 772-781.

68. Kadam, L., H.R. Kohan-Ghadr, and S. Drewlo, *The balancing act - PPAR-gamma's roles at the maternal-fetal interface.* Syst Biol Reprod Med, 2015. **61**(2): p. 65-71.

69. Parast, M.M., et al., *PPARgamma regulates trophoblast proliferation and promotes labyrinthine trilineage differentiation.* PLoS One, 2009. **4**(11): p. e8055.

70. McCarthy, F.P., et al., *Peroxisome Proliferator-Activated Receptor-gamma as a Potential Therapeutic Target in the Treatment of Preeclampsia.* Hypertension, 2011. **58**(2): p. 280-U319.

71. Wieser, F., et al., *PPAR Action in Human Placental Development and Pregnancy and Its Complications.* PPAR Res, 2008. **2008**: p. 527048.

72. Liu, F., et al., *C1431T Variant of PPARγ Is Associated with Preeclampsia in Pregnant Women.* Life (Basel), 2021. **11**(10).

73. Adair, T.H. and J.P. Montani, *Angiogenesis*. 2010.

74. Sweeney, M.D., S. Ayyadurai, and B.V. Zlokovic, *Pericytes of the neurovascular unit: key functions and signaling pathways.* Nat Neurosci, 2016. **19**(6): p. 771-83.

75. Kliche, S. and J. Waltenberger, *VEGF receptor signaling and endothelial function.* IUBMB Life, 2001. **52**(1-2): p. 61-6.

76. Chau, K., A. Hennessy, and A. Makris, *Placental growth factor and pre-eclampsia.* J Hum Hypertens, 2017. **31**(12): p. 782-786.

77. McLaughlin, K., et al., *PlGF (Placental Growth Factor) Testing in Clinical Practice: Evidence From a Canadian Tertiary Maternity Referral Center.* Hypertension, 2021: p. HYPERTENSIONAHA12117047.

78. Agrawal, S., et al., *Predictive Performance of PlGF (Placental Growth Factor) for Screening Preeclampsia in Asymptomatic Women: A Systematic Review and Meta-Analysis.* Hypertension, 2019. **74**(5): p. 1124-1135.

79. Ashar-Patel, A., et al., *FLT1 and transcriptome-wide polyadenylation site (PAS) analysis in preeclampsia.* Sci Rep, 2017. **7**(1): p. 12139.

80. Drewlo, S., et al., *Heparin promotes soluble VEGF receptor expression in human placental villi to impair endothelial VEGF signaling.* J Thromb Haemost, 2011. **9**(12): p. 2486-97.

81. Maynard, S.E., et al., *Excess placental soluble fms-like tyrosine kinase 1 (sFlt1) may contribute to endothelial dysfunction, hypertension, and proteinuria in preeclampsia.* J Clin Invest, 2003. **111**(5): p. 649-58.

82. McGinnis, R., et al., *Variants in the fetal genome near FLT1 are associated with risk of preeclampsia.* Nat Genet, 2017. **49**(8): p. 1255-1260.

83. Margioula-Siarkou, G., et al., *The role of endoglin and its soluble form in pathogenesis of preeclampsia.* Mol Cell Biochem, 2022. **477**(2): p. 479-491.

84. Marasciulo, F.L., M. Montagnani, and M.A. Potenza, *Endothelin-1: the yin and yang on vascular function.* Curr Med Chem, 2006. **13**(14): p. 1655-65.

85. Kang, B.Y., et al., *Peroxisome Proliferator-Activated Receptor γ and microRNA 98 in Hypoxia-Induced Endothelin-1 Signaling.* Am J Respir Cell Mol Biol, 2016. **54**(1): p. 136-46.

86. Kurihara, Y., et al., *Elevated blood pressure and craniofacial abnormalities in mice deficient in endothelin-1.* Nature, 1994. **368**(6473): p. 703-10.

87. Kappou, D., et al., *Role of the angiopoietin/Tie system in pregnancy (Review).* Exp Ther Med, 2015. **9**(4): p. 1091-1096.

88. Akwii, R.G., et al., *Role of Angiopoietin-2 in Vascular Physiology and Pathophysiology.* Cells, 2019. **8**(5).

89. David, S., et al., *Angiopoietin 2 and cardiovascular disease in dialysis and kidney transplantation.* Am J Kidney Dis, 2009. **53**(5): p. 770-8.

90. Lee, K.W., G.Y. Lip, and A.D. Blann, *Plasma angiopoietin-1, angiopoietin-2, angiopoietin receptor tie-2, and vascular endothelial growth factor levels in acute coronary syndromes.* Circulation, 2004. **110**(16): p. 2355-60.

91. Patel, J.V., et al., *Angiopoietin-2 levels as a biomarker of cardiovascular risk in patients with hypertension.* Ann Med, 2008. **40**(3): p. 215-22.

92. Hirokoshi, K., et al., *Increase of serum angiopoietin-2 during pregnancy is suppressed in women with preeclampsia.* Am J Hypertens, 2005. **18**(9 Pt 1): p. 1181-8.

93. Han, S.Y., et al., *Angiopoietin-2: a promising indicator for the occurrence of severe preeclampsia.* Hypertens Pregnancy, 2012. **31**(1): p. 189-99.

94. Bolin, M., et al., *Angiopoietin-1/angiopoietin-2 ratio for prediction of preeclampsia.* Am J Hypertens, 2009. **22**(8): p. 891-5.

95. Nugent, M.A. and R.V. Iozzo, *Fibroblast growth factor-2.* Int J Biochem Cell Biol, 2000. **32**(2): p. 115-20.

96. Murphy, P.R., et al., *Fibroblast growth factor-2 stimulates endothelial nitric oxide synthase expression and inhibits apoptosis by a nitric oxide-dependent pathway in Nb2 lymphoma cells.* Endocrinology, 2001. **142**(1): p. 81-8.

97. Okada-Ban, M., J.P. Thiery, and J. Jouanneau, *Fibroblast growth factor-2.* Int J Biochem Cell Biol, 2000. **32**(3): p. 263-7.

98. Arany, E. and D.J. Hill, *Fibroblast growth factor-2 and fibroblast growth factor receptor-1 mRNA expression and peptide localization in placentae from normal and diabetic pregnancies.* Placenta, 1998. **19**(2-3): p. 133-42.

99. Ozkan, S., et al., *Placental expression of insulin-like growth factor-I, fibroblast growth factor-basic, and neural cell adhesion molecule in preeclampsia.* J Matern Fetal Neonatal Med, 2008. **21**(11): p. 831-8.

100. Murakami, M., et al., *FGF-dependent regulation of VEGF receptor 2 expression in mice.* J Clin Invest, 2011. **121**(7): p. 2668-78.

101. Hohlagschwandtner, M., et al., *Basic fibroblast growth factor and hypertensive disorders in pregnancy.* Hypertens Pregnancy, 2002. **21**(3): p. 235-41.

102. Perry, R.J., *Leptin revisited: The role of leptin in starvation.* Mol Cell Oncol, 2018. **5**(5): p. e1435185.

103. Ladyman, S.R., R.A. Augustine, and D.R. Grattan, *Hormone interactions regulating energy balance during pregnancy.* J Neuroendocrinol, 2010. **22**(7): p. 805-17.

104. Myers, M.G., M.A. Cowley, and H. Munzberg, *Mechanisms of leptin action and leptin resistance.* Annu Rev Physiol, 2008. **70**: p. 537-56.

105. Sylvia, K.E., et al., *Physiological predictors of leptin vary during menses and ovulation in healthy women.* Reprod Biol, 2018. **18**(1): p. 132-136.

106. Herrid, M., et al., *An updated view of leptin on implantation and pregnancy: a review.* Physiol Res, 2014. **63**(5): p. 543-57.

107. Su, R.W. and A.T. Fazleabas, *Implantation and Establishment of Pregnancy in Human and Nonhuman Primates.* Adv Anat Embryol Cell Biol, 2015. **216**: p. 189-213.

108. Jansson, T., M. Wennergren, and N.P. Illsley, *Glucose transporter protein expression in human placenta throughout gestation and in intrauterine growth retardation.* J Clin Endocrinol Metab, 1993. **77**(6): p. 1554-62.

109. Zhang, Y., et al., *The leptin receptor mediates apparent autocrine regulation of leptin gene expression.* Biochem Biophys Res Commun, 1997. **240**(2): p. 492-5.

110. Taylor, B.D., et al., *Serum leptin measured in early pregnancy is higher in women with preeclampsia compared with normotensive pregnant women.* Hypertension, 2015. **65**(3): p. 594-9.

111. Salimi, S., et al., *Different profile of serum leptin between early onset and late onset preeclampsia.* Dis Markers, 2014. **2014**: p. 628476.

112. Armant, D.R., et al., *Reduced expression of the epidermal growth factor signaling system in preeclampsia.* Placenta, 2015. **36**(3): p. 270-8.

113. Jessmon, P., R.E. Leach, and D.R. Armant, *Diverse functions of HBEGF during pregnancy.* Mol Reprod Dev, 2009. **76**(12): p. 1116-27.

114. Leach, R.E., et al., *Multiple roles for heparin-binding epidermal growth factor-like growth factor are suggested by its cell-specific expression during the human*

endometrial cycle and early placentation. J Clin Endocrinol Metab, 1999. **84**(9): p. 3355-63.

115. Large, M.J., et al., *The epidermal growth factor receptor critically regulates endometrial function during early pregnancy.* PLoS Genet, 2014. **10**(6): p. e1004451.

116. Imudia, A.N., et al., *Expression of heparin-binding EGF-like growth factor in term chorionic villous explants and its role in trophoblast survival.* Placenta, 2008. **29**(9): p. 784-9.

117. Hastie, R., et al., *EGFR (Epidermal Growth Factor Receptor) Signaling and the Mitochondria Regulate sFlt-1 (Soluble FMS-Like Tyrosine Kinase-1) Secretion.* Hypertension, 2019. **73**(3): p. 659-670.

118. Leach, R.E., et al., *Pre-eclampsia and expression of heparin-binding EGF-like growth factor.* Lancet, 2002. **360**(9341): p. 1215-9.

119. Fullerton, P.T., et al., *Follistatin is critical for mouse uterine receptivity and decidualization.* Proc Natl Acad Sci U S A, 2017. **114**(24): p. E4772-E4781.

120. Köninger, A., et al., *Follistatin during pregnancy and its potential role as an ovarian suppressing agent.* Eur J Obstet Gynecol Reprod Biol, 2017. **212**: p. 150-154.

121. Petraglia, F., *Inhibin, activin and follistatin in the human placenta--a new family of regulatory proteins.* Placenta, 1997. **18**(1): p. 3-8.

122. Luisi, S., et al., *Inhibins in female and male reproductive physiology: role in gametogenesis, conception, implantation and early pregnancy.* Hum Reprod Update, 2005. **11**(2): p. 123-35.

123. Prakash, A., et al., *Inhibin A and activin A may be used to predict pregnancy outcome in women with recurrent miscarriage.* Fertil Steril, 2005. **83**(6): p. 1758-63.

124. Prakash, A., et al., *A study of luteal phase expression of inhibin, activin, and follistatin subunits in the endometrium of women with recurrent miscarriage.* Fertil Steril, 2006. **86**(6): p. 1723-30.

125. Prakash, A., et al., *A preliminary study comparing the endometrial expression of inhibin, activin and follistatin in women with a history of implantation failure after IVF treatment and a control group.* BJOG, 2008. **115**(4): p. 532-6; discussion 536-7.

126. Choi, A.M. and J. Alam, *Heme oxygenase-1: function, regulation, and implication of a novel stress-inducible protein in oxidant-induced lung injury.* Am J Respir Cell Mol Biol, 1996. **15**(1): p. 9-19.

127. Otterbein, L.E., et al., *Heme oxygenase-1: unleashing the protective properties of heme.* Trends Immunol, 2003. **24**(8): p. 449-55.

128. Levytska, K., et al., *Heme oxygenase-1 in placental development and pathology.* Placenta, 2013. **34**(4): p. 291-8.

129. Ryter, S.W. and A.M. Choi, *Targeting heme oxygenase-1 and carbon monoxide for therapeutic modulation of inflammation.* Transl Res, 2016. **167**(1): p. 7-34.

130. Gallardo, V., et al., *Role of heme oxygenase 1 and human chorionic gonadotropin in pregnancy associated diseases.* Biochim Biophys Acta Mol Basis Dis, 2020. **1866**(2): p. 165522.

131. Martínez-Casales, M., R. Hernanz, and M.J. Alonso, *Vascular and Macrophage Heme Oxygenase-1 in Hypertension: A Mini-Review.* Front Physiol, 2021. **12**: p. 643435.

132. Consoli, V., et al., *Heme Oxygenase-1 Signaling and Redox Homeostasis in Physiopathological Conditions.* Biomolecules, 2021. **11**(4).

133. Kaartokallio, T., et al., *Microsatellite polymorphism in the heme oxygenase-1 promoter is associated with nonsevere and late-onset preeclampsia.* Hypertension, 2014. **64**(1): p. 172-7.

134. Denschlag, D., et al., *The size of a microsatellite polymorphism of the haem oxygenase 1 gene is associated with idiopathic recurrent miscarriage.* Mol Hum Reprod, 2004. **10**(3): p. 211-4.

135. Otterbein, L.E., et al., *Carbon monoxide has anti-inflammatory effects involving the mitogen-activated protein kinase pathway.* Nat Med, 2000. **6**(4): p. 422-8.

136. Deramaudt, B.M., et al., *Gene transfer of human heme oxygenase into coronary endothelial cells potentially promotes angiogenesis.* J Cell Biochem, 1998. **68**(1): p. 121-7.

137. Deshane, J., et al., *Stromal cell-derived factor 1 promotes angiogenesis via a heme oxygenase 1-dependent mechanism.* J Exp Med, 2007. **204**(3): p. 605-18.

138. Zhao, H., et al., *Heme oxygenase-1 in pregnancy and cancer: similarities in cellular invasion, cytoprotection, angiogenesis, and immunomodulation.* Front Pharmacol, 2014. **5**: p. 295.

139. Li Volti, G., et al., *Carbon monoxide signaling in promoting angiogenesis in human microvessel endothelial cells.* Antioxid Redox Signal, 2005. **7**(5-6): p. 704-10.

140. George, E.M., et al., *Induction of heme oxygenase-1 attenuates sFlt-1-induced hypertension in pregnant rats.* Am J Physiol Regul Integr Comp Physiol, 2011. **301**(5): p. R1495-500.

141. Zhao, H., et al., *Effect of heme oxygenase-1 deficiency on placental development.* Placenta, 2009. **30**(10): p. 861-8.

142. Wong, R.J., H. Zhao, and D.K. Stevenson, *A deficiency in haem oxygenase-1 induces foetal growth restriction by placental vasculature defects.* Acta Paediatr, 2012. **101**(8): p. 827-34.

143. Staff, A.C., *The two-stage placental model of preeclampsia: An update.* J Reprod Immunol, 2019. **134-135**: p. 1-10.

144. McDonald, C.R., et al., *Angiogenic proteins, placental weight and perinatal outcomes among pregnant women in Tanzania.* PLoS One, 2016. **11**(12): p. e0167716.

145. Zur, R.L., et al., *The Placental Basis of Fetal Growth Restriction.* Obstet Gynecol Clin North Am, 2020. **47**(1): p. 81-98.

146. Phipps, E.A., et al., *Pre-eclampsia: pathogenesis, novel diagnostics and therapies.* Nat Rev Nephrol, 2019. **15**(5): p. 275-289.

147. Myers, J.E., et al., *Angiogenic factors combined with clinical risk factors to predict preterm pre-eclampsia in nulliparous women: a predictive test accuracy study.* BJOG, 2013. **120**(10): p. 1215-23.

148. Levine, R.J., et al., *Circulating angiogenic factors and the risk of preeclampsia.* N Engl J Med, 2004. **350**(7): p. 672-83.

149. Doherty, A., et al., *Altered hemodynamics and hyperuricemia accompany an elevated sFlt-1/PlGF ratio before the onset of early severe preeclampsia.* J Obstet Gynaecol Can, 2014. **36**(8): p. 692-700.

150. Zeisler, H., et al., *Soluble fms-Like Tyrosine Kinase-1-to-Placental Growth Factor Ratio and Time to Delivery in Women With Suspected Preeclampsia.* Obstet Gynecol, 2016. **128**(2): p. 261-269.

151. Zeisler, H., et al., *Predictive Value of the sFlt-1:PlGF Ratio in Women with Suspected Preeclampsia.* N Engl J Med, 2016. **374**(1): p. 13-22.

152. McLaughlin, K., et al., *Placental Growth Factor Testing In Clinical Practice: Evidence From A Canadian Tertiary Maternity Referral Centre* 2021: Hypertension.

153. Ganss, R., *Maternal Metabolism and Vascular Adaptation in Pregnancy: The PPAR Link.* Trends Endocrinol Metab, 2017. **28**(1): p. 73-84.

154. Fan, X., et al., *Endometrial VEGF induces placental sFLT1 and leads to pregnancy complications.* J Clin Invest, 2014. **124**(11): p. 4941-52.

155. Chang, M., et al., *Glial cell missing 1 regulates placental growth factor (PGF) gene transcription in human trophoblast.* Biology of reproduction, 2008. **78**(5): p. 841-851.

156. Kendall, R.L. and K.A. Thomas, *Inhibition of vascular endothelial cell growth factor activity by an endogenously encoded soluble receptor.* Proceedings of the National Academy of Sciences, 1993. **90**(22): p. 10705-10709.

157. Kendall, R.L., G. Wang, and K.A. Thomas, *Identification of a Natural Soluble Form of the Vascular Endothelial Growth Factor Receptor, FLT-1, and Its Heterodimerization with KDR.* Biochemical and Biophysical Research Communications, 1996. **226**(2): p. 324-328.

158. Jebbink, J., et al., *Expression of placental FLT1 transcript variants relates to both gestational hypertensive disease and fetal growth.* Hypertension, 2011. **58**(1): p. 70-6.

159. Thomas, C.P., et al., *A recently evolved novel trophoblast-enriched secreted form of fms-like tyrosine kinase-1 variant is up-regulated in hypoxia and preeclampsia.* J Clin Endocrinol Metab, 2009. **94**(7): p. 2524-30.

160. Baczyk, D., et al., *Complex patterns of GCM1 mRNA and protein in villous and extravillous trophoblast cells of the human placenta.* Placenta, 2004. **25**(6): p. 553-559.

161. Bainbridge, S.A., et al., *Effects of Reduced Gcm1 Expression on Trophoblast Morphology, Fetoplacental Vascularity, and Pregnancy Outcomes in Mice.* Hypertension, 2012. **59**(3): p. 732-739.

162. Mohammadi, H., et al., *HIV antiretroviral exposure in pregnancy induces detrimental placenta vascular changes that are rescued by progesterone supplementation.* Sci Rep, 2018. **8**(1): p. 6552.

163. Ruebner, M., et al., *Regulation of the human endogenous retroviral Syncytin-1 and cell-cell fusion by the nuclear hormone receptors PPARgamma/RXRalpha in placentogenesis.* J Cell Biochem, 2012. **113**(7): p. 2383-96.

164. Tache, V., et al., *Hypoxia and trophoblast differentiation: a key role for PPARgamma.* Stem Cells Dev, 2013. **22**(21): p. 2815-24.

165. Lane, S.L., et al., *Pharmacological activation of peroxisome proliferator-activated receptor gamma (PPAR-gamma) protects against hypoxia-associated fetal growth restriction.* FASEB J, 2019. **33**(8): p. 8999-9007.

166. Julian, C.G., et al., *Inhibition of peroxisome proliferator-activated receptor gamma: a potential link between chronic maternal hypoxia and impaired fetal growth.* FASEB J, 2014. **28**(3): p. 1268-79.

167. Rodie, V.A., et al., *Human Placental Peroxisome Proliferator-Activated Receptor δ and γ Expression in Healthy Pregnancy and in Preeclampsia and Intrauterine Growth Restriction.* Journal of the Society for Gynecologic Investigation, 2005. **12**(5): p. 320-329.

168. Waite, L.L., R.E. Louie, and R.N. Taylor, *Circulating activators of peroxisome proliferator-activated receptors are reduced in preeclamptic pregnancy.* J Clin Endocrinol Metab, 2005. **90**(2): p. 620-6.

169. Holdsworth-Carson, S.J., et al., *Peroxisome proliferator-activated receptors are altered in pathologies of the human placenta: Gestational diabetes mellitus, intrauterine growth restriction and preeclampsia.* Placenta, 2010. **31**(3): p. 222-229.

170. Permadi, W., et al., *Differences in expression of Peroxisome Proliferator-activated Receptor-gamma in early-onset preeclampsia and late-onset preeclampsia.* BMC Res Notes, 2020. **13**(1): p. 181.

171. *ACOG Practice Bulletin No. 202: Gestational Hypertension and Preeclampsia.* Obstet Gynecol, 2019. **133**(1): p. e1-e25.

172. Becker, J., et al., *Detecting endogenous SUMO targets in mammalian cells and tissues.* Nat Struct Mol Biol, 2013. **20**(4): p. 525-31.

173. Drewlo, S., K. Levytska, and J. Kingdom, *Revisiting the housekeeping genes of human placental development and insufficiency syndromes.* Placenta, 2012. **33**(11): p. 952-954.

174. Leach, R.E., et al., *High throughput, cell type-specific analysis of key proteins in human endometrial biopsies of women from fertile and infertile couples.* Human Reproduction, 2012. **27**(3): p. 814-828.

175. Altman, D.G. and J.M. Bland, *Standard deviations and standard errors.* BMJ, 2005. **331**(7521): p. 903.

176. Knofler, M. and J. Pollheimer, *Human placental trophoblast invasion and differentiation: a particular focus on Wnt signaling.* Front Genet, 2013. **4**: p. 190.

177. Shahul, S., et al., *Circulating Antiangiogenic Factors and Myocardial Dysfunction in Hypertensive Disorders of Pregnancy.* Hypertension, 2016. **67**(6): p. 1273-1280.

178. Tache, V., et al., *Placental expression of vascular endothelial growth factor receptor-1/soluble vascular endothelial growth factor receptor-1 correlates with severity of clinical preeclampsia and villous hypermaturity.* Hum Pathol, 2011. **42**(9): p. 1283-8.

179. Rajakumar, A., et al., *Transcriptionally active syncytial aggregates in the maternal circulation may contribute to circulating soluble fms-like tyrosine kinase 1 in preeclampsia.* Hypertension, 2012. **59**(2): p. 256-64.

180. Brust, R., et al., *A structural mechanism for directing corepressor-selective inverse agonism of PPARgamma.* Nat Commun, 2018. **9**(1): p. 4687.

181. Lee, G., et al., *T0070907, a selective ligand for peroxisome proliferator-activated receptor gamma, functions as an antagonist of biochemical and cellular activities.* J Biol Chem, 2002. **277**(22): p. 19649-57.

182. Abheiden, C.N.H., et al., *Cardiovascular risk factors in women with inheritable thrombophilia a decade after single or recurrent hypertensive disorder of pregnancy.* Hypertension in Pregnancy, 2016. **35**(4): p. 461-469.

183. Ackerman, C.M., et al., *Severe cardiovascular morbidity in women with hypertensive diseases during delivery hospitalization.* Am J Obstet Gynecol, 2019. **220**(6): p. 582 e1-582 e11.

184. Bernardes, T.P., et al., *Delivery or expectant management for prevention of adverse maternal and neonatal outcomes in hypertensive disorders of pregnancy: an individual participant data meta-analysis.* Ultrasound in Obstetrics & Gynecology, 2019. **53**(4): p. 443-453.

185. Braunthal, S. and A. Brateanu, *Hypertension in pregnancy: Pathophysiology and treatment.* SAGE Open Med, 2019. **7**: p. 2050312119843700.

186. Kadam, L., et al., *Rosiglitazone Regulates TLR4 and Rescues HO-1 and NRF2 Expression in Myometrial and Decidual Macrophages in Inflammation-Induced Preterm Birth.* Reprod Sci, 2017. **24**(12): p. 1590-1599.

187. Kohan-Ghadr, H.R., et al., *Rosiglitazone augments antioxidant response in the human trophoblast and prevents apoptosis†.* Biol Reprod, 2019. **100**(2): p. 479-494.

188. Levytska, K., et al., *PPAR- γ Regulates Trophoblast Differentiation in the BeWo Cell Model.* PPAR Res, 2014. **2014**: p. 637251.

189. Xu, Y., et al., *An M1-like Macrophage Polarization in Decidual Tissue during Spontaneous Preterm Labor That Is Attenuated by Rosiglitazone Treatment.* J Immunol, 2016. **196**(6): p. 2476-2491.

190. Jung, H.Y., et al., *Heme Oxygenase-1 Protects Neurons from Ischemic Damage by Upregulating Expression of Cu,Zn-Superoxide Dismutase, Catalase, and Brain-Derived Neurotrophic Factor in the Rabbit Spinal Cord.* Neurochem Res, 2016. **41**(4): p. 869-79.

191. Kim, C.S., et al., *Quercetin reduces obesity-induced hepatosteatosis by enhancing mitochondrial oxidative metabolism via heme oxygenase-1.* Nutr Metab (Lond), 2015. **12**: p. 33.

192. Lee, P.J., et al., *Regulation of heme oxygenase-1 expression in vivo and in vitro in hyperoxic lung injury.* Am J Respir Cell Mol Biol, 1996. **14**(6): p. 556-68.

193. Lee, J.C., et al., *Ischemic preconditioning protects hippocampal pyramidal neurons from transient ischemic injury via the attenuation of oxidative damage through upregulating heme oxygenase-1.* Free Radic Biol Med, 2015. **79**: p. 78-90.

194. Zuckerbraun, B.S., et al., *Carbon monoxide protects against liver failure through nitric oxide-induced heme oxygenase 1.* J Exp Med, 2003. **198**(11): p. 1707-16.

195. Wang, G., et al., *A novel hypothesis: up-regulation of HO-1 by activation of PPARγ inhibits HMGB1-RAGE signaling pathway and ameliorates the development of ALI/ARDS.* J Thorac Dis, 2013. **5**(5): p. 706-10.

196. Xu, J., et al., *The PPARγ agonist, rosiglitazone, attenuates airway inflammation and remodeling via heme oxygenase-1 in murine model of asthma.* Acta Pharmacol Sin, 2015. **36**(2): p. 171-8.

197. McCarthy, F.P., et al., *Peroxisome proliferator-activated receptor-γ as a potential therapeutic target in the treatment of preeclampsia.* Hypertension, 2011. **58**(2): p. 280-6.

198. Lee, C. and C.H. Huang, *LASAGNA-Search 2.0: integrated transcription factor binding site search and visualization in a browser.* Bioinformatics, 2014. **30**(13): p. 1923-5.

199. Kohan-Ghadr, H.R., et al., *Rosiglitazone augments antioxidant response in the human trophoblast and prevents apoptosisdagger.* Biol Reprod, 2019. **100**(2): p. 479-494.

200. Skene, P.J. and S. Henikoff, *An efficient targeted nuclease strategy for high-resolution mapping of DNA binding sites.* Elife, 2017. **6**.

201. Skene, P.J., J.G. Henikoff, and S. Henikoff, *Targeted in situ genome-wide profiling with high efficiency for low cell numbers.* Nat Protoc, 2018. **13**(5): p. 1006-1019.

202. Kovo, M., et al., *The relationship between hypertensive disorders in pregnancy and placental maternal and fetal vascular circulation.* Journal of the American Society of Hypertension, 2017. **11**(11): p. 724-729.

203. Carpentier, G., et al., *Angiogenesis Analyzer for ImageJ - A comparative morphometric analysis of "Endothelial Tube Formation Assay" and "Fibrin Bead Assay".* Sci Rep, 2020. **10**(1): p. 11568.

204. Schneider, C.A., W.S. Rasband, and K.W. Eliceiri, *NIH Image to ImageJ: 25 years of image analysis.* Nat Methods, 2012. **9**(7): p. 671-5.

205. Kappou, D., et al., *Placental mRNA expression of angiopoietins (Ang)-1, Ang-2 and their receptor Tie-2 is altered in pregnancies complicated by preeclampsia.* Placenta, 2014. **35**(9): p. 718-23.

206. Zhang, J., et al., *Peroxisome proliferator-activated receptor γ mediates porcine placental angiogenesis through hypoxia inducible factor-, vascular endothelial growth factor- and angiopoietin-mediated signaling.* Mol Med Rep, 2017. **16**(3): p. 2636-2644.

207. Yoon, J.C., et al., *Peroxisome proliferator-activated receptor gamma target gene encoding a novel angiopoietin-related protein associated with adipose differentiation.* Mol Cell Biol, 2000. **20**(14): p. 5343-9.

208. Saleh, L., et al., *The emerging role of endothelin-1 in the pathogenesis of pre-eclampsia.* Ther Adv Cardiovasc Dis, 2016. **10**(5): p. 282-93.

209. Lankhorst, S., A.H. Danser, and A.H. van den Meiracker, *Endothelin-1 and antiangiogenesis.* Am J Physiol Regul Integr Comp Physiol, 2016. **310**(3): p. R230-4.

210. Delerive, P., et al., *Peroxisome proliferator-activated receptor activators inhibit thrombin-induced endothelin-1 production in human vascular endothelial cells by inhibiting the activator protein-1 signaling pathway.* Circ Res, 1999. **85**(5): p. 394-402.

211. McLaughlin, K., et al., *PlGF (Placental Growth Factor) Testing in Clinical Practice: Evidence From a Canadian Tertiary Maternity Referral Center.* Hypertension, 2021. **77**(6): p. 2057-2065.

212. Li, S. and M.S. Roberson, *Dlx3 and GCM-1 functionally coordinate the regulation of placental growth factor in human trophoblast-derived cells.* J Cell Physiol, 2017. **232**(10): p. 2900-2914.

213. Chiu, Y.H., et al., *New insights into the regulation of placental growth factor gene expression by the transcription factors GCM1 and DLX3 in human placenta.* J Biol Chem, 2018. **293**(25): p. 9801-9811.

214. Yasuda, E., et al., *PPAR-gamma ligands up-regulate basic fibroblast growth factor-induced VEGF release through amplifying SAPK/JNK activation in osteoblasts.* Biochem Biophys Res Commun, 2005. **328**(1): p. 137-43.

215. Kushwaha, R., et al., *Rosiglitazone up-regulates glial fibrillary acidic protein via HB-EGF secreted from astrocytes and neurons through PPARγ pathway and reduces apoptosis in high-fat diet-fed mice.* J Neurochem, 2019. **149**(5): p. 679-698.

216. Necela, B.M., W. Su, and E.A. Thompson, *Peroxisome proliferator-activated receptor gamma down-regulates follistatin in intestinal epithelial cells through SP1.* J Biol Chem, 2008. **283**(44): p. 29784-94.

217. Wang, L., Y.Y. Shao, and R.T. Ballock, *Leptin Antagonizes Peroxisome Proliferator-Activated Receptor-γ Signaling in Growth Plate Chondrocytes.* PPAR Res, 2012. **2012**: p. 756198.